BIOMIMETIC MATERIALS PROCESSING: IMPLEMENTATION OF MOLECULAR IMPRINTING AND STUDY OF BIOMINERALIZATION THROUGH THE DEVELOPMENT OF AN AGAROSE GEL ASSAY

by

Sajiv Boggavarapu

A Dissertation Submitted to the Faculty of the

DEPARTMENT OF MATERIALS SCIENCE AND ENGINEERING

In Partial Fulfillment of the Requirements
For the Degree of

DOCTOR OF PHILOSOPHY

In the Graduate College

THE UNIVERSITY OF ARIZONA

2 0 0 6

THE UNIVERSITY OF ARIZONA
GRADUATE COLLEGE

As members of the Dissertation Committee, we certify that we have read the dissertation

prepared by Sajiv Boggavarapu

entitled Biomimetic Materials Processing: Implementation of Molecular Imprinting and Study of Biomineralization through the Development of an Agarose Gel Assay

and recommend that it be accepted as fulfilling the dissertation requirement for the

Degree of Doctor of Philosophy

_____ Date: March 20, 2006
Brian Zelinski

_____ Date: March 20, 2006
Pierre Deymier

_____ Date: March 20, 2006
John Lombardi

_____ Date: March 20, 2006
James Collins

Final approval and acceptance of this dissertation is contingent upon the candidate's submission of the final copies of the dissertation to the Graduate College.

I hereby certify that I have read this dissertation prepared under my direction and recommend that it be accepted as fulfilling the dissertation requirement.

_____ Date: March 20, 2006
Dissertation Director: Brian Zelinski

STATEMENT BY AUTHOR

This dissertation has been submitted in partial fulfillment of requirements for an advanced degree at The University of Arizona and is deposited in the University Library to be made available to borrowers under rules of the Library.

Brief quotations from this dissertation are allowable without special permission, provided that accurate acknowledgment of source is made. Requests for permission for extended quotation from or reproduction of this manuscript in whole or in part may be granted by the head of the major department or the Dean of the Graduate College when in his or her judgment the proposed use of the material is in the interests of scholarship. In all other instances, however, permission must be obtained from the author.

SIGNED: Sajiv Boggavarapu

ACKNOWLEDGEMENTS

First and foremost I would like to thank my parents, Dr. Rao L. Boggavarapu and Vani S. Boggavarapu, for the endless support and encouragement throughout this whole educational adventure. It has been a long road, but in the end it has truly been worthwhile. Next I would like to thank my brothers, Dr. Jagadish Boggavarapu and Dr. Deepak Boggavarapu, for their support and occasional late night phone conversations dealing with anything from high tech to the day's currents sports stories.

I would like to thank Professor Pierre Deymier and Professor Brian Zelinski for helping make that last push such that I could finish this work. Professor Deymier showed an appreciation for my work and efforts and helped to make the final run to finishing possible. Thanks to Professor Zelinski for taking the time to read through the dissertation and clearing those last administrative hurdles. Special thanks to Dr. John Lombardi who as a fellow graduate student provided endless scientific knowledge and laboratory entertainment and after his graduation provided even more scientific knowledge along with personal encouragement which made the completion of this Doctoral work possible. I would also like to personally thank Professor James Collins of the Veterinary Science/Microbiology department for his time and efforts for being on my committee. I thank Dr. Keith Runge of the University of Florida for offering to help evaluate my dissertation and providing some encouragement that I had done some good work.

Finally, I would like to thank all my friends and acquaintances who have come and gone throughout my academic career and throughout life.

TABLE OF CONTENTS

TABLE OF CONTENTS - continued

LIST OF FIGURES

LIST OF FIGURES - continued

LIST OF FIGURES - continued

LIST OF FIGURES - continued

LIST OF FIGURES - continued

LIST OF FIGURES - continued

LIST OF FIGURES - continued

LIST OF FIGURES - continued

LIST OF FIGURES - continued

LIST OF TABLES

ABSTRACT

Biomimetics is defined as an approach in which naturally occurring materials processes are mimicked in laboratory situations. The ultimate goal is to develop synthetic analogues of naturally occurring materials such as bone and teeth, classified as biocomposites, which possess similar chemical and mechanical properties. The work presented here provides the initial work in furthering the progress of biomimetic materials processing.

The first element of the work utilizes molecular imprinting as a selective recognition, or sensing tool, for detection of low molecular weight organic molecules. Molecular imprinting is a phenomenon in which crosslinked synthetic polymers exhibit selective binding towards small organic molecules. Initial work in the field was done in which numerous processing steps were involved with bulk polymer samples while the achievement here lies in the development of molecular imprinted polymer films which greatly facilitate the processing and characterization. Molecularly imprinted polymers are sometimes referred to as artificial antibodies due to the selective binding aspects that are highly analogous to natural antibodies.

Additional work involves transforming the recognition aspects of molecular imprinting into a biomineralization analogue. Biomineralization is the process in which organisms convert freely soluble minerals (namely calcium carbonates and calcium phosphates) into solid parts, such as bones and teeth, at ambient conditions via the influence of organic molecules such as proteins and carbohydrates. The molecular imprinting approach with biomineralization led to limited success but formed the

foundation for a more detailed study into the effects of small organic functional groups ($COOH^-$, OH^-) on the growth of calcium carbonates and calcium phosphates, the core components of important biocomposites such as bone.

In order to study the effects of organic molecules on the calcium based crystals, a mineralization assay was developed in an agarose gel matrix for studying inhibition and growth as influenced by various organic molecule functionalities. The gel mineralization assay is a novel approach in which quantitative and qualitative data could be generated in a high throughput fashion to determine organic molecule mediation of calcium based crystal growth. Such methods provide an approach for eventually providing control in development of synthetic biocomposites with customized materials properties.

1.0 INTRODUCTION

The term biomimetics is applied to understanding the underlying science and engineering carried out by biological organisms and extending this toward mimicking the processes in laboratory situations. The end result and primary goal is to achieve the development of functional materials.

The goal of the research presented here is a study in utilizing biomimetic techniques for materials synthesis and development in a quest to develop an artificial bone analogue. This has been approached by focusing on two primary areas: molecular imprinting and biomineralization.

Molecular imprinting is a phenomenon in which crosslinked synthetic polymers exhibit selective recognition towards small organic molecules. Such organic molecules are often interchangeably referred to as either imprint, template or target molecules. Polymerization is conducted around an imprint molecule and the resulting polymer retains a memory in terms of a shape based on the locations of the functional groups of the imprint molecule and a resulting host polymer. Molecular imprinting literature frequently refers to molecular imprinting polymer systems with varying terminology. (It is often times represented as imprint molecule-imprinted polymer, target-host molecules, template molecule-imprinted polymer etc.)

Biomineralization is defined as the process by which organisms convert ions in solution into solid materials. Organic molecules play a role in the formation of inorganic minerals such as calcium carbonate and calcium phosphate. These are the primary components of such biologically important materials-minerals as seashells, bones and

teeth. Such materials are also described as biocomposites due to the nature of organic/inorganic components of the end materials.

As the general goal of this research is the utilization of biomimetic techniques it is worth noting that molecular imprinting illustrates a selective recognition system that is analogous to the natural antigen-antibody systems. The natural antigen-antibody system involves molecules of much larger size and molecular weight than what has been achieved via molecular imprinting. However, the underlying interactions are fundamental to either system, e.g. hydrogen bonding, van der Waals forces, electrostatic interactions and even shape selectivity [1, 2]. The majority of work in molecular imprinting of polymers has been illustrated utilizing bulk polymer samples while this research shows molecular imprinting in polymer films.

Biomineralization plays a major role in the development of natural materials, frequently referred to as biocomposites, such as bones, teeth and seashells. The concept of biomineralization may also be described as organic molecule mediated crystallization of inorganic salts i.e. calcium carbonate, calcium phosphate. In nature, organic molecules in the form of proteins and polysaccharides mediate the transport, through intercellular fluids, and precipitation of inorganic salts throughout the organisms resulting in the aforementioned functional materials e.g. teeth, bone etc[3, 4]. Many of the organic molecules responsible for influencing crystal formation possess ordinary functionalities that are readily available in more common chemicals as low and high molecular weight polymers. Studies in biomineralization have been carried out utilizing a broad array of techniques including the use of self-assembled monolayers, bulk polymers

and other polymer films. The major issue has been the control or placement of the varying functional groups in order to better characterize the crystallization (or mineralization) process.

The initial motivation of the current research is to integrate molecular imprinting in polymer films with the principles of biomineralization as a stepping point for biomimetic materials processing. Although the reasoning seemed feasible the results were inconsistent and the system proved to be very difficult to characterize. However, the experiments provided some interesting questions and therefore led to studying biomineralization with a different approach, studying mineralization in an agarose gel form. This approach led to the development of a novel gel mineralization assay in which the influence of organic molecules on the crystallization of calcium based biominerals was studied and quantified. Briefly stated, the gel mineralization assay is done with agarose gels deposited in Petri dishes. A sufficient amount of gel is deposited in the Petri dish to allow an easily measurable thickness. During processing, the gel is incorporated with a calcium salt. After the gel cools and sets an organic molecule inhibitor/modifier/additive is added and allowed to diffuse into the gel. Once the organic molecule diffuses into the gel another salt solution is deposited onto the gel. The interactions between the salt solutions within the gel and the solution that is deposited allows the development of calcium crystals e.g. calcium carbonate, calcium phosphate. The effect of the organic modifier/inhibitor may show an inhibition of calcium crystal formation, thus resulting in an easily observable ring of inhibition. The primary effort was in calcium carbonate studies.

The shift in focus also allowed the preliminary steps to be taken such that true biocomposites could be developed using solid freeform fabrication techniques. Solid free-form fabrication (SFF) is a form of rapid prototyping for part making. It is a processing method in which a three dimensional part is produced without the use of molds. There are several variations of solid-freeform fabrication and all essentially rely upon the conversion of some matter, which can be solid or liquid, into a solid material by sequential addition of layers. The layers are injected through a syringe type dispensing head.

The resulting gel mineralization data provides the groundwork for estimating and controlling relative amounts of crystal formation. One can envision creating customized parts via solid freeform fabrication (SFF) and introducing inhibitors in selected areas to control mechanical properties e.g. control relative flexibility and rigidity by reducing or increasing crystal content via control and/or inhibition of calcium mineral growth.

1.1 Overview and Progression of Projects

It is worth noting that as the project focus was altered several times this dissertation is presented in a form of short papers and reports as opposed to an extended, and perhaps more easily unified, singular project. The initial goals of the project were to develop a molecular imprinted polymer system in film form. This was successfully completed and the synthesis and characterization of molecular imprinted polymer films are presented in Chapter 4, entitled 'Molecular Imprinting in Cross Linked Acrylic Polymers' while the background and theory behind molecular imprinting are presented in

Chapter 2. The primary advantages of molecular imprinted polymer films lie in the ease of post synthesis processing and characterization. Bulk imprinted polymers, although highly effective, require collection of particles, grinding and a somewhat more involved solvent extraction methodology. It is noted that the resulting MIP (molecular imprinted polymer) is a crosslinked polymer with imprint molecules that are essentially encapsulated within. Exposure, or more precisely, submersion, in a proper solvent allows for swelling of the polymer and hence subsequent removal, or extraction, of the imprint molecule. The polymer film form for MIPs is done by depositing thin layers of polymer upon soda-lime microscope slides. The post processing analysis and characterization is easily carried out via simple dipping and removal of an entire slide into desired solvents or mixtures of solvents.

Once appropriate success of MIP films was illustrated the project focus was taken towards incorporating molecular imprinting and biomineralization. Since molecular imprinting provided a memory effect via the selective recognition with organic molecules the focus shifted to inorganic entities, primarily calcium based minerals e.g. calcium carbonate, calcium phosphate etc. The proposed reasoning was such that if molecular imprinted polymers exhibit selective recognition towards organic molecules, could the same effect be observed with inorganic crystals. An imprinted polymer is synthesized based on prior knowledge of functional groups and placement. Based on this it was deemed possible that insertion of an inorganic crystal, calcium based mineral, would interact with the functional groups of the imprinted polymer. The resulting terminology, for ease of understanding, was called crystal imprinting.

Crystal imprinting is described briefly as follows. While conventional imprinting relies on incorporating an organic imprint molecule during polymerization crystal imprinting involves the incorporation of an inorganic crystal during polymerization. The crystals that were primarily used were calcium carbonate, calcium phosphate and calcium oxalate. The intent was to polymerize around the crystal, dissolve the crystal and then subsequently attempt to precipitate a new crystal within the matrix. It was assumed that some characterization could be done in order to determine the placement of the new crystal. However, the characterization proved to be far too prohibitive to succeed. However, this led to some interesting observations including the fact that the selected methacrylic acid polymer which has a -COOH functionality appeared to have inhibited the formation of crystals.

The results in the crystal imprinting project provided the impetus to gain a greater understanding of the effects of organic molecules on the formation of calcium based minerals. More detailed explanations of the current understanding of biomineralization principles and processes are presented in Chapter 3.

As the efforts in developing a 'pure' crystal imprinting system were unsuccessful the approach was changed and the gel mineralization assay was developed. Chapter 5, entitled 'A Test for Mineralization Inhibition for Calcium Salts Using Agarose Hydrogels' presents a published paper with the initial proof of concept of the gel mineralization assay. A limited number of conditions were utilized in the initial study; however, it is clear that injecting organic molecules into a gel does provide a procedure for determining the resulting effects on crystallization. Chapter 6, 'Test for

Mineralization – Additional Analysis' presents a more thorough analysis of the initial work presented in Chapter 5. It was noted after publication that the data had to be analyzed again for several potential inconsistencies, primarily depth of penetration of crystal growth and inhibition.

Chapter 7, entitled 'Gel Mineralization: Series 2' is the first step in developing a thorough method and protocol for gel mineralization assay screening. The concentration regime of the precipitating salts (calcium salt and carbonate solution) is more organized with a range of 0.1 M to 1.0 M. Data are presented in a thorough fashion with the attempt to detect consistent trends dependent on concentrations of inhibitors, concentrations of salt solutions, and various other parameters. A large number of graphs are presented as detection of specific trends proved elusive. Much like the initial work of Chapter 5 and 6 it is shown that polyacrylic acid had the most pronounced and easily detectable effects on calcium carbonate formation.

Chapter 8, entitled "Gel Mineralization: Series 3" furthers the studies into the gel mineralization assays. The previous experiments were done with a pH of 10.3 as that was optimized in some external projects prior to the initiation of the gel mineralization assays. In Series 3 the pH is not adjusted for any of the salt solutions, calcium chloride within the gel upon gel formation, and the sodium bicarbonate. The motivation behind this is that with solid freeform fabrication in mind limiting the number of steps involved in the chemistry could prove to be useful. Additionally, the comparison of molecules is altered. In addition to polyacrylic acid that has been previously established to inhibit calcium carbonate growth a newer molecule was introduced. Tetrasodium pyrophosphate (TSPP)

was chosen as another molecule in the screening of calcium carbonate inhibitors. It has previously been shown that certain phosphates play an inhibitory role in mineralization of calcium minerals[5, 6]. Once again the data presented is thorough and yet no distinct and consistent trends are easily noticeable. Polyacrylic acid did not show the large inhibitory effect as seen in the pH 10.3 systems.

Chapter 9, 'Gel Mineralization Screening', presents a basis for utilizing the gel mineralization assay as a screening method utilizing small organics and inorganics and studying the effects of calcium carbonate formation. Various molecules were chosen to sample their effects. The choice was somewhat systematic and arbitrary at the same time. This chapter primarily presents images indicating the observation of inhibited and uninhibited areas based on which inhibitor/modifier molecules were used. The concentration regimes varied from 0.1 M to 1.0 M salt solutions and the pH was not adjusted.

Chapter 10, 'Gel Mineralization: Calcium Phosphates', describes a limited more qualitative effort into the adaptation of the gel mineralization assay in the formation of calcium phosphates. Calcium phosphates proved to be a logical extension as the ultimate goal of biomimetic processing is to make functional biomaterials/biocomposites such as bone, which is primarily made of calcium phosphate in the form of hydroxyapatite. The chapter presents the preliminary stages involved in determining viability of analyzing various molecules as they influence the formation of calcium phosphates. Due to limited resources this aspect of the project was not extensively finished. However, a brief

analysis shows that the groundwork is present for a thorough study of biomineralization of calcium phosphates.

Chapter 11, ‘Applications Future Work’, is an introduction to the application of the gel mineralization assay as it is incorporated into a freeform fabrication protocol. This chapter describes some initial work on the mechanical properties of calcium based biocomposites. Additionally, some potential directions in future work in molecular imprinting and gel mineralization are described

2.0 MOLECULAR IMPRINTING

In regards to the molecular imprinting concept it is important to keep several fundamental issues in mind. Molecular imprinting is based on core molecular recognition fundamentals and is described in the following sections. Molecular imprinting is a phenomenon in which a crosslinked polymer exhibits a selective recognition towards low molecular weight organic molecule[7, 8]. Molecular recognition is an underlying characteristic of the structure and function of the entire biological world. All living processes are reliant on specific interactions at the molecular level, including examples such as DNA replication, transcription, and translation; antibody-antigen, enzyme-substrate/inhibitor recognition; and many other systems. Because of such importance there is extensive research in the fields of molecular recognition both for the sake of further understanding as well for finding uses for practical applications[9, 10]. Rational design of artificial receptors, including macrocyclic compounds, is dependent on a thorough knowledge of the structure of guest molecules. Host systems have been successfully created that involve complex and involved organic chemistry including developments by Cram, Lehn and Pedersen which led to a Nobel Prize in 1987[11]. The formation of host-guest complexes is driven by a range of intermolecular interactions that involve ionic pairing, hydrogen bonding, van der Waals forces, hydrophobic effects and others. All of these interactions are also prevalent in the phenomena known as molecular imprinting.

Molecular imprinting is a seemingly simple technique that can be characterized as a synthetic approach towards a molecular host via a template-guided synthesis in a self-

assembly mode. It may also be described as a cross-linked self-assembled polymer that exhibits selective recognition. In the process of molecular imprinting an imprint (in the molecular imprinting field also referred to as template or target molecule) molecule is used to induce the arrangement of functional monomers around the imprint and then the monomer chains are chemically fixed via co-polymerization with a crosslinking agent (monomer). The end result is a rigid polymer matrix that has an embedded imprint molecule. This imprint molecule may then be removed by exposure/submersion in an appropriate solvent and results in presence of recognition sites specific to the imprint molecule within the host polymer. A typical molecular imprinting system consists of a functional monomer, crosslinker, porogenic solvent and an imprint (template, target) molecule. As in most polymer systems the solvent is responsible for bringing all the components together during the polymerization i.e. the imprint molecule, the functional monomer(s), the crosslinker and the initiator. It also serves an additional purpose and that is the creation of pores in the macroporous polymers and hence the solvent is frequently referred to as a porogenic solvent or porogen[12]. An appropriate initiator is also required to induce free radical polymerization. The formation of the initial imprint-functional monomer complex (or template-functional monomer) is commonly referred to as the imprinting process. The resulting polymer is referred to as the molecular imprinted polymer or MIP in abbreviated form. The imprint molecule may be removed from the host MIP and is referred to as either the extraction or the removal process. Molecular imprinting involves selective recognition and testing of this involves the formation of the MIP, removal of the imprint molecule and in order to appreciate the value of the

recognition process a rebinding aspect is also required. The rebinding is the process in which the imprint molecule (previously unprocessed), in solvent, is introduced to the preexisting MIP after the imprint molecule has been removed. The rebinding process may be executed with either the original imprint molecule or any other molecule in order to illustrate the selective recognition, or selective binding, of the original MIP.

The entire molecular imprinting process is driven either by covalent or non-covalent interactions. The non-covalent approach was first realized by Mosbach and coworkers and is the easier method. However, it generates greater numbers of heterogeneous binding sites due to the relatively weaker interactions utilized. The covalent approach was pioneered by Wulff and co-workers and should provide more homogeneous binding sites but the rebinding is slower to the required formation of covalent bonds between the imprint and MIP[13, 14]. Additionally, a derivatization step of the imprint is required prior to the processing. Some attempts have been made to combine the two approaches whereby the imprinting is executed using polymerization of functional monomer being covalently coupled to the imprint molecule and the selective rebinding utilizes the non-covalent interactions.

Molecularly imprinted polymers(MIPs) have been mentioned as antibody and receptor binding mimics and have displayed high affinity and specificity for many systems[15]. The MIPs are favorable both physically and chemically and have been used in harsher conditions such as in organic solvents, at pH extremes, high pressures and elevated temperatures which is of great interest as naturally occurring biological molecules tend to denature in such conditions[16]. Hence, MIPs have potential applications

in the areas of separation, trace analysis, biomimetic sensors and biochemical and chemical synthesis. The end resulting MIPs have primarily been synthesized in bulk monolithic form and subsequent processing involves transforming the polymer into powders or small beads.

2.1 Theory and Principles

A valuable tool involved in the challenge to develop a synthetic system of recognition is the concept of molecular imprinting, which entails the creation of selective recognition sites in synthetic polymers. The concept of utilizing a specific imprint (also referred to as template or target) molecule to coordinate an assembly of synthetic monomers around some target molecule, in order to create a specific host, has been under consideration for some time. A new approach was developed to prepare the specific cavities with the functional groups arranged in a specific desired manner. This involves having functional groups bound to a suitable template molecule in the form of polymerizable vinyl derivatives [17, 18]. The monomer was copolymerized such that highly crosslinked polymers formed with chains in a fixed arrangement. These cavities possess a specific shape and arrangement of the functional groups that correspond to the template molecule. The functional groups in the polymer are located at various points of the polymer chain and are held in the specific spatial relationship by crosslinking.[7, 19] Essentially, two different approaches were developed - covalent and noncovalent. In either case the functional monomers undergo polymerization with the presence of the template, or target, molecule. This template molecule possesses some functionality that is complementary to the functionality of the host polymer chains.[20, 21]

The covalent approach has been researched primarily by Wulff in Germany and Shea in California, while the noncovalent approach is being investigated by Mosbach in Sweden. In this covalent approach the imprint molecule and the polymerizable host molecule are bound covalently. Upon completion of polymerization with a crosslinker the imprint molecule may be cleaved from the resulting highly crosslinked polymer.[7, 12, 19] The covalent approach has been utilized in the preparation of imprinted polymers that are selective for derivatized and free sugars[22, 23], glyceric acid and derivatives[1, 24], amino acids and amino acid derivatives[25-27], aromatic ketones[20].

In the non-covalent approach the imprint, or target, molecules are included with the functional monomers which are then polymerized together, thus allowing for non-covalent interactions between the two. The resulting polymer is a crosslinked, rigid structure. The imprint molecules are removed once polymerization is complete leaving recognition sites that are complementary to the imprint molecules both in shape and positioning of the functional groups.[7, 12, 28] This provides an induced molecular memory within the polymer which makes the polymer capable of selectively recognizing the imprint molecules.[28] The imprint molecules may interact during the extraction and rebinding processes with the host polymer via non-covalent interactions, e.g. ionic, hydrophobic and hydrogen bonding.[19, 29-31] The use of the non-covalent approach has been utilized in the preparation of polymers that are selective for dyes[32-34], diamines[33, 35],amino acid derivatives[36-48],peptides[42], β-adrenergic blockers[49], pharmaceuticals: theophylline and diazepam[1] and nucleotide bases[50].

2.2 Polymer Properties

The polymers utilized in molecular imprinting must meet some structural criteria in order to be effective. Once the template is removed from the host polymer the polymer must be able to restore the cavity shape of the template. The polymer structure must be optimized along several lines for this reason. The polymer chains should possess high rigidity in order to preserve the shape of the cavities upon removal of the template molecules. This is primarily achieved with a high a degree of crosslinking. Polymers that had less than 10% crosslinking showed no specificity for the template and as degree of crosslinking is increased the template specificity increases. As the degree of crosslinking approaches 95% the specificity for the template is nearly four-fold that at 10% crosslinking.[7, 51] In contrast to the requirements of rigidity the polymer must also possess some flexibility in the whole arrangement. This allows for rapid binding and splitting of the templates within the cavities [52]. Cavities may be present without reasonable flexibility in which case the kinetics of reversible binding are adversely affected [53]. The extent of flexibility may be tailored by changing the crosslinking agents, which also affect the polymer chain swellability. Crosslinked polymer chains swell when exposed to certain solvents and this swelling phenomenon allows the chain to expand and therefore release the template molecule.

Accessibility of the cavities is another important characteristic that the polymer must possess. As many cavities as possible should be available to the template molecules. The accessibility may be measured as the percentage of the templates that are separated from the host polymer. This is dependent on the flexibility of the polymer chains, the inner surface

area, and on the pore size distribution in the macroporous polymer [54, 55]. Higher degrees of crosslinking result in higher inner surface areas within the polymer matrix [56, 57]. The degree of crosslinking is once again the controlling factor in the development and formation of the pores, or cavities. These macroporous polymers are generated when the polymerization is done with a high degree of the crosslinking agent (5-90%) along with inert solvents (also known as porogens).[56] As the polymerization is taking place, phase separation occurs and upon removal of the porogen, followed by drying, the permanent pore structure remains. The pores will change size during swelling but will remain present throughout. A relatively large inner surface (50-600 m^2g^{-1}) will result in the bulk polymerizations, and along with the large pores(10-60 nm) ensures that specific microcavities are formed by the imprinting process(approx. 0.5-1.5 nm in diameter) which are readily accessible and allow smaller molecules to diffuse into the pores.[56] Another key characteristic required for the polymer is mechanical stability which is primarily a factor in applications with High Performance Liquid Chromatography (HPLC). The mechanical stability is a function of the degree of crosslinking and with the higher degrees of crosslinking providing the greater mechanical stability.[7, 51, 58]

2.3 Selectivity and Binding

The formation of the binding sites by the imprinting procedure generates two primary functions for the binding groups. Initially, during the polymerization a strong interaction between the template and the binding groups is required so the template molecule

can fix the binding groups at the growing polymer chains with a defined stereochemistry. Once the template splits off, the binding groups of the

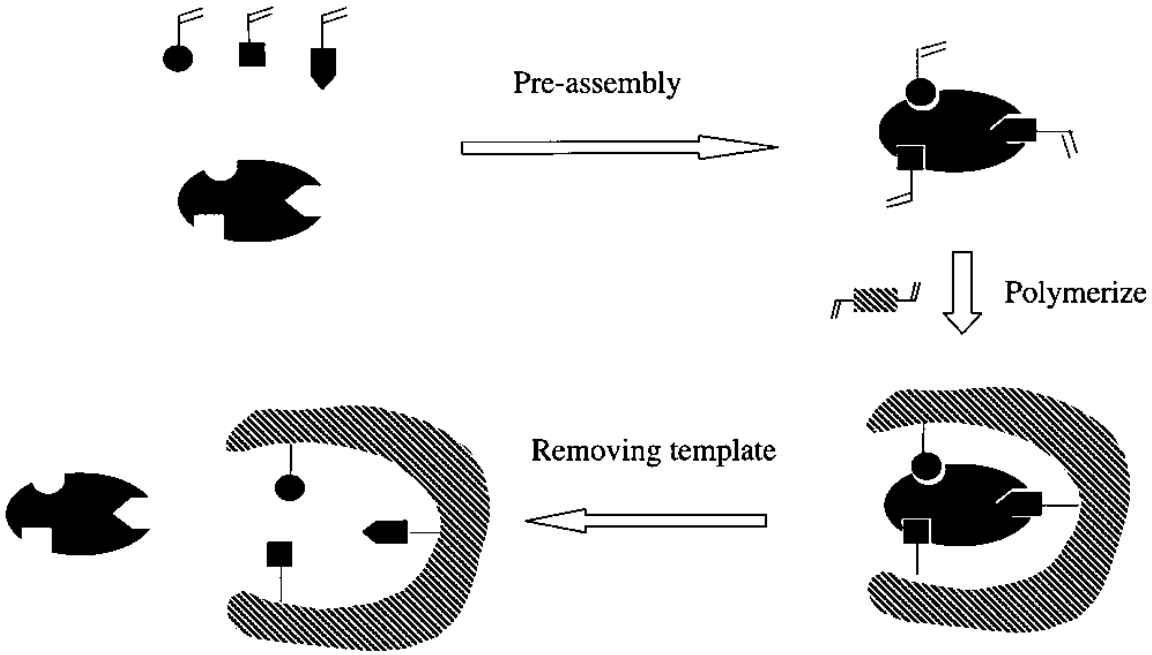

Figure 2.1 A schematic of the molecular imprinting process. Steps include a preassembly of the functional monomer with the imprint molecule. A copolymerization with the crosslinker essentially freezes the binding groups to form an imprint defined cavity. The template is removed by solvent extraction thus providing a cavity that is specific to the original imprint molecule that is complementary to the position of the functional groups and shape of the cavity.[59]

polymer should be able to undergo a reversible binding interaction with the template (fig 1). During the polymerization the binding should be strong and afterwards the activation energy should be minimal[28, 60]. Possible interactions between the binding groups and the polymer include hydrophobic, electrostatic, charge-transfer, and dipole-dipole and in some cases covalent[7, 19, 51].

Molecularly imprinted polymers exhibit selectivity towards the template molecules based on several aspects of chemistry. These factors may affect the selectivity either during the synthesis of the polymers or during the protocols that are actually testing the ability of the imprinted polymer to rebind to the template molecule. These fundamentals of molecular imprinting include chirality of the imprinted polymers, temperature of extractions and polymer synthesis and shape specificity[61, 62]. The origin of the chirality of the imprinted polymer is important in determining whether or not the polymer can correctly incorporate the template molecule. The cavities are asymmetrical and this asymmetry is measured by the racemate resolution ability or is directly measured by measuring optical activity. The polymer is suspended in a solvent that has the same refractive index as the polymer followed by measurements of the molar optical rotation. The imprints may either adversely affect the molar optical rotation, in which case proper imprinting may not occur, or it will enhance the molar optical rotation thus allowing for more favorable binding of the template[19, 56].

The selectivity of the imprinted polymers to the template is also dependent on the temperature at which the polymer synthesis occurs as well as the temperature at which rebinding experiments are attempted[63]. Polymer synthesis may occur at a wide range of temperatures from 0°C (via photoinitiation) to upwards of 100°C. This may influence the selectivity since the imprinting may occur at one temperature, e.g. 65°C, while the rebinding may be attempted at 40°C and therefore the cavity may be better preserved at the synthesis temperature than at the lower temperature[40, 63]. Another reason for the temperature dependence may be that at higher temperatures the embedding of the template molecule is more rapid and that more cavities, primarily the more selective ones, are filled. At higher

temperatures the swelling of the polymer chains is also increased and therefore embedding of the template is faster and easier. Upon separation from the template some polymers that are highly crosslinked possess swellability of more than 100% in the solvent used in the original synthesis. When the template is added the original volume is restored by deswelling. If the swelling does occur with solvation of the functional groups within the microcavities they restore their original form upon binding. This may be regarded as being analogous to the 'induced fit' in enzymes[27, 63].

The primary characteristic involved in the molecular recognition of molecularly imprinted polymers is the shape selectivity. The selectivity is a result of the combination of the accuracy of the cavity-shape fitting and the exactness of the arrangement of the introduced functional groups. The exact distances between the functional groups influence the clefts that will be present in the imprinted polymer. It has been observed that even differences in the positions of the functional groups by as little as 0.33 nm may adversely affect the rebinding of the template to the host polymer[45, 63].

2.4 Applications

The groundwork for understanding the theory of molecular imprinting has been achieved by many research groups. Sufficient understanding has allowed for the direct use of molecular imprinting in several areas. Molecular imprinting has been utilized in an array of different applications, ranging from tailor-made separation materials to enzyme and antibody mimics to custom made biosensors. Several of the more promising applications will be mentioned here. The three primary areas for the application of molecularly imprinted

polymers include (1) the use as tailor-made separation materials, (2) the use in organic synthesis and enzyme technology as catalytically active polymers of enzyme mimics and (3) as sensors in biosensor-like systems, where the polymers are used as substitutes for the biological molecules that are normally utilized[7, 8, 40, 45].

2.5 Chiral Separations

The more widely studied areas for molecularly imprinted molecules are the separations of mixtures. Stereo- and regioselective separations have been accomplished using various sugars, both derivatized [64] and free[23] have been separated into their optical counterparts. Other applications of chiral separations have been made with amino acid derivatives[42] and with drugs like β-blockers(aryloxy propanolamines)[49] and have yielded systems that are capable of achieving baseline separations. Eventually, it is hoped that the usage of molecularly imprinted polymers will challenge that of traditional chiral stationary phases(CSPs)[45, 65]. Molecularly imprinted polymers provide the option of making specific imprint polymers for the desired separation which is much more efficient than the conventional trial and error methods associated with CSPs. In fact of the approximately 500 optically active drugs currently sold close to 90% are administered as racemic mixtures. Reinforcing the fact that faster alternatives to CSPs are desired, the FDA recently passed regulations stating that for new drugs to receive approval both enantiomers must be tested as separate substances in pharmacokinetic and toxicological profiling[8].

2.6 Antibody Mimics

A more alluring application of molecularly imprinted polymers is that in which the polymer is used as an antibody mimic. This application shows great promise in greatly influencing biological separations in clinical situations e.g., detection of substances in the blood. Conventionally, ligand-binding assays are used to measure small amounts of some substance in the bloodstream. These assays require some receptor that is specific for the target substance and most often antibodies are used. As those in the field of immunology can attest to, the production of antibodies(monoclonal), though seemingly optimized, is still expensive and time consuming[66, 67]. Molecular imprinting has been used to prepare certain polymers that mimic the antibody combining sites. These imprinted molecules showed binding and crossreactivity profiles comparable to those of the antibodies. In addition a radiolabelled ligand-binding assay, the molecularly imprinted sorbent assay, which uses the antibody mimics, has been developed. This assay accurately measures the drug levels in the human serum that are within detection ranges obtained using the conventional immunoassay technique[1].

2.7 Enzyme Mimics

The creation of synthetic polymers displaying enzyme like properties, substrate-selective catalytic behavior, has been a goal for scientists for some time[27, 63, 68]. The success in antibody mimics provides incentives to take the concept further to develop systems that possess catalytic functionality in the binding site. Imprints have been prepared against transition state analogues, the molecularly imprinted polymer displayed preference to the

transition state analogue, and did influence an increase in hydrolysis rates in these reactions[63, 69]. Enzyme cofactors are understood to be complementary to the construction of enzymatic systems and imprints have been made to certain cofactors in which cases the imprinted polymer once again enhanced the rate of reaction[69]. Recently it has been reported that selective recognition properties of molecularly imprinted polymers can be utilized to change the course of chemical reactions involving amino acid derivatives[70]. The results obtained from catalytically active polymers are limited, but the stability of these preparations coupled with the possibility of introducing new catalytic properties, indicates that research in this area will continue. In addition, success in using the imprint as a model for the catalytic stereo- and regioselective reactions remains feasible[70].

2.8 Biosensors

Molecular imprinting has shown impressive results in antibody or receptor-site mimics and this leads to the possibility of utilizing these as substrate-selective sensors, or biosensors. Although there are a wide variety of biosensors currently existing there is a need for improvement[46]. By using catalytically active or ligand-specific polymers prepared from molecular imprints a stronger sensing element would result. In many cases there is no suitable specific biomolecule, but with molecular imprinting this would be made possible. Mosbach et al have developed molecularly imprinted polymers into field effect devices, in which C-V (Capacitance vs. Voltage) measurements may be taken as a function of absence or presence of the imprint molecule[46]. Advantages to using imprinted polymers as the sensing layer in devices include high mechanical stability and thermal stability of the

polymers. In addition: (i) the sensor may be sterilized for use in e.g. fermentors, (ii) a long lifetime of the sensor is expected, and (iii) the sensor may be tailor-made for specific compounds or groups of compounds[46]. Detection principles include the use of fluorescence, optical reflectometry, changes in mass, and surface plasmon resonance. Another illustration of the use of molecular imprinting in biosensors is the separation of optical isomers of amino acid derivatives in a column containing an imprint molecule for one of the enantiomers based on measuring streaming potentials[43].

3.0 BIOMIMETIC CRYSTALLIZATION: BIOMINERALIZATION

3.1 Introduction

Technologies requiring crystallization protocols that require control over the structure, size and morphology of inorganic crystals have been desired for some time[71-74]. This primarily exists since many of the areas of materials fabrication involve particles of modal size and shape as well as the use of inorganic materials with specific crystallographic attributes. The knowledge of the thermodynamics and kinetics of crystallization is extensive but the reproducible fabrication of customized crystalline materials with specific designs remains to be seen[75]. The primary challenge is to understand the molecular processes that are responsible for the phase transformation from a supersaturated solution into a crystalline solid. In order to attain this goal, a greater understanding of the dynamic forces dictating the aggregation of molecular species into stable clusters and the subsequent stabilization and amplification of the crystal nuclei into three dimensional form must be achieved[76]. The conventional crystal growth methods that are based on the supersaturation of aqueous solutions have not advanced to the point where they generate consistency with regard to the control of particle size, morphology, orientation, and crystal texture[75, 77, 78]. However, epitaxial crystallization strategies utilizing organized substrates to facilitate the formation and orientation of critical nuclei from supersaturated solutions have proven somewhat successful[79]. Substrate-mediated growth strategies have now found greater usage in widespread situations. Seeding techniques may be used to induce control over product size and size distribution[80, 81]. In addition, metals, polymers, and small molecules not prone to form large single crystals have been processed into oriented structures via epitaxial

crystallization on single crystal substrates[82], and on moderately oriented polymers[83]. Although there are more widespread applications, the molecular origins of the orientational effects remain to be completely understood, since assuming that a one-to-one lattice match is the only requirement is insufficient [84]. The more probable reason is that oriented nucleation and growth may be achieved by the cooperative influence of several interfacial features: selective charge accumulation, geometric and stereochemical disposition of active chemical groups within the substrate and forming crystal, and the inherent symmetry requirements of ions within the crystal faces[76]. Such demands and criteria in the areas of crystal engineering lead to utilization of novel methods in controlling crystallization products[85].

3.2 Nucleation, Crystallization

The formation of crystals from single molecules from supersaturated solutions is dependent on processes in which the molecules assemble at early stages in the form of structured aggregates or nuclei. This originates from the intermolecular forces and entropy within. Nucleation, in general, depends on an activation energy barrier preventing the spontaneous formation of a solid phase from a supersaturated solution.

3.3 Biomineralization: Fundamentals

One particular area of interest is in biomineralization and the mechanisms inspired thereof. Many of the aforementioned influences of oriented crystallization have come from the study of biomineralization, in which the organized organic surfaces dictate the nucleation and crystal growth of the inorganic phases. Simply stated, biomineralization is the process by which organisms convert ions in solution into solid materials[72, 73, 79]. Though many

colloidal and solution processing techniques have been used, the biological synthesis of the inorganic solids often yields materials of uniform size, unusual habit, organized texture, and defined structure and composition under conditions of supersaturation and temperature[86]. Prime examples include magnetotactic bacteria, which synthesize oriented intracellular chains of single domain crystals of magnetite[76, 80] or the metastable ferrimagnetic iron sulfide, geigite (Fe_3S_4)[80]. These organisms have gained scientists' interest because of the ability to carry out low temperature synthesis of magnetic materials. The mineral particles are uniformly sized and characterized by unique crystal habits that come between the space group symmetries of the materials[76].

3.4 Controlling Factors in Biomineralization

In order for the processes of biomineralization to take place, and for the synthetic analogues to take place, several controlling factors are deemed fundamental in controlling the crystallization processes. Many factors must play a role at the site of the mineralization [87]. The site must be predetermined from the rest of the possible substrates, must be activated only at specific times by the organism, and must be highly regulated in regards to the chemistry of the mineralization process.[73, 86, 88] These principle factors may be noted as follows:

(I) spatial delineation by supramolecular assemblies,

(II) chemical regulation by transport processes, and

(III) molecular recognition at inorganic-organic interfaces.

3.5 Spatial Delineation

In order for the mineralization to take place there must be a selected area for this to occur. This mineralization zone is restricted by the physical shape of the polymer assemblies. In some instances the mineral particles are often seen trapped by bilayer vesicles[72] and results in crystal sizes from 20 nm to several microns[89]. In order to get crystals smaller than these the use of polypeptide micelles and polymeric crystals like collagen can be used to get the nanoscale volumes optimized[90]. The cellular forces are responsible for shaping of the supramolecular systems and subsequently induce differing morphologies based on the basic principles that the mineral will grow into whatever space it is given[91-93].

3.6 Chemical Regulation

The chemical processes of the biomineralization process are essentially regulated by the transport and/or the reaction-mediated mechanisms. Since the mineralization is localized within the supramolecular assemblies, it allows for complete variation of the supersaturation levels to be regulated via facilitated ion-flux, complexation/decomplexation switches, local redox and pH modifications and changes in local ion activities through ionic strength and vectorial water fluxes[94]. These reaction mechanisms are also responsible for affecting the kinetics of these surface-mediated processes, including, the stability of embryonic clusters in nucleation, expression of crystal faces, pathways of phase transformations, and aggregation(maturation) which all depend on the activation energy barriers of the interfacial properties[94-96].

3.7 Molecular Recognition

The primary reason that biomineralization differs from conventional mineralization is the influence of the organic substrates. In nature this is governed by the presence of macromolecular substrates responsible for the "organic-matrix-mediated" processes that provide the mineral with conditions in which specific crystallographic orientation with respect to the underlying organic surface occurs[86, 97].

There should be some form of complementarity that exists between the surface chemistry, structure and the nucleated crystal face. This illustrates the concept of molecular recognition at the inorganic-organic interface[71, 76, 88, 91, 98, 99]. In order to achieve some form of molecular recognition there must be some interactions between the organic interface and the mineral. The chemical bonding at the surface of the mineral nuclei is primarily ionic hence the organic interface should possess areas of high local charge where electrostatic, dipolar and hydrogen bonding interactions take place during the nucleation. If these forces are responsible for the molecular recognition between the stereochemical requirements of the ions of the nucleus surface and the charged groups at the macromolecular interface, then the structure and orientation of the mineral deposit may be determined[71, 100]. Certain features of the organic matrix are required to create the crystallochemical specificity: an existing organization of the organic matrix (molecular preorganization) and molecular complementarity between the inorganic ions and the local binding sites on the matrix[71, 88, 91].

An extensive description of the molecular forces that would be in an idealized inorganic-organic interface are still under investigation and information regarding the structure(periodic, amorphous, polyhedral) size, or composition of critical clusters or

whether or not the initial interactions involve ion-binding or larger scale polynuclear events is still unclear and hence the molecular recognition is still only regarded in the broadest sense[88, 101, 102]. However, it is still firmly postulated that the role of the matrix is essentially to lower the activation energy of nucleation by reducing the time between ionic collisions. It is also possible, in a more complex manner, that the matrix stabilizes a specific conformation of the transition state (nucleus) by structural and stereochemical recognition. General features of the organic matrix may be classified into three categories[88]. The Primary structures is the term used in which the matrix is matched to the coordination chemistry of the ionic species that comprise the mineral through the choice of ligands exposed to the interface. This is illustrated in calcified invertebrate tissues with macromolecules rich in carboxylate residues[3, 103] in which the Ca binding mimics Ca-CO_3 interactions in the crystal structures of calcite and aragonite. There are also secondary and tertiary structures in which only two options exist; nucleation may take place at a planar organic surface or at one that is curved. Planar organic surfaces are generated by antiparallel β-sheets while other planar surfaces can occur with phospholipid membranes. The curved surfaces are more prevalent since localized protein pockets and grooves, membrane-bound vesicles, α-helical, and triple-helical conformations all are possible. Finally the quaternary structures may play a more fundamental role in biomineralization[104, 105]. Mann[71, 88] has summarized the two key structural factors in the use of organic matrices in controlled nucleation as follows. The matrix is preorganized with respect to nucleation through several processes such as self-assembly, aggregation, membrane vesiculation, and controlled polymerization(cross-

linking) which influences spatial regulation of the surface functional groups. Secondly, the nucleation at the matrix surface is regiospecific with a limit on the number of sites that are confined to each location[106-109].

3.8 Crystal Engineering

Currently, several approaches to the biomimetic crystallization processes are possible:

(I) use of supramolecular assemblies in nanoscale synthesis,

(II) organic surfaces as molecular templates for nucleation,

(III) organic additives in the control of crystal morphology, and

(IV) synthetic polymeric matrices as frameworks for composite structures.

As mentioned previously, unilamellar vesicles may be used in which the vesicles' bilayer membrane confines an internal aqueous volume to only 20-50 nm in diameter. Materials such as Ag_2O [110], $CoSiO_3$ [111], calcium phosphates, $Fe_2O_3 \bullet nH_2O$ and Fe_3O_4 [112] have been prepared as nanometer-size intravesicular particles. These vesicles are formed with the organic membrane in a curved shape thus having an influence on the crystallization reactions. Changes in the crystal structure, size, and morphology may be observed contrasting to those resulting in similar reactions occurring without the aid of the vesicles[72].

The use of tailor made additives that will modify the crystal shape through specific interactions with the adsorbed molecules at the crystal faces has shown some promise. More detailed studies utilizing stereochemical calculations have been used to observe effects on inorganic crystallization[88, 113, 114].

Attempts to develop structured composites using inorganic precipitation *in situ* are also being pursued. Polymeric matrices are being used as the organic matrices though problems with the volume fractions of the inorganic phase may pose limitations. The presence of nucleator molecules and framework polymers may provide a suitable biomimicking environment[88, 99, 115].

3.9 Crystal Growth in Gels

The fundamentals of crystal growth in gels were pioneered by Henisch[116-118]. Several procedures for crystal growth were illustrated. The first concept is that of a charged gel that is covered with a counter ion solution and a second counter ion incorporated directly in the gel. Upon diffusion of these counter ions, in selected and proper concentrations, a precipitate forms. Such methods have been utilized to precipitate such materials as calcium carbonate, calcium sulfate and even some metals such as copper, iron and cobalt.

It is believed that the gel creates a stable pattern of concentrations and since crystal growth is directed by the diffusion of the reactant to the surface, the precipitation rates and subsequent mechanics may be altered. Such alterations may result in larger sized crystals and even more pure crystals. Additionally, the gel acts as a matrix that supports the crystals. Once the crystal grows however, the gel may also exert pressures upon the crystals. The gel also is known to suppress nucleation and thus reduces the number of growing crystals and may induce growth of more perfect crystals that are also larger.

The importance of crystal growth in gels is mirrored in biological systems where important biominerals such as calcium carbonate and calcium phosphates precipitate within swollen polymers. These materials may be described as natural biocomposites.

In this study agarose gel matrices are utilized for the study of the formation of calcium carbonates and some conceptual tests with calcium phosphates. Such studies will lead to a greater understanding of biomineral development as applied to bones, teeth and other functional biominerals/biomaterials such as seashells.

3.10 Agarose

Agarose is a linear polysaccharide obtained from red marine algae. It is an essentially uncharged polysaccharide and is frequently used as a model biopolymer in gelation. It consists of an alternating 1,3-linked β-D-galactose and 1,4-linked 3,6-anhydro- α -L-galactose[119].

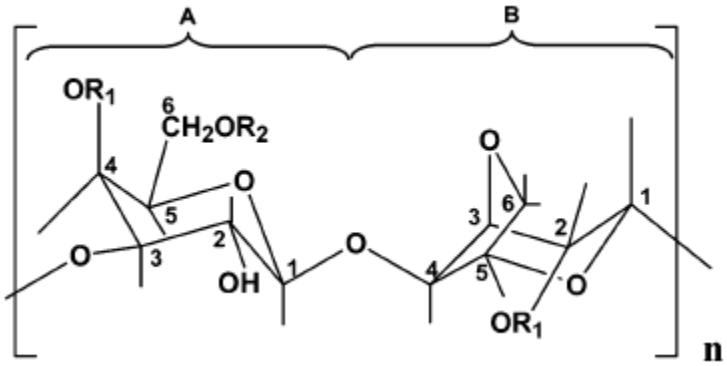

Figure 3.1 Ideal AB repeat unit of agarose polymer: The portion represented as (A) is a 1,3 linked β-D-Galactosidase residue while section (B) is a 1,4 linked 3,6-anhydro-α-L-galactose residue. In a native agarose gel, $R_1=R_2=R_3=H$. [120]

It forms a gel when a homogeneous solution is cooled below an ordering temperature of approximately 35° C and subsequently an infinite three dimensional network of fibers is formed. The melting of agarose occurs at an expectedly higher temperature of 85° C. The chemical structure of agarose provides the ability to form somewhat strong gels even

at low temperatures. The generally open mesh allows for control by varying the gel concentration of the agarose[121].

Agarose is a neutral polysaccharide that primarily consists of hydroxyl functionalities. While in some matrices such as gelatin the acid proteins exert effects on the crystallization of $CaCO_3$ the polysaccharide matrices usually do not solely effect crystallization of calcium carbonate. Hence it is expected that the agarose molecules play more a role of reaction media that control diffusion processes of ions and may hinder crystal growth when the sizes become prohibitively large e.g. exceed the pore sizes of the agarose network. The pore size of a 1% agarose gel is approximately 140 nm [122] .

4.0 MOLECULAR IMPRINTING OF CROSS LINKED ACRYLIC FILMS

4.1 Molecular Imprinting

Molecular imprinting is the phenomena utilizing functionalized polymers synthesized with a template, or print, molecule for developing selective binding assays. The host polymer exhibits selectivity to the imprint or a structurally similar one[7, 19]. The underlying concepts of utilizing a specific imprint molecule to coordinate an assembly of synthetic monomers around a target molecule have been around for some time. This approach was developed in order to prepare specific cavities with the functional groups arranged in some desired manner. The functional groups of the host monomer are bound to a template molecule in the form of polymerizable vinyl derivatives and the monomer is copolymerized such that highly crosslinked polymers are formed with the chains in a fixed arrangement[7, 11, 19, 31]. Two different approaches have been developed- the covalent and noncovalent. In both cases the functional monomers undergo polymerization in the presence of a template molecule. This template will possess some functionality complementary to the functionality of the host polymer[20, 123]. Here we illustrate usage of the noncovalent approach.

In the noncovalent approach the imprint, or target, molecules are included with the functional monomers which are then polymerized together, thus allowing for the non-covalent interactions to take place. The imprint molecules may be removed once the polymerization is complete, leaving recognition sites that are complementary to the imprint molecules both in shape and positioning of the functional groups[7, 28, 124, 125]. This

provides an induced molecular memory within the polymer which then makes the polymer capable of selectively recognizing the imprint molecules[28, 52].

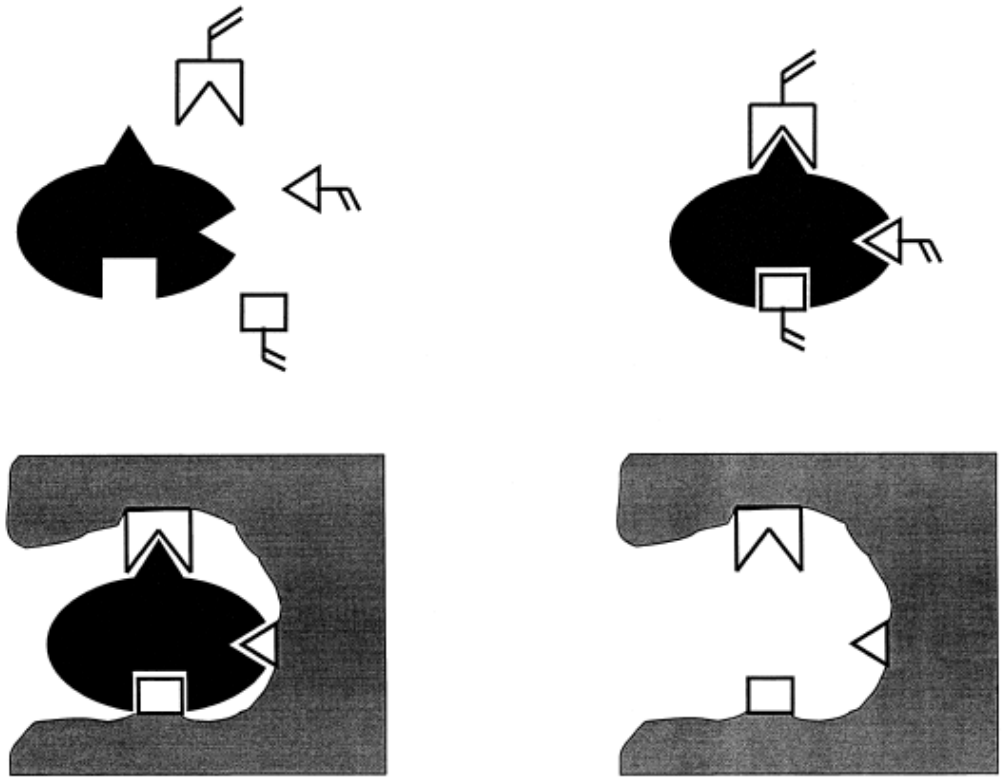

Figure 4.1 Schematic of molecular imprinting preparation. Adapted from [11]

The noncovalent approach interacts via ionic, hydrophobic and hydrogen bonding[19, 29, 30, 126], and has been used for preparation of polymers towards dyes[32, 33], amino acid derivatives[36-38, 44, 45, 127], , and pharmaceuticals, including, theophylline and diazepam[1, 66, 128, 129].

The polymers used in molecular imprinting must meet certain structural criteria in order to be effective. When the template is removed from the host polymer the polymer must be able to restore the cavity shape of the template. The polymer thus needs to be

optimized. The polymer chains must possess high rigidity in order to preserve the shape of the cavities upon removal of the templates. This is achieved with a high degree of crosslinking. Polymers that are less than 10% crosslinked tend to show no specificity for the template and as the degree of crosslinking is increased the specificity increases. As the degree of crosslinking(expressed here as volume percent of the monomer) approaches 95% the specificity is nearly four-fold that of the 10% crosslinked polymers[7, 130]. Though the polymer must possess such rigidity, it must simultaneously exhibit chain flexibility allowing for the rapid binding and splitting of the templates within the cavities. The kinetics of reversible binding are adversely affected when the cavities lack reasonable flexibility. The flexibility is tailored by changing the crosslinking agents, subsequently affecting the chain swellability. The cavities should also be easily accessible such that a maximum number of cavities are available to the template molecules. This may be measured as a percentage of templates separated from the host polymer and is dependent on chain flexibility, inner surface area and the pore size distribution[56, 123].

Much of the work done in molecular imprinted polymers has been with bulk polymers[7, 19, 36-38, 44, 45]. Here we illustrate the phenomena of molecular imprinting with the use of polymer films of methacrylic acid and 3-trimethoxysilyl propyl methacrylate imprinted with either caffeine or theophylline. The imprint molecules were chosen because of their structural similarity, with the only difference being the additional methyl group at the number 7 position in caffeine, and the previous successful work by Mosbach and others [8, 128]. The synthesis of films allows for facilitated processing conditions. Once the films are cast and dried they are ready for immediate processing without further

grinding or filtering steps. The choice of using UV characterization allows for direct and quick determination of associated peaks of the imprint molecules and determination of imprint concentrations.

4.1.1 Polymer synthesis

Methacrylic acid, theophylline, caffeine, 3-(trimethoxysilyl)propyl methacrylate were purchased from Aldrich (Milwaukee, WI). The initiator, azo-bis-isobutyronitrile (AIBN), was obtained from Pfaltz and Bauer. Dioxane was purchased from Mallinkcrodt and Alfa-Aesar. Standard soda-lime microscope slides were used as substrates for the membranes. The solutions were initially mixed in two flasks as follows: In Flask A AIBN(0.1g, 0.61 mmol) was added along with the imprint, theophylline(.150 g, 0.83 mmol) or caffeine(0.150 g, 0.82 mmol) to 25 ml dioxane. Flask B, with 25 ml dioxane, received Methacrylic acid(1.5 ml, 0.18 mol) and 3-(trimethoxysilyl) propyl methacrylate(1 ml, 4.2 mmol). The control

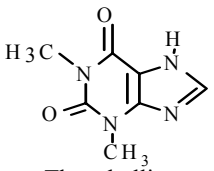

Theophylline

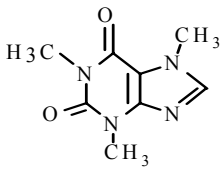

Caffeine

Figure 4.2 The selected imprint molecules. Note identical structure except for additional methyl group at no. 7 position of Caffeine.

solutions were prepared as above without the imprints. Contents of flask A and B were mixed separately until all components were dissolved into homogeneous solutions at

which point they were mixed into one 100 ml beaker and stirred again at room temperature. The monomer-imprint solutions were vigorously bubbled with argon gas, in order to purge solution of oxygen which is known to adversely affect polymerization[131], for 2 minutes and placed in warm oil baths (50° C). Polymerization of the solutions occurred at about 110 hours, at which time 1 ml aliquots of solution were removed with Pasteur pipettes and coated onto standard soda lime slides in a drop by drop manner on the slide surface. The polymerization time was elected so as to increase the degree of polymerization. At 110 hours the polymer solution had a notable increase in viscosity suggesting that polymerization was occurring thoroughly[131]. Previous experiments with shorter polymerization times yielded unsuccessful in regards of creating resulting polymer films with satisfactory coupling/adhesion to the glass slides. Samples were then dried, as crosslinking occurred, at room temperature for 130 hours before sample processing was initiated. Average membrane thickness was 10-12μm.

4.1.2 Binding and Rebinding Assays

Once dried, the samples were purged of all imprint molecules. The membranes, on slides, were washed in 40 ml of spectral quality dioxane. The slides were placed in 50 ml flat bottom beakers, tilted against the side and the contents stirred. At this angle 60% of the slide area was washed and only this portion of the membrane was subject to the testing. The beakers were placed in a heated water bath with continuous stirring at 40°C (temperatures of dioxane inside beakers reached 33-35°C) in two hour increments. Following each 2-hour extraction UV absorbance measurements were taken vs. a blank

dioxane reference. The absorbance peaks of interest are 272 nm for Theophylline and 274 nm for Caffeine. Repeated extractions were done as needed until no peaks were detected. In order to thoroughly determine the necessary timing increments of extraction and rebinding several tests were done. After each two hour extraction, for originally imprinted samples, a UV spectroscopy measurement was completed. The bulk of any imprint removal occurred after the initial two extraction. The second two hour extraction yielded very little extracted imprint and the third extraction yielded no detectable imprint molecule. Several iterations were done in order to confirm this behavior with theophylline-imprinted, caffeine-imprinted and non-imprinted(control) films. Following purging of the imprint molecules the films: (1) Theophylline imprinted, (2) Caffeine imprinted and (3) non-imprinted(control) were subjected to a treatment regime of various concentrations of either theophylline or caffeine. The following molar concentrations of theophylline or caffeine(in dioxane) were used: 0.007, 0.010, 0.014, 0.017, 0.020, and 0.025. The caffeine-, theophylline- and non-imprinted samples were all subjected to a complete treatment cycle of rebinding with both the caffeine and theophylline solutions. Each concentration was prepared in 40 ml aliquots and placed in a 50 ml flat bottom beaker with the selected membrane, theophylline-, caffeine- or non-imprinted, and placed in heated oil bath with continuous stirring at 40°C for two hours.

Following the two hour treatment with the selected concentration the membranes were removed and rinsed with 1.5 ml of dioxane to remove any surface excesses. The membranes were then prepared for extraction by placing in 40 ml clean dioxane in a 50 ml flat bottom beaker for two hours as described earlier. After the two hour extraction

UV absorbance measurements were taken. Two 2-hour extractions were required to remove any imprint and subsequent extractions were done as needed to ensure removal of the imprint. Subsequent concentrations were then used for the treatments until a complete cycle was run. (see next page for experimental schematic) The complete cycle is referred to as a full extraction, two 2-hour extractions, a rebinding(2-hour exposure to solution with selected imprint molecule) and then the subsequent two 2-hour extractions. Concentrations were determined from absorbance peaks. Figure 4.3 shows the raw data UV spectral peak of two extractions of caffeine from a caffeine-imprinted film. Note the first scan indicates a rather notable peak indicating the presence of caffeine. The second scan peak indicates the spectra after the second 2-hour extraction. It is noted that there is no detection of caffeine. This is just a representative sample graph and in some cases where larger amounts of imprint were extracted the second scan would reveal small amounts of imprint removal.

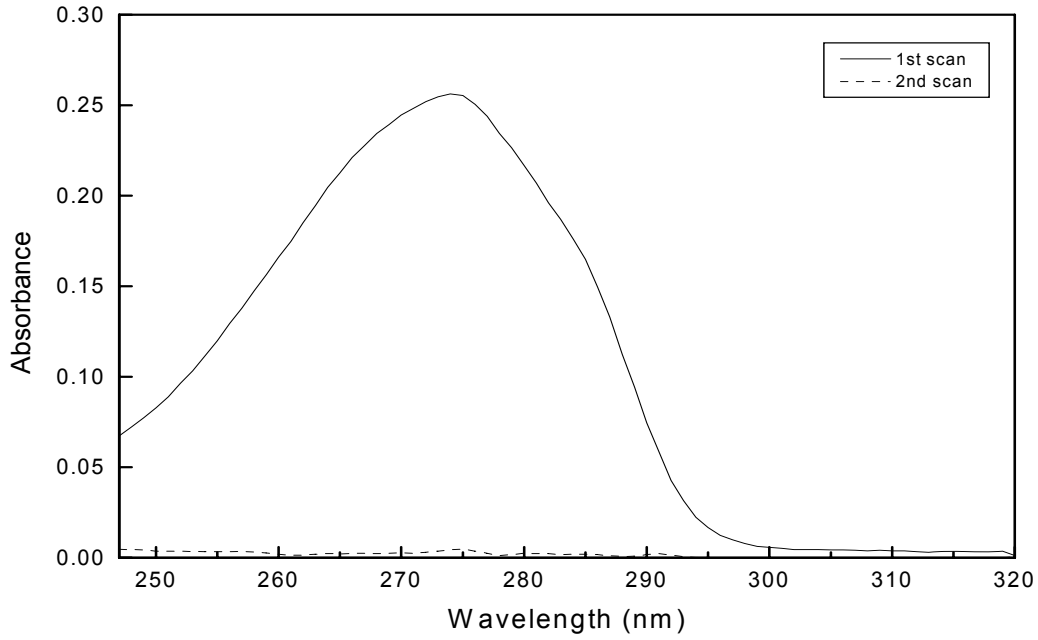

Figure 4.3 UV spectral peaks upon extraction of imprint molecules. (Caffeine peak raw data)

An experimental schematic of the physical processes is shown below. The slides are with the attached polymer films are submerged in chosen solvent. After a given time the slide+film combos are removed and necessary steps are taken.

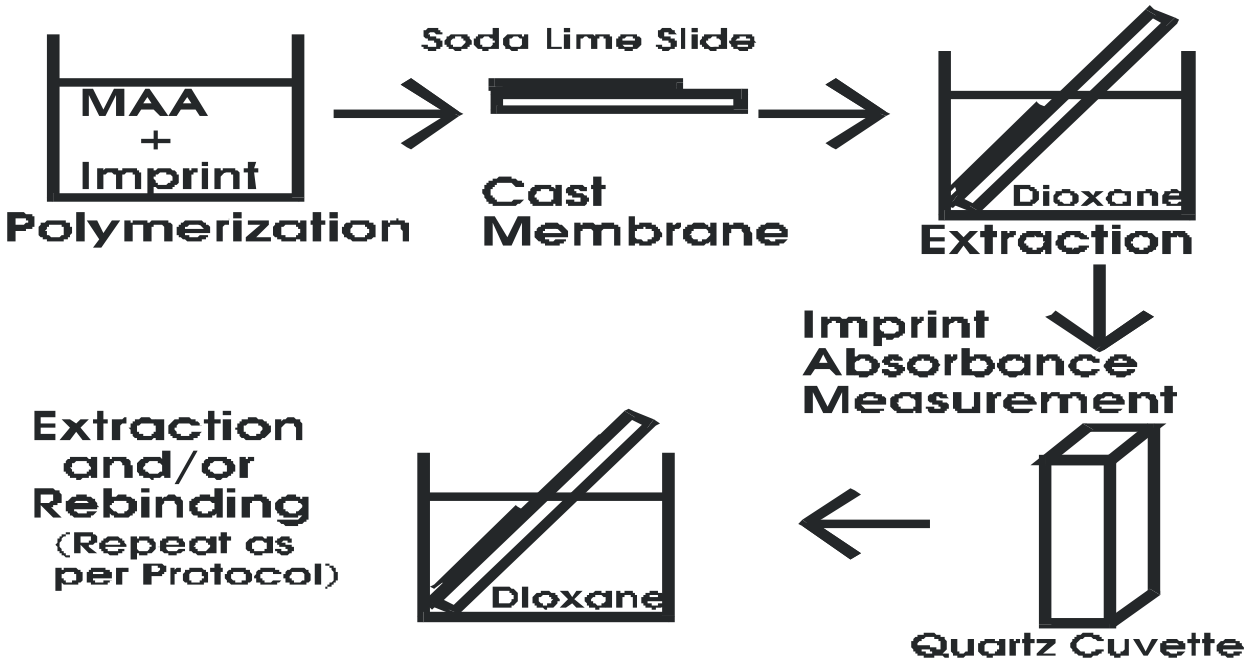

Figure 4.4 The experimental schematic of the molecular imprinting procedure.

4.2 Results and Discussion: Molecular Imprinting

Current progress in molecular imprinting has primarily been dominated by bulk polymerizations in which the particles are ground and treated with solvent in order to extract/rebind the imprint molecules. Here the molecular imprinting phenomenon is illustrated in thin membranes synthesized with methacrylic acid, crosslinked with a silica coupling agent (3-(trimethoxysilyl) propyl methacrylate). The drugs are caffeine, a common stimulant, and theophylline, a bronchodilator, which were chosen as per previous studies[1], as the imprint molecules to be tested in membranes. The two molecules, caffeine and theophylline, are identical except for an additional methyl(CH_3) group on the caffeine. The membranes were imprinted for caffeine and theophylline. Ultraviolet absorption spectra

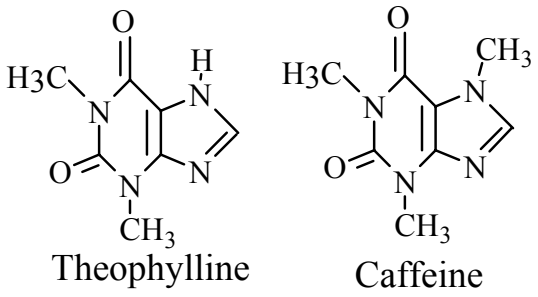

Figure 4.5 The chemical Structures of Theophylline and Caffeine. Note the identical structure except the additional methyl(CH_3) group on the caffeine.

were used to determine presence of the molecules with caffeine absorbing at 274 nm and theophylline at 272 nm[132]. The membranes were purged of any imprint molecules following synthesis and were then cycled through a regime of various treatment concentrations(.007,

.010, .014, .017, 0.02, .025 M either caffeine or theophylline). This was done to test for specific and non specific binding of the molecules in the two types of membranes.

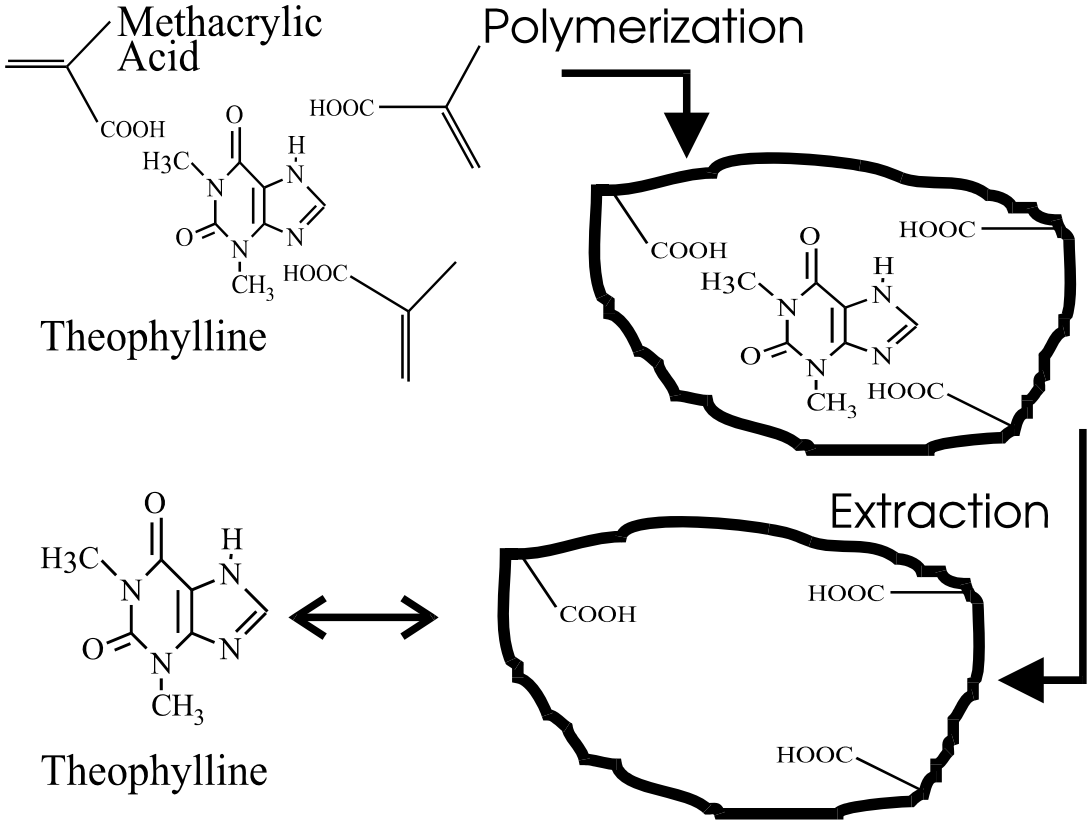

Adapted From Mosbach 1994. Trends in Biochemical Sciences v.19,n0.1

Figure 4.6 The chemistry schematic of molecular imprinting of theophylline and caffeine membranes. This illustrates the interaction between the COOH groups of the host matrix polymer and the imprint molecule.

Solvent extraction of the membranes following rebinding and extraction were tested for absorption spectra of the respective molecules. The results indicated that selectivity is illustrated for the imprint molecules. The two types of membranes, caffeine imprinted and theophylline imprinted, were tested against caffeine and theophylline solutions for rebinding/extraction tests. The caffeine molecule, because of its extra functional group,

is expected to create larger clefts within the host polymer and therefore theophylline uptake within the caffeine imprinted membrane is expected. However, when the theophylline imprinted membranes were tested the binding was strongly favored for the theophylline over the caffeine thus illustrating selective binding.

The imprints were prepared by the copolymerization of methacrylic acid and the silane coupling agent 3-trimethoxysilyl propyl methacrylate in the form of membranes on soda lime microscope slides. The polymerizations were done with imprint molecules of caffeine or theophylline, and control membranes were prepared with no imprint molecule. Each imprinted membrane, and control, was tested against both caffeine and theophylline, separately, to test for selectivity and rebinding capabilities. Theophylline imprinted polymers exhibited greater selectivity for theophylline, as expected, while caffeine membranes showed greater cross reactivity. Control membranes indicated greater uptake of theophylline than caffeine, primarily due to the hydrogen binding abilities of the theophylline molecule.

4.2.1 Binding analysis

Correlations between specific and non-specific binding were made by expressing data as molar uptake ratios of theophylline to caffeine(T/C) in the three types of films. In order to complete a thorough investigation of the quantification of imprint extraction and rebinding a number of samples were tested. The data indicate the results of testing eight different samples of each kind e.g. caffeine-imprinted film, theophylline-imprinted film and non-imprinted(control) film. Each film was subsequently cycled four times each. As

mentioned previously a cycle is a synthesis of a film, extraction of imprint, rebinding of imprint followed by an extraction regime. The data is the result of averaging each of the 32 data points as a whole regardless of what each sample showed. The molar uptake ratios were obtained by analyzing the resulting UV spectroscopic data and incorporating the Beer-Lambert law to calculate resulting imprint concentrations. The Beer-Lambert law is stated as $A=\varepsilon bc$; where A, is the absorbance and in this case is measured by the UV instrument, ε is the molar absorptivity coefficient(wavelength specific), b is the path length(1 cm in this case for standard quartz cuvette), and c is the concentration. In this case the concentration, c, is calculated based on the resulting absorbance measurement. The molar absorptivity coefficients, ε, are as follows, for caffeine the value is 10486 $M^{-1}cm^{-1}$ 274 nm and for theophylline the value of the coefficient is 10450 $M^{-1}cm^{-1}$ at 272 nm[133-135]. Based on these values the resulting concentration of imprint is calculated and subsequent comparisons are made. A sample calculation would proceed as follows. Sample A with caffeine, for example, results in two UV spectra with absorbance measurements of 0.322 and 0.022. Solving for 'c' in the Beer-Lambert Law yields $c=A/\varepsilon b$, where once again, b=1 and hence results in a concentration of $3.1x10^{-5}$ M. This calculation is done for each absorbance value and the resulting concentrations are added to yield a quantity giving a molar concentration value. This resulting value multiplied by the total volume of solvent, 40 ml in each extraction/rebinding, gives a number of moles. Subsequently this can be used either in molar quantities or in numbers of moles to calculate the ratios are mentioned in the results analysis.

The data may be analyzed in several ways and the initial look is to present the data as molar uptake ratios utilizing the previously mentioned calculations involving the Beer-Lambert law. Graphs with molar uptake ratios in caffeine-, theophylline- and non-imprinted films show the variations in the specificity of the films.

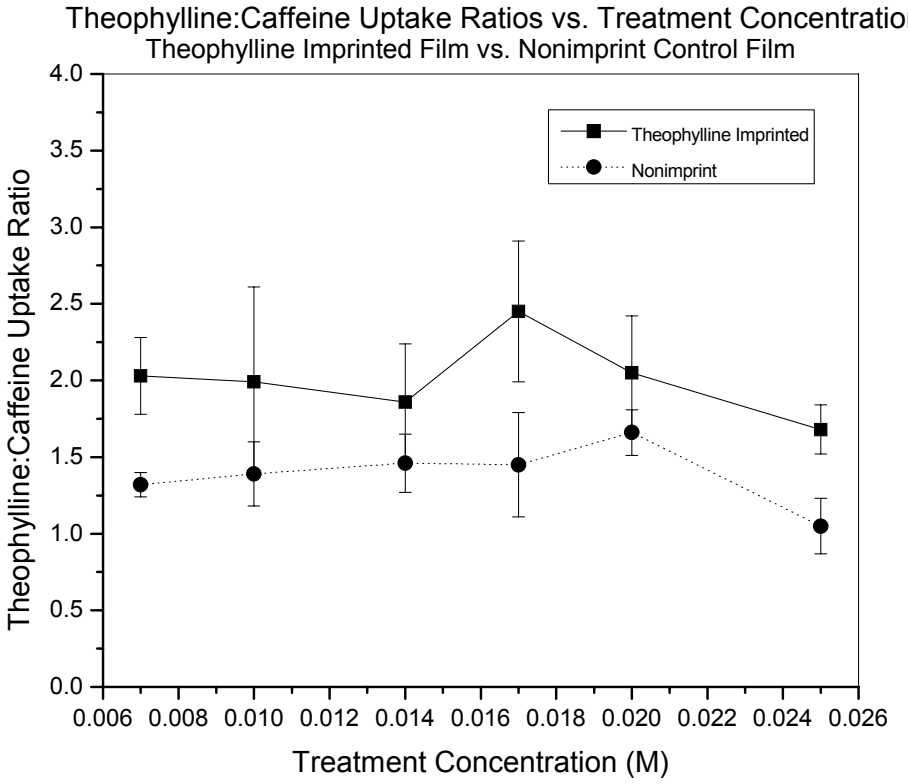

Figure 4.7 Molar uptake ratios of Theophylline:Caffeine in theophylline imprinted films vs. nonimprinted(control) films. A clear preference is indicated in the theophylline imprinted film versus the control film. Indicates a favorable effect by imprinting the polymer.

Figure 4.7 shows that by imprinting the film with theophylline, in this case, that it creates a favorable situation in that theophylline is preferentially rebound as opposed to caffeine.

Although the nonimprint polymer indicates uptake, as is expected, the specificity is increased by imprinting in the polymer.

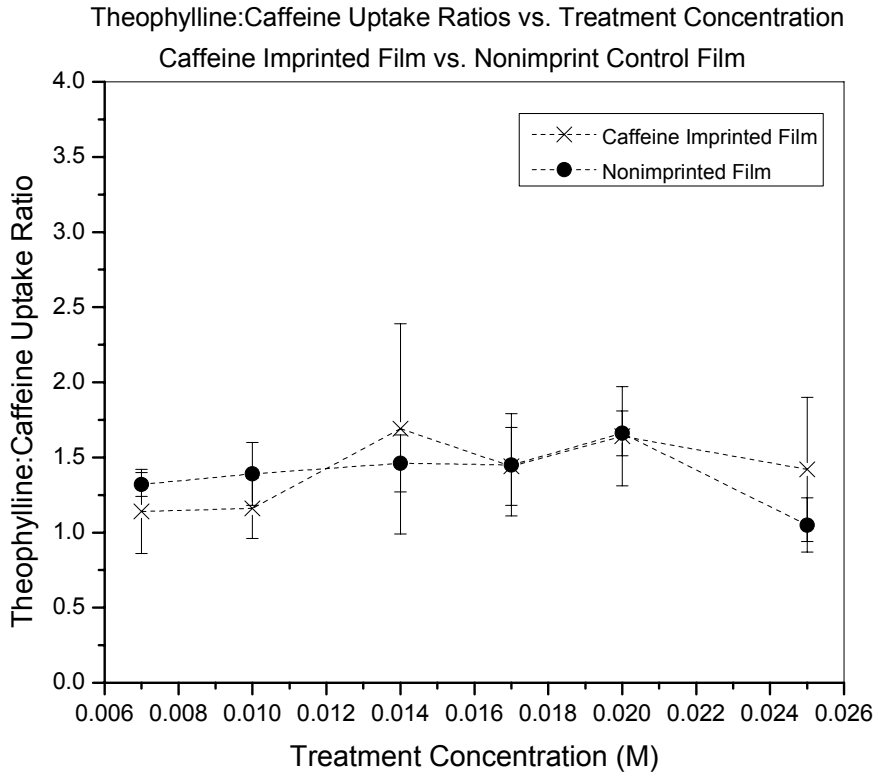

Figure 4.8 Molar uptake ratio of Theophylline:Caffeine in Caffeine imprinted film vs. nonimprinted(control) film. Indicated cross reactivity and no real specificity. Additionally, the magnitude of the ratios is slight smaller than the similar ratio in theophylline imprinted films.

Figure 4.8 illustrates the molar uptake ratio of theophylline:caffeine in the caffeine imprinted films versus the nonimprinted films. As opposed to the previous comparison of theophylline imprinted films there is no clear preferential binding in this situation. Both indicate a greater quantity, as seen by the molar uptake ratio, of theophylline uptake but neither film indicates a preference in terms of more favorable selectivity to theophylline

e.g. both films will rebind theophylline and caffeine but neither shows more specificity. This is essentially what is expected in terms of showing that imprinting induces preferential binding.

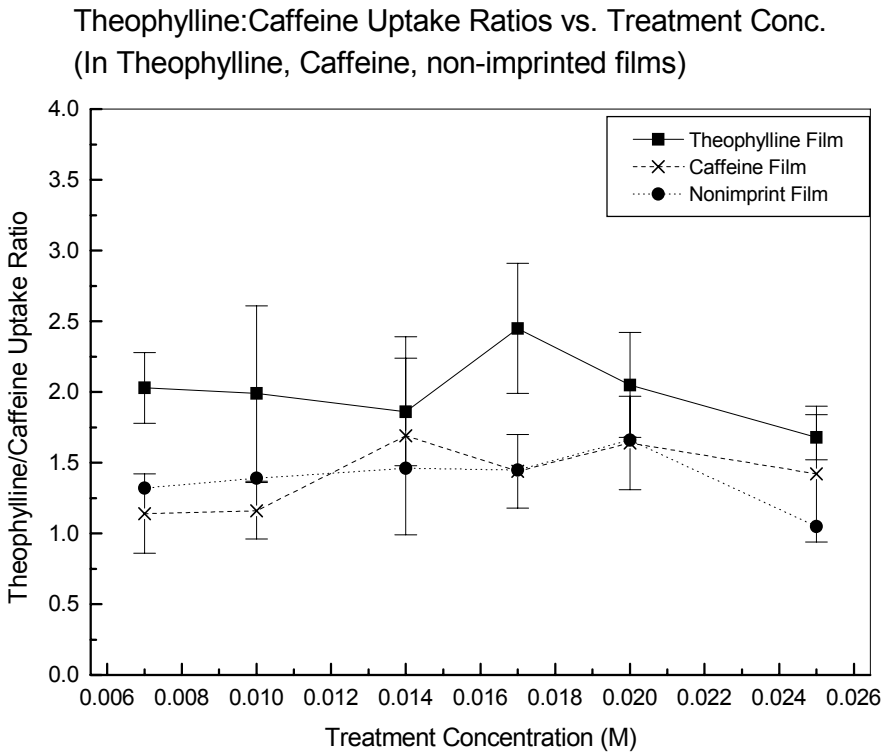

Figure 4.9 Theophylline versus Caffeine uptake Ratio vs. Treatment Concentration (shown for Theophylline-, Caffeine- and non-imprinted films). Notable preference of theophylline uptake versus the caffeine- and non-imprinted films.

Figure 4.9 illustrates the comparative ratios of theophylline:caffeine uptake in the theophylline and caffeine imprinted films, as well as in the non-imprinted(control) films. The data indicate a preferential uptake of theophylline in the treatment concentration regime in all three types of films. Through the whole regime the T/C uptake ratio is

greater than one indicating the greater propensity of theophylline binding primarily due to the structural difference, the H group at the number 7 carbon(theophylline) instead of the CH_3(caffeine), in the two imprint molecules. The T/C ratios in theophylline imprinted films ranged from 1.7 to as high as 2.5 while ratios in caffeine imprinted films ranged from 1.1 to 1.7. The ratios in the nonimprinted films remained in a much narrower range of 1.05 to 1.46. Across the entire regime the theophylline imprinted films indicated an average T:C ratio of 2.01 while the caffeine imprinted films had an average T:C ratio of 1.42 and for nonimprinted films was 1.39.

In addition to analyzing the theophylline:caffeine uptake ratios it is important to analyze the imprinted films from the opposite standpoint of Caffeine:Theophylline uptake ratios to determine if any form of selective binding is introduced by imprinting.

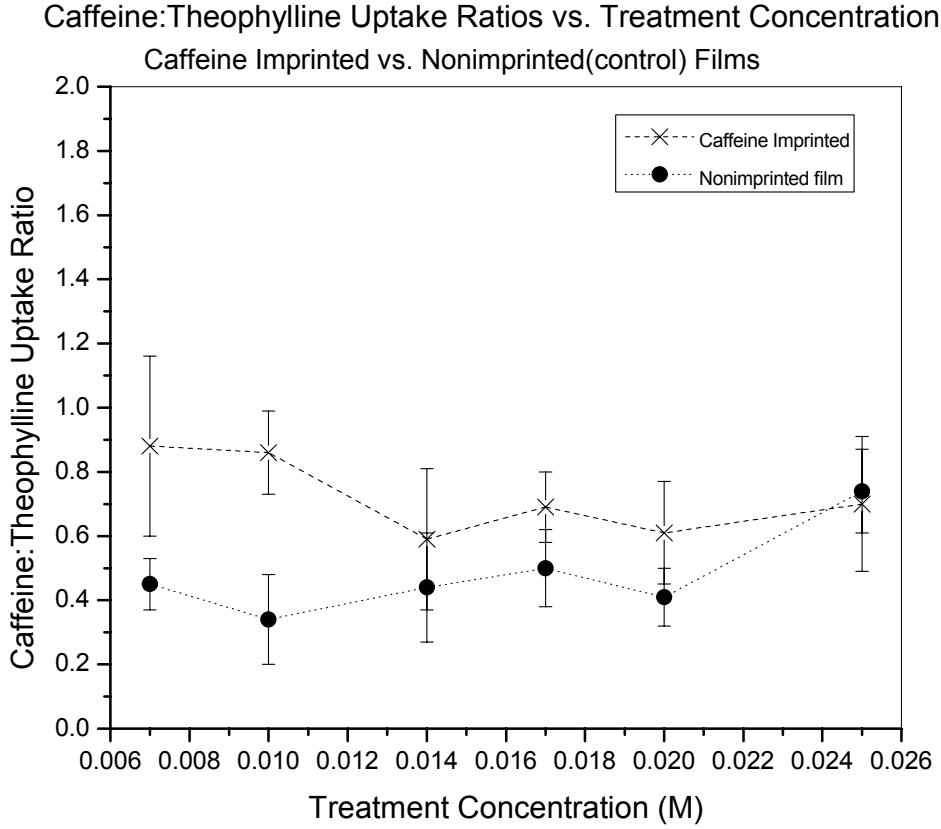

Figure 4.10 Caffeine:Theophylline molar uptake ratio in caffeine-imprinted film vs. nonimprinted(control) film.

The data in figure 4.10 show the caffeine:theophylline molar uptake ratio in caffeine imprinted versus nonimprinted polymer films. The ratios show some favorable binding in the caffeine imprinted film versus the nonimprinted film. Some effects of imprinting, and hence a form of induced specificity are present. However, it is important to note that even for the caffeine imprinted films the molar uptake ratios of caffeine:theophylline are less than 1. This indicates, as is extrapolated from the previous theophylline:caffeine uptake

ratio data, that there is some imprinting effect but theophylline is more readily bound to the polymers than caffeine(this is discussed in this chapter).

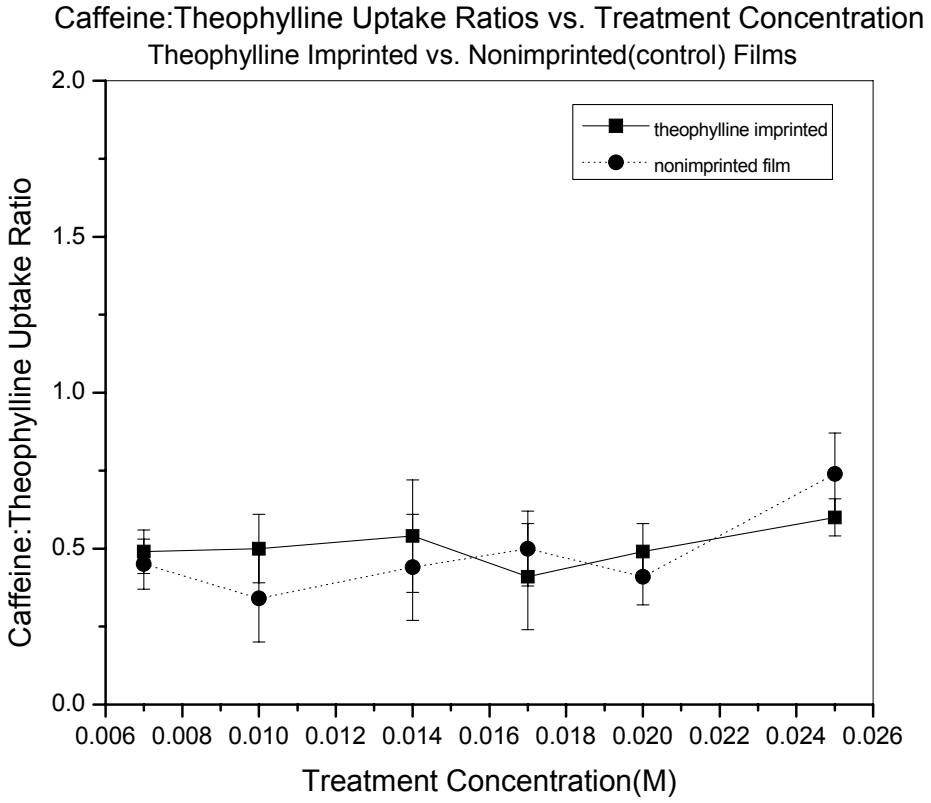

Figure 4.11 Caffeine:Theophylline molar uptake ratios for theophylline-imprinted films vs. nonimprinted(control) films.

In figure 4.11 the uptake ratios of caffeine:theophylline are shown for theophylline imprinted films versus the nonimprinted control films. In this case there is no readily apparently preference shown. When analyzed within the error limits there is no difference in caffeine:theophylline uptake in theophylline imprinted films versus nonimprinted

films. As mentioned for figure 4.10 it is noteworthy that the uptake ratios are less than 1 and are in the 0.5 range.

In order to get a more thorough comparison it is necessary to look at a graph comparing the caffeine:theophylline uptake ratios for all three films.

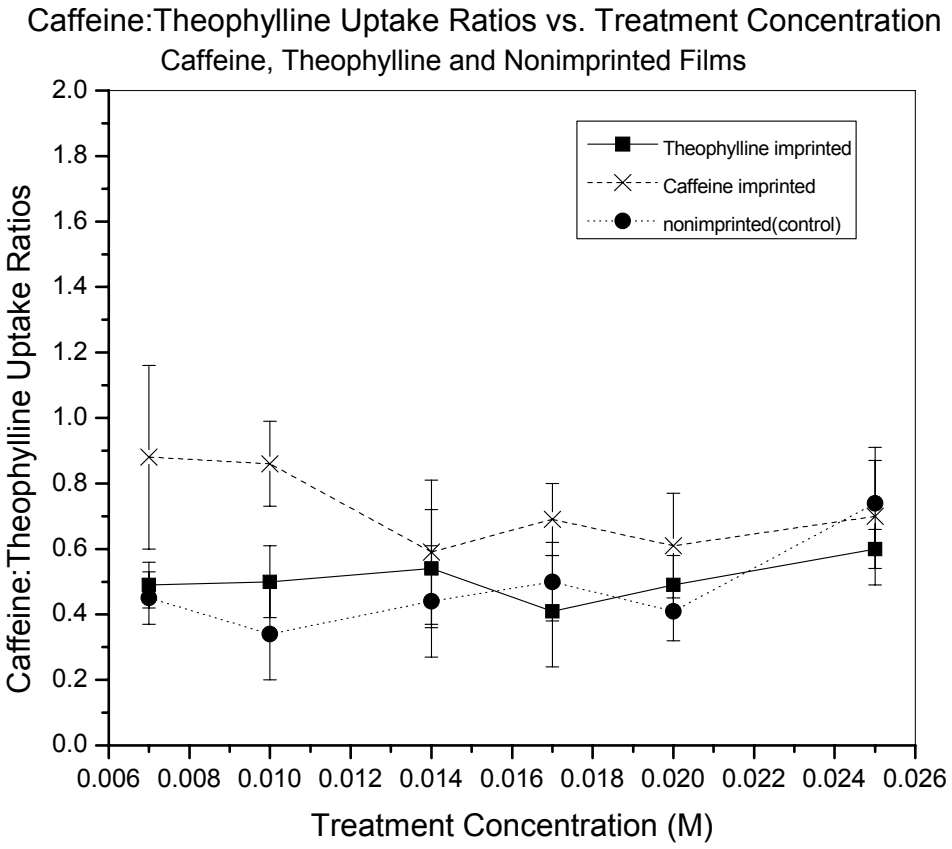

Figure 4.12 Caffeine:theophylline uptake ratios vs. treatment concentration for caffeine-, theophylline- and non-imprinted films.

Figure 4.12 illustrates the comparison of the uptake ratios of caffeine:theophylline for the three types of imprinted films, caffeine-, theophylline- and nonimprinted. The results indicate that the caffeine imprinted films show some favorable binding to caffeine over

the other types of imprinted films. However, as the uptake ratio is less than 1 the preference isn't nearly as significant as the theophylline rebinding preference illustrated in the theophylline:caffeine uptake ratios. This indicates some cross reactivity with the caffeine imprinted films and is explained in part by looking the molar volumes of the two molecules as well as the pKa values and is discussed later in this chapter.

4.2.2 Imprint Removal

In order to illustrate the efficiency of the polymer matrix in binding and removal of the imprint, the data is presented in terms of quantities of imprint in solution upon synthesis of the film, total quantity of imprint removed upon initial extraction steps and quantities of imprint involved in subsequent rebinding and removal steps. It is assumed that the polymerization has gone to completion and that the only loss of mass/volume from the resultant polymer is from the solvent evaporation. The two types of imprinted films were synthesized with 300 μmol imprint per gram of polymer. Subsequent data were expressed in terms of micromoles of imprint per gram of polymer to facilitate comparisons. The quantification of imprint removal/rebinding data in moles or micromoles/gram of polymer has developed as a somewhat standard methodology in molecular imprinting research[1, 9, 45] as a simplified form of comparing different imprinting methodologies and synthesis approaches.

Table 4.1 Site occupation data. Indication of active nos. of sites and theoretical sites.

Imprinted with:	**Imprint in film upon synthesis** μmol/ g polymer	**Total Imprint removed.** μmol/ g polymer	**Percentage of total imprint removed**.(%)
Theophylline	300	104 ± 12	35 ± 4
Caffeine	300	127 ± 14	42 ± 5

Based upon the initial amounts of imprint within the polymer, calculations were made regarding imprint removal. The theophylline imprinted films showed an average removal(Table 4.1) of 104 μmol/g polymer, which translates to 35% of total imprint removal, while the caffeine imprinted films indicated an average removal of 127 μmol/g polymer, or 42% total imprint. These quantities of imprint removal may be interpreted as those sites that are active in the imprinting scheme. Imprint molecules that have not been removed are those that have remained inaccessible within the matrix i.e. within the highly crosslinked portions of the matrix. This may be attributed to the fact that upon removal of templates, in this noncovalent approach, there is relaxation of strain and swelling of the matrix that cause cavities to change shape such that subsequent uptake of the molecules is hindered[56]. Such data provides a reference as to how many of the imprinted sites within the film are viable sites for subsequent rebinding and removal.

4.2.3 Rebinding

Selective rebinding of imprints was done with the concentration range that was previously indicated and is seen in the graphs such as figure 4.11. The uptake of each imprint is determined as follows. Once all the available imprint has been removed the imprinted polymer films are subsequently exposed to the aforementioned concentration regime of either caffeine or theophylline solutions. Then after the rebinding step the imprint molecules are once again extracted in solvent and the UV spectra is taken. Once again utilizing the Beer-Lambert law the resulting concentrations are calculated and expressed as quantity of imprint per gram of polymer. Rebinding data(Table 4.2) were expressed, as above, in terms of micromoles of imprint per gram polymer rebound. Column 2 in the table 4.2 refers to the amount of theophylline uptake by the two types of imprinted films. The theophylline imprinted film had

Table 4.2. Rebinding data for caffeine and theophylline imprinted films.

Imprinted for:	**Uptake of Theophylline** μmol/ g polymer	**Uptake of Caffeine** μmol/ g polymer	**Percentage rebound vs. removed**
Theophylline	21.2±3.2	11.3±1.8	20%
Caffeine	24.2±5.6	21.4±5.6	17%

similar quantities of theophylline uptake as the caffeine imprinted film. This is attributable to the greater hydrogen bonding ability of theophylline over caffeine. In

addition, since the caffeine is slightly larger than the theophylline molecule, certain nonspecificity is expected. Based upon quantities of imprint removed from initial films comparisons are made in terms of participation of sites involving removal and uptake. Theophylline imprinted films on average were able to rebind 21.2 μmol/ g polymer which translates to 20% of the imprint that was removed. Similarly, caffeine imprinted films rebound 21.4 μmol/ g polymer which amounts to 17% of the quantity of imprint that was removed. Further interpretation of the data suggest that up to 11 μmol/ g polymer of sites specific to theophylline are present in the theophylline imprinted films while the caffeine imprinted films show no clear indication of caffeine specific sites.

Further analysis was done with theophylline imprinted films by altering the concentration of the crosslinker upon synthesis. The above films were prepared with molar ratios as follows: monomer:imprint of 22:1 and monomer:crosslinker of 4:1. To determine if increased crosslinker would influence the selectivity the samples were prepared with 1:1 monomer:crosslinker ratio. Results were as follows:

Table 4.3 Comparison of values for crosslink variation in theophylline imprinted films.

Imprinted for: (mol ratio of monomer to crosslinker)	**Uptake of Theophylline** μmol/ g polymer	**Uptake of Caffeine** μmol/ g polymer	**Percentage rebound vs. removed**	**Percentage of total imprint removed**.(%)
Theophylline 4:1	21.2±3.2	11.3±1.8	20%	35 ± 4
Theophylline 1:1	37.6±5.6	24.0±3.7	26%	68±11

Analysis of this data indicate that by keeping the monomer:imprint ratio constant and increasing the monomer:crosslinker ratio(1:1) there was not an increase in the selectivity, the average T:C uptake ratio throughout the concentration regime was determined to be 1.2. The notable differences are that the uptake of theophylline increased to 37.6 μmol/ g polymer while the uptake of caffeine increased to 24 μmol/ g polymer. In addition the participation of active sites increased to 26%, an increase of six percent. Further interpretation of the data indicate that approx. 13 μmol/ g polymer remain selective for theophylline.

4.3 Discussion

The work here illustrates that molecular imprinting can be observed in crosslinked methacrylic acid-(3-(trimethoxysilyl)propyl methacrylate) polymer films.

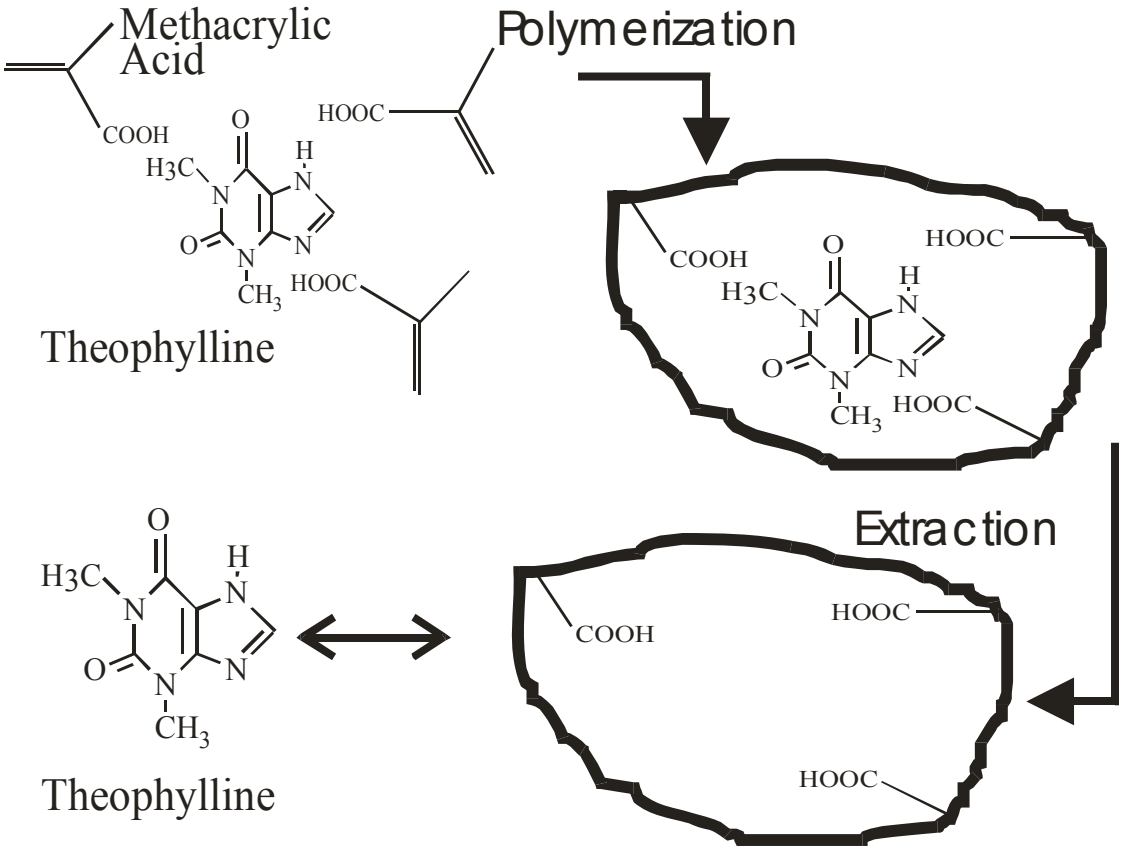

Adapted From Mosbach 1994. Trends in Biochemical Sciences v.19,n0.1

Figure 4.13 The imprinting scheme with methacrylic acid as the host monomer. Theophylline scheme is depicted.

The data indicate that all films were capable of uptake of the imprint molecules. However, the salient is point is that a selective uptake preference was induced into the films by imprinting as observed in the theophylline:caffeine (T:C) uptake ratio. The theophylline imprinted films, though indicating cross reactivity with caffeine molecules, showed a preferential uptake throughout the concentration regime. Meanwhile, the caffeine-imprinted and nonimprinted films showed analogous behavior in terms of selectivity. A slight preference for theophylline over caffeine is observed with no notable difference between caffeine uptake in a caffeine imprinted film vs. the nonimprinted

control film. This may be caused by nonspecific binding throughout the network polymer. Nonspecific binding may be attributed to the geometrical fit between the imprint molecule and the polymer matrix[56, 136]. It is suggested that several types of binding may occur between the two as in figure 4.14. One point binding, in which one functional group of the imprint and matrix interact, provides nonspecific binding but as it is only a single interaction it doesn't allow additional binding/interaction points for the remaining functional groups of the imprint/polymer matrix and hence may be considered non-productive or non-selective binding. In addition the favorable two point binding in which two functional groups between the matrix and imprint interact is labeled as a more productive binding and hence a more selective binding is assumed[56]. Additionally, figure 4.14 illustrates the potential binding configurations and introduces the terminology of continuate and discontinuate words. Figure 4.14(d) shows the most desirable and productive form of binding and likely introduces the best overall selectivity[56]. However, it is difficult to control or to characterize such chain confirmations and hence is provided as a potential guidance for what may be going on within the polymer-imprint entity. Such interactions may account for observed nonspecificity and cross reactivity with each type of film.

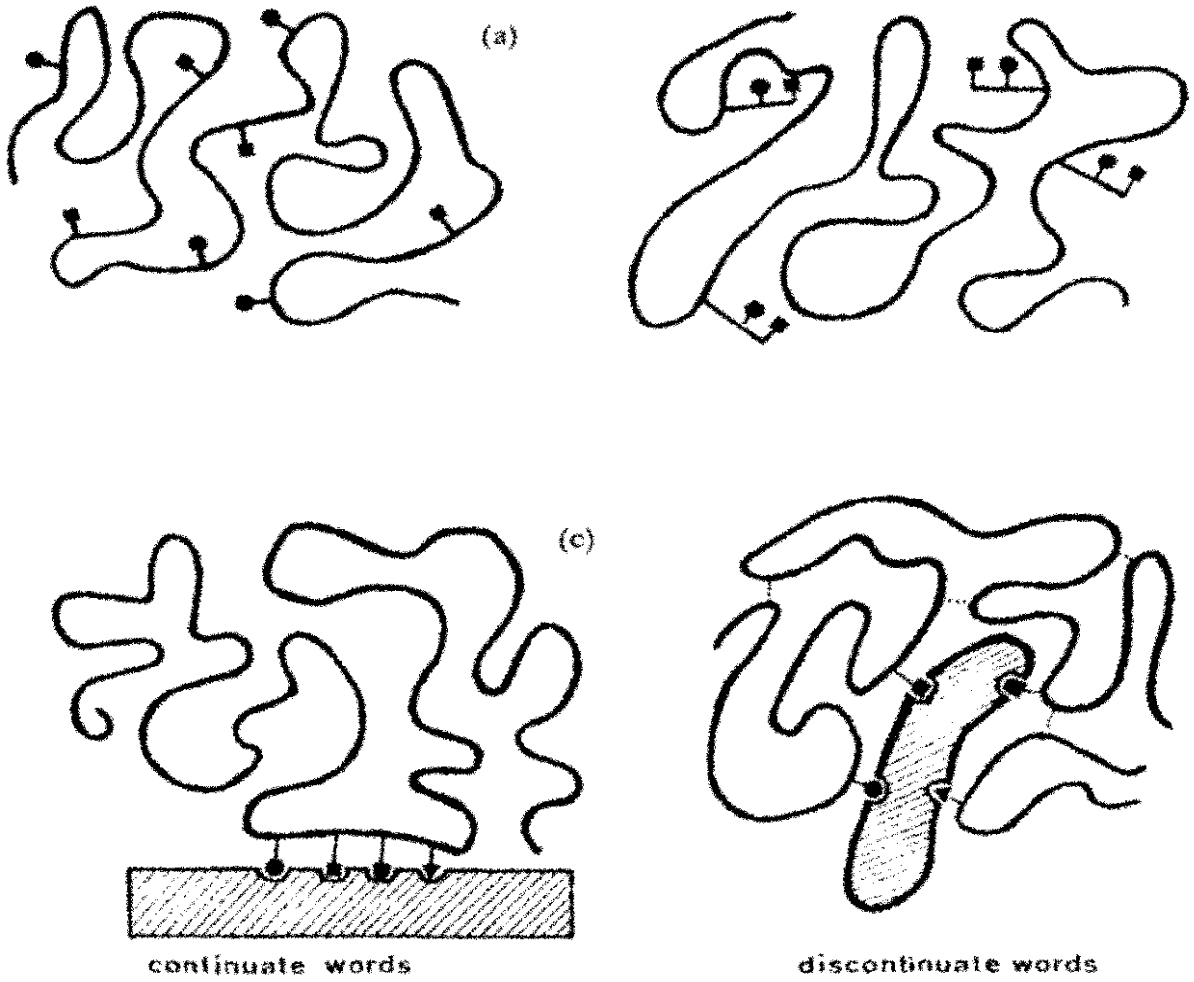

FIGURE 1. Possible arrangements of functional groups in synthetic and natural polymers (Wulff *et al.*, 1

Figure 4.14 Illustration of point binding variations in imprinting. The discontinuate words configuration is most favorable in terms of overall specificity. (from Wulff [19])

Table 4.4 Comparison of uptake amounts, three films, caffeine imprinted, theophylline imprinted and the nonimprinted control sample.

Sample Label	**Moles theophylline uptake (μmols/g polymer)**	**Moles caffeine uptake (μmols/g polymer)**
Theophylline imprinted	21.2±3.2	11.3±1.8
Caffeine imprinted	24.2±5.6	21.4±5.6
Nonimprinted	152.5±13.4	125.6±9.7

Table 4.4 illustrates the quantities of imprint/nonimprint bound to the types of films. The three films represented here were synthesized with identical molar ratios of monomer:crosslinker(4:1) and, in the case of the two imprinted films, with identical monomer:imprint(22:1) molar ratios. The data may suggest the influence of the types of binding mentioned earlier and that imprinting provides chain rearrangements that favor specific binding thus limiting overall quantities of bound molecule.

It has been determined that the molecular imprinting process is reliant on the location of functional groups of the imprint molecule and host polymer but the size of the imprint molecule is also important. The molar volumes of the theophylline(123.7 cc/mol)[137] and caffeine (140-157.8 cc/mol)[138, 139] present notable variation such as to provide cause for the caffeine imprinted films to exhibit greater nonspecific binding that the theophylline imprinted samples. The caffeine molecule is noted to have some variation dependent on temperature[138] but is approximately 15-22% larger(dependent on temperature) than the theophylline and hence the subsequent cavities developed in the

host polymer of the caffeine imprinted polymer may allow for cross reactivity, e.g. the caffeine imprinted polymer exhibiting uptake of theophylline in greater quantities than the theophylline imprinted polymer exhibiting non-specific binding towards caffeine.

There is also some potential concern that the imprint removal and rebinding may be limited to a surface effect where the bulk of the film is not participating in the removal and rebinding cycles. It has been noted that not all of the imprint that is incorporated into the polymer is not removed but in order confirm that it is not only a surface effect a few basic calculations, and general assumptions, will reaffirm that it is a whole bulk-film effect. This is calculated by utilizing such parameters as the density of the imprinted polymer (0.98/cc as calculated by an Archimedes method) , the molar volume of the imprint molecule(Table 4.5), an average film thickness of 15 μm and some simplified approximations and assumptions. In this case a surface effect was assumed as the top 1 μm of the film. To simplify the calculation a 1 μm cube is utilized.

The density of the imprinted polymer of 0.98 g/cc this is converted into $g/\mu m^3$(1 $cc=1x10^{12}$ μm^3) which yields $9.8x10^{-12}$ $g/\mu m^3$. For comparison purposes the quantity of imprint removed/rebound is converted into units of moles/unit volume, more specifically in terms of $\mu mol/\mu m^3$, and compared. The stock solution, e.g. stock imprinted polymer 300 μmol theophylline imprint/g polymer, multiplied by the polymer density, yields $2.49x10^{-10}$ μmol imprint/μm^3 . The amount of theophylline removed was $1.02x10^{-10}$ $\mu mol/\mu m^3$ and the amount of theophylline rebound is calculated/converted to $1.49x10^{-10}$ $\mu mol/\mu m^3$. A critical comparison is done by assuming that a pure theophylline is present in the 1 μm cube to note whether the imprinting removal/rebinding process is

somewhat surface related as opposed to more of the bulk film related. Pure theophylline in a 1 μm cube would yield $8.08x10^{-9}$ μmol/$μm^3$. This was calculated by using the molar volume of theophylline, 123.7 cc/mol, and converting into units of μmol theophylline/$μm^3$. As is expected the pure theophylline approximation yields a large amount of theophylline. This, upon first look, indicates that it is possible that all the interactions were taking place in the surface layers. However, it is important to note the oversimplification of the approximations. The stock imprinted polymer has a density of 0.98 g/cc but upon synthesis, assuming all the solvent is removed (this was confirmed by mass loss measurements after polymer synthesis in film form), the quantity of theophylline(in this case) comprises 2.6 wt% of the whole polymer. It is not possible to pinpoint an exact mapping of the final chain confirmations and additionally the potential conformational changes during extraction of imprint and rebinding of imprint[140]. These calculations may not thoroughly prove that the interactions are not limited to the surface but it is important to note that the selectivity created in imprinted polymers is still valid as is seen from previous data. In order to further analyze the potential of surface versus bulk effects further analysis is required. One potential method is to use optical properties, such as choosing imprint molecules that possess fluorescent properties and tracing them in a fluorescence spectrometer. Further investigation into this is important but the imprinting effect is still illustrated in by the observing the selectivity.

Upon further analysis it is important to note that in addition to the molar volumes of the two molecules an equally significant factor is the associated pKa, or dissociation/ionization constants of the imprint molecules.

Table 4.5 pKa values of Caffeine, Theophylline and Hypoxanthine(core chemical structure class of caffeine and theophylline).

	pKa	Molar Volume (cc/mol)
Caffeine	0.8-3.6	140-155
Theophylline	8-8.7	123.7
Xanthine	6.6	
Hypoxanthine	8.7	

Table 4.5 shows the values of pKa for Caffeine, Theophylline[141] and Hypoxanthine, Xanthine[142]. As is seen from the table the pKa value variation between caffeine and theophylline is significant. The low pKa of caffeine indicates a far more acidic molecule than the theophylline with the high pKa. Since the theophylline is far more of basic molecule it is retained more strongly within the polymer. This mention of the pKa analysis along with the molar volume differences contributes to the variation of the retention of theophylline versus caffeine in the imprinted and non-imprinted polymer membranes.

4.4 Conclusions

Molecular imprinting of crosslinked polymer films has been illustrated. Theophylline imprinted films show preferential uptake for theophylline over caffeine throughout the concentration regime. Caffeine imprinted films indicated slight preferential binding in terms of caffeine:theophylline uptake ratios but as the ratio value was less than 1 it confirms the fact of some cross reactivity and not the overall specificity

as seen in the theophylline imprinted films and the preferred binding of theophylline. It is important to note the imprinting does have an effect in both types of films and can induce some form of specificity as compared to control polymers. Additionally, it is important to take into account the pKa values even when dealing with molecules of highly similar molecular structure. Nonimprinted films showed greater theophylline uptake attributable to the hydrogen bonding issue. Variation of the crosslinker amount in the theophylline imprinted films contributed to greater uptake of theophylline and caffeine but did not contribute to greater overall selectivity.

4.5 Molecular Imprinting Project Summary and Progression

The original intent of the molecular imprinting experimentation was to show the ability to observe an imprinting phenomena in a membrane form as much of the work had been in molecular imprinting of bulk polymers. After showing the conceptual and quantitative proof of molecular imprinting polymer films with organic imprint, or template, molecules the focus was shifted. The new focus of molecular imprinting was geared toward illustration of the memory effect utilizing inorganic crystals such as calcium carbonate and calcium oxalate as the imprint, or template.

The procedure was analogous to the formation of molecular imprinting polymers with organic molecules. During synthesis the calcium oxalate or calcium carbonate was included in the mix of solvent, crosslinker and monomer. The crystals were not soluble in the solvent as the solvent was utilized more as a carrier to allow for some distribution of crystals during polymerization. The temperature schemes and timings of the

polymerization were essentially the same as with the organic molecule imprinted polymers. After the crystal imprinted polymer films were synthesized they were analyzed under both optical and electron microscopy(SEM).

The challenge of crystal imprinting was not in the crystal imprinted polymer synthesis but in the subsequent experimentation. An abundance of crystals were easily apparent both through optical microscopy and SEM. However, the molecular imprinting phenomena is defined by the host polymer developing selective binding areas around the organic imprint molecule and is tested by extracting the imprint molecule and then subjecting the host polymer to a regime which illustrates rebinding. In the case of crystal imprinting the memory effect was to be illustrated via dissolving away the original crystals and then trying to reprecipitate them back into the host/imprinted polymer. This facet of the experimental protocols proved to be exceedingly challenging.

The first step was to be able to dissolve the imprinted crystals. The process was difficult in that proper solvents had to be used in order to remove the crystal and not damage the structural or chemical integrity of the host crystal imprinted polymer. After many iterations it was found that utilizing and EDTA solution was successful in removing the crystals and was assumed that the chemical structural integrity of the host polymer was kept in tact. The films were analyzed primarily by optical microscopy to ensure that all crystals were removed and proved to be successful. The next step was to show that crystals could be reprecipitated under the assumption that the host polymer would exhibit some memory effect towards the location where the crystals were previously located. This is based on the assumption that much like in the organic

molecule imprinting the host polymer chains organized around the crystals and a selective binding site/crystal formation site was left. The goal was to determine if the crystals would reprecipitate with selective locations or just precipitate in any location as per the nature of some heterogeneous nucleation and growth. This step proved to be the most challenging for several reasons. The primary reason is that the ability, or lack thereof, of keeping track of where the original crystals were located. The results proved to be very scattered. In some cases crystals of either calcium carbonate or calcium oxalate were precipitated in control polymer films(films that were synthesized without crystals) and in crystal imprinted polymer films. The salient point was that the crystals precipitated in greater abundance on control films as opposed to the previously crystal imprinted films. The results were highly inconclusive but one interesting question arose, and that was why was there seemed to be an inhibition of crystal growth exhibited by the previously crystal imprinted polymers. Some of the 'theories' of explanation that arose were that for some reason the carboxyl(-COOH) groups may have acted in an inhibitory role.

It was with this information and observation that the true form of crystal imprinting was set aside and the investigation of influence of various organic functionalities on the precipitation of calcium based crystals became the focus. This was a primary reason along with the fact that characterization and analysis of the crystal imprinting process proved to be too difficult with the tools at hand. One of the greatest limitations was the inability to have a noninvasive test method to determine locations of crystals upon imprinted polymer synthesis and removal. The complexities of the crystal

imprinting process lead to the formation of the gel mineralization assays that are described in subsequent chapters. The gel method proved to be very effective in ease of implementation and analysis of results.

5.0 GEL MINERALIZATION PART I: A TEST FOR MINERALIZATION INHIBITION FOR CALCIUM SALTS USING AGAROSE HYDROGELS

5.0 Introduction

The deposition of calcium carbonate from solution is a major problem in water systems. Anionic polymers, such as polyacrylic acid (PAA) and polymethacrylic acid, are used to inhibit the precipitation process. They are believed to do so by binding to the surface of the growing crystal. Proteins with high anionic contents are found in mineralizing biological tissues, such as bone, tooth and shell. In solution, they can act to prevent deposition, to control shape, or to select specific crystal polymorphs, by binding to specific crystal surfaces [143, 144]. When the proteins are bound to a solid substrate, they may also act to nucleate crystals. Polycarboxylates are not the only known inhibitors, various polydentate phosphate species, such as pyrophosphate, are also known to be effective in vitro and important in vivo.

Probably the most elegant method to demonstrate these effects is to monitor the adsorption of the inhibitor to growing crystal surfaces using in situ AFM [145] . More usually, the effect of additives is monitored by following the extent of crystallization in a solution held at constant composition or in solution where one reagent is allowed to slowly increase in concentration.

In previous work, we have reported forming hard bonelike composites by building shapes using agarose gel that is heavily doped with soluble calcium salts [146]. These gels are then mineralized by diffusion from a solution of carbonate or phosphate

and dried to make a stiff material. This approach has now been extended to observe the effect of mineralization inhibitor on precipitation in these gels.

The inhibitor used here is PAA, which has long been known to prevent crystallization of calcium salts [147-149] . There have been many studies on anionic polypeptides, which also inhibit mineralization [150] . Highly anionic proteins extracted from mollusk shell act similarly and are believed to be part of the control mechanism for shell growth. In this study, control tests with acrylic acid AA and EDTA were carried out to eliminate possible effects due to simple chelation of calcium ions or pH changes.

5.1 Experimental Method

Initially, a conceptual approach was taken in order to determine the feasibility of an agarose gel assay for the study of calcium carbonate in gels. If successful, then a more thorough approach would be developed.

A thin layer of calcium-containing agarose is poured into a Petri dish to a thickness of about 1 mm and allowed to cool. A drop of inhibitor is injected into the gel and the whole is then exposed to a mineralizing carbonate solution. Calcium carbonate forms in the gel except where the inhibitor is present. Calcium chloride solution, 0.01 M, was adjusted to pH 10.3. This is heated to 75–80 ºC and 2.5% w/v of agarose is dissolved. The solution was further heated to 85–90 ºC to ensure dissolution of the agarose. The calcium chloride/agarose is poured into Petri dishes and allowed to cool.

The PAA Aldrich, MW 2000 and AA were made up to concentrations of 1%, 0.1% and 0.01%w/v. Ethylenediamine tetracarboxylic acid sodium salt EDTA was made

up to give equivalent concentrations of carboxylate 0.139 M in COOH . These solutions were added into the gel using a syringe with a sharp needle in amounts of 2–4 μl. The drops of modifiers are allowed to soak into the gel. Sodium bicarbonate 0.01 M, pH 10.3 is added in quantities of 5 ml and allowed to spread uniformly over the gel. The samples are allowed to sit at room temperature for 16 h and observed using optical microscopy. The mineralization time was chosen to be several times the characteristic time for diffusion through a 1 mm layer of gel with a diffusion coefficient estimated at about 10^{-6} cm^2/s.

Numbers of crystals were counted at the center of the modifier spot and in unmodified areas of gel and the results expressed in terms of numbers per square millimeter. The boundary between the inhibited and uninhibited regions is quite sharp. The radii of the inhibited regions were measured from the center of the circle to the mid-point of the transition zone, as estimated by eye. These radii and the gel thickness were used to calculate the inhibited volume.

Similar studies were carried out with higher calcium chloride concentrations, up to 1 M. Sodium bicarbonate concentrations were increased to be equal to the calcium concentration

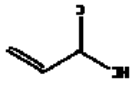

Figure 5.1 Chemical structure of acrylic acid($C_3H_4O_2$) and hence, the monomer unit of polyacrylic acid.

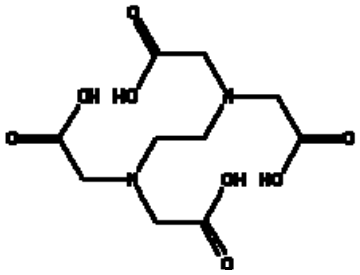

Figure 5.2 Chemical structure of EDTA($C_{10}H_{16}N_2O_8$), Ethylenediaminetetraacetic acid.

5.2 Results

The figure below(Fig. 5.3a and 5.3b) illustrates heavily mineralized layers of gel with clear zones where PAA has been added. The central dark mark is the needle stab.

The following Table 5.1 shows the numbers of crystals found in the inhibited spots and in the surrounding unmodified regions.

Table 5.1 Crystal Counts in gels with polyacrylic acid, acrylic acid and EDTA, respectively.

Sample Label	Count/$mm^{2.}$ Area of injected modifier	Count/mm^2. Unmodified(plain) area
P1 (1% PAA)	6±2	117±8
P2 (0.1% PAA)	8±3	108±9
P3 (0.01 % PAA)	39±4	83±9
A1 (1% AA)	97±9	89±8
A2 (0.1% AA)	86±8	83±12
A3 (0.01% AA)	67±9	75±10
E1 (1% EDTA)	128±15	133±21
E2 (0.1% EDTA)	133±19	139±18
E3 (0.01% EDTA)	125±14	114±15

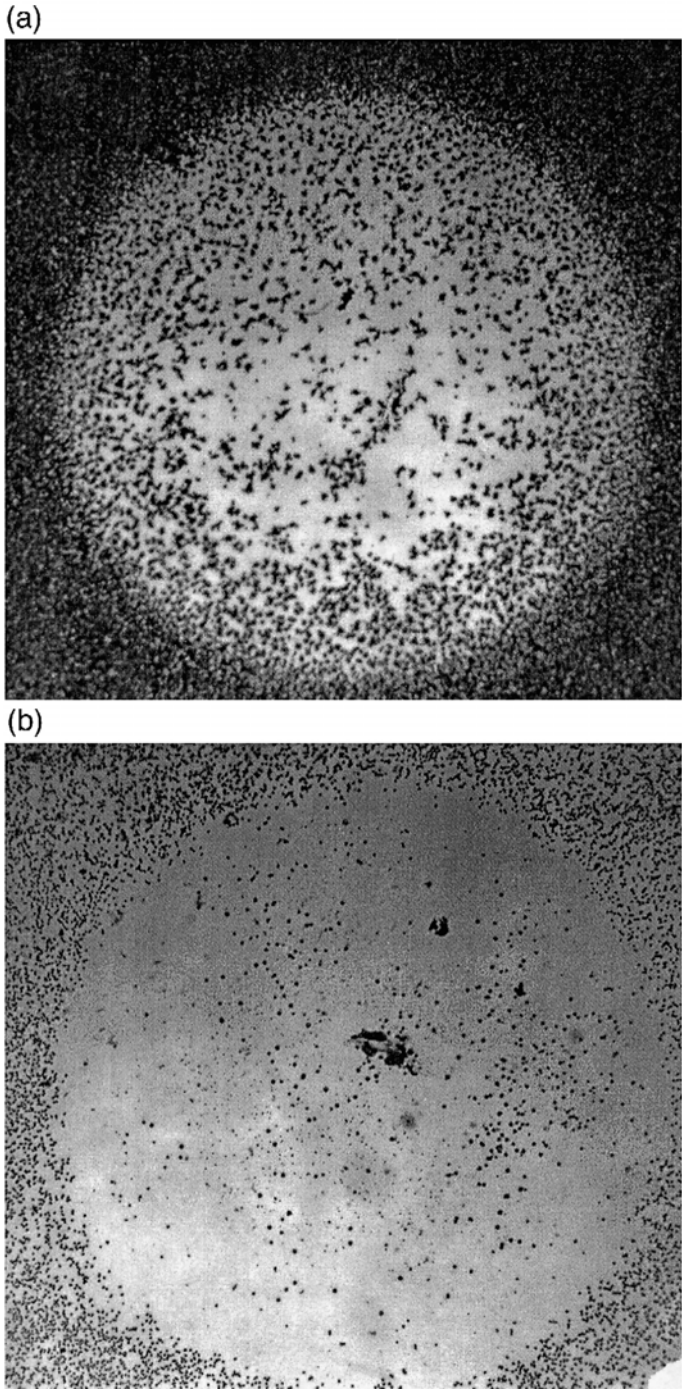

Figure 5.3 (a) Calcium carbonate formed in agarose gel from 0.5 M calcium chloride and sodium bicarbonate. One microliter of 0.1% PAA added at center of ring. Ring diameter is about 5 mm. (b) as in part (a) with 0.075 M calcium chloride and sodium bicarbonate, 4 ml of 0.1% PAA added at center of ring. Magnification as in (a).

It can be seen that EDTA and AA controls have no effect at these concentrations. These small molecules are not effective inhibitors and the concentrations are too low to bind enough calcium ions and reduce the activity significantly. PAA does have a large effect, through its action as a crystal growth inhibitor. Differences in the counts for the unmodified area reflect differences in the thickness of the gel layer.

The absence of inhibition in zones modified by EDTA and AA does suggest that the PAA is acting as an inhibitor in the blank zones and is not just modifying pH or ion concentrations. However, it is possible that the smaller molecules simply diffuse faster to reach a lower effective concentration in the gel. This could be due either to the larger size of the PAA or to its tendency to be crosslinked by calcium into gel particles.

The area of agarose gel, where inhibition by PAA occurred, was measured and converted to a volume on the basis of the measured thickness of the gel. This volume was measured for two inhibitor concentrations, four added volumes of inhibitor and a range of calcium concentrations from 0.01 to 1 M. Table 5.2 shows some of these results and the calculated average COOH/Ca ratio in this volume.

Table 5.2 COOH/Ca Ion Ratios in samples with 0.01 M salts and 0.5 M salts.

Inhibitor Volume, µl	0.01 M Calcium in Gel		0.5 M Calcium in Gel	
	Inhibited Volume (mm^3)	COOH/Ca	Inhibited Volume(mm^3)	COOH/Ca
1	28	0.05	8	0.003
2	59	0.05	26	0.002
4	34	0.16	19	0.006
6	49	0.17	27	0.006

At the highest levels of inhibitor and lowest calcium concentrations, the fraction of bound calcium, assuming every carboxylate binds a cation, can be as large as 50%, but the ratio is 1% or less over much of the range. Hence, there is no reason to assume that the calcium ion activity is significantly reduced by the presence of the inhibitor. It can be seen from Fig. 5.4 that the inhibited volume does increase with the concentration and volume of added

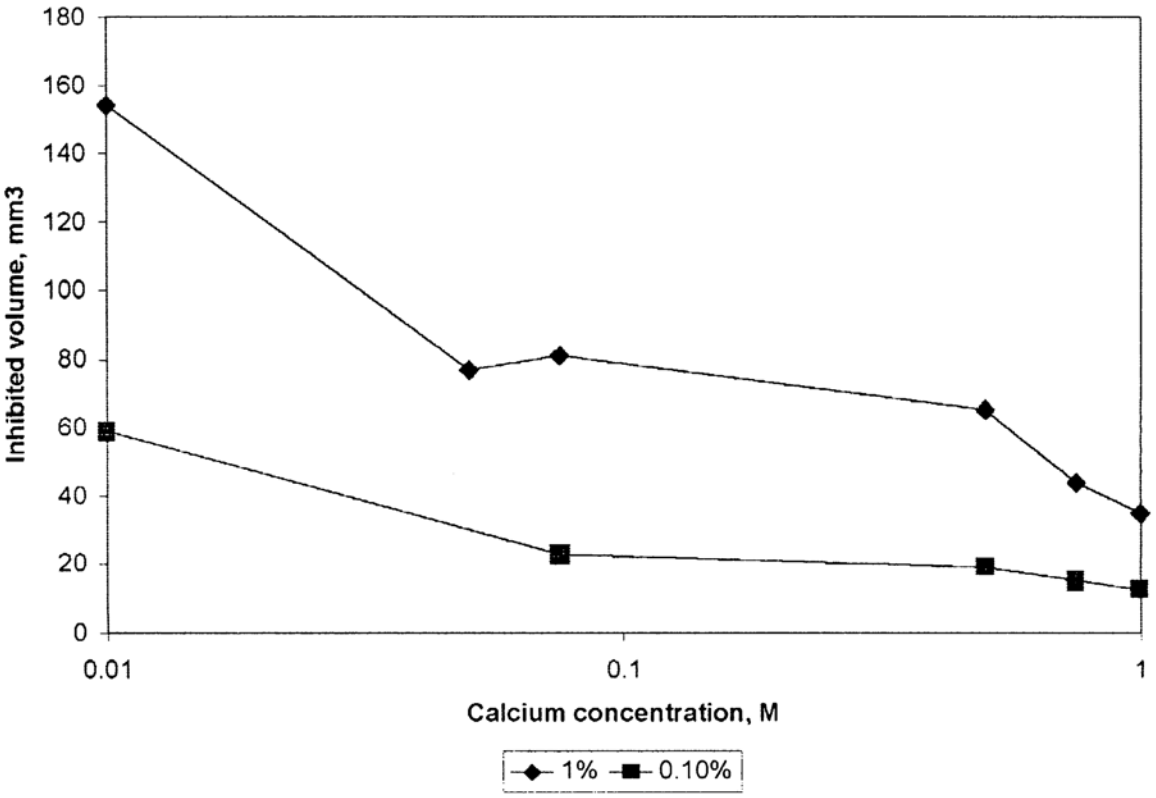

Figure 5.4 Inhibited volume of gel as a function of calcium concentration for two concentrations of added PAA. Two microliters of inhibitor solution added.

inhibitor and does decrease with increasing concentration of calcium in the gel. There is no simple linear relationship between added inhibitor and affected volume. Rather, this

change in affected volume must reflect some combination of diffusion and relative concentration.

5.3 Summary

The gel mineralization method offers a simple way of testing inhibition of crystallization by PAA and could readily be extended to other small molecule inhibitors and to proteins. The volume inhibited is not simply proportional to the volume or concentration of inhibitor added, so more work would be needed to establish a quantitative scale of inhibitor effectiveness. This technique would readily lend itself to screening methods.

6. A TEST FOR MINERALIZATION INHIBITION FOR CALCIUM SALTS PART II: GEL MINERALIZATION PART II

The previous chapter(Chapter 5) introduced the basics of the gel mineralization assay and illustrated a conceptual and somewhat quantitative proof of the feasibility of a gel mineralization approach. At this point a more thorough and systematic methodology was introduced where a more thorough analysis of the previously used molecules is carried out. Additionally, certain parameters are varied.

6.1 General Mineralization Assay Setup

6.1.1 Selected Molecules

As in chapter 5 the molecules to be analyzed here are Polyacrylic Acid(PAA), Acrylic Acid(AA) and Ethylenediamine tetracarboxylic acid sodium salt(EDTA).

6.1.2 Experimental Setup

The agarose gels were formed in circular Petri dishes. In order to develop a somewhat combinatorial/high throughput approach the outside of the Petri dish was marked by dividing the gel into a selected number of divisions ranging from four to eight divisions. The following illustration depicts the markings.

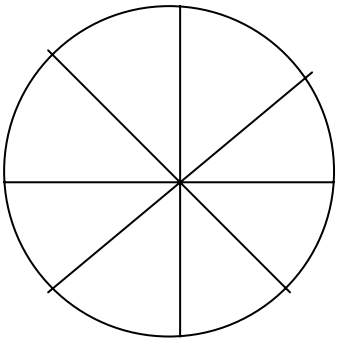

Figure 6.1 The schematic of gel division in Petri dish. The gel, in many cases, was divided into eight equal parts such that various quantities could be used.

As per previously mentioned protocols the gels are deposited within the Petri dish and while the calcium chloride is incorporated upon mixing and heating the agarose.

Initially, water is heated and a select concentration of $CaCl_2$ is added to the water in predetermined molar concentrations. In nearly all subsequent tests the chosen regime is 0.1 M to 1.0 M solutions in increments of 0.1 M. The pH of the solution is adjusted, in this case pH 10.3 by using NaOH. Once the solution is at the desired pH the solution is subsequently heated to approx 85-90 ºC and the agarose powder is added. Once dissolution is ensured the agarose-calcium chloride solution is deposited in the previously marked Petri dishes. The dishes may be labeled after the gel has cooled as the markings are on the underside of the Petri dish bottom.

Once the gels are cooled and gelled the process of injecting the organic molecules is initiated. A microliter syringe is used and previously determined volume quantities are injected into the gel. The primary quantities used in this study are 1, 2, 4 and 6 µl quantities. Once the molecules are absorbed into the gel the next step of adding a 'developing' solution is carried out. Here, the choice of solution is sodium bicarbonate

primarily for its buffering ability in avoiding localized pH fluctuations. This solution is mixed in water and the pH is adjusted to match the pH of the initial $CaCl_2$. Molar concentration e.g. a gel that was synthesized with 0.5 M $CaCl_2$ will be developed with a 0.5 M $NaHCO_3$ solution. The system is then set for predetermined time before analysis is initiated. Usually 12-16 hours after the sodium bicarbonate solution is added.

6.1.3 Data Collection

After the sodium bicarbonate solution is added and allowed to sit the formation of crystals is readily apparent. The surface of the gel and a certain depth are subsequently impregnated with newly formed calcium carbonate crystals.

6.1.3.1 Data Collection: XRD

Prior to a more quantitative analysis of the crystal formation it is necessary to characterize the resulting crystals. Following is the XRD analysis for the crystals harvested from the agarose gels.

Crystals were harvested by allowing the gel to dry slightly and scraping a portion of the surface and a thickness of the gel. The resulting XRD analysis is below.

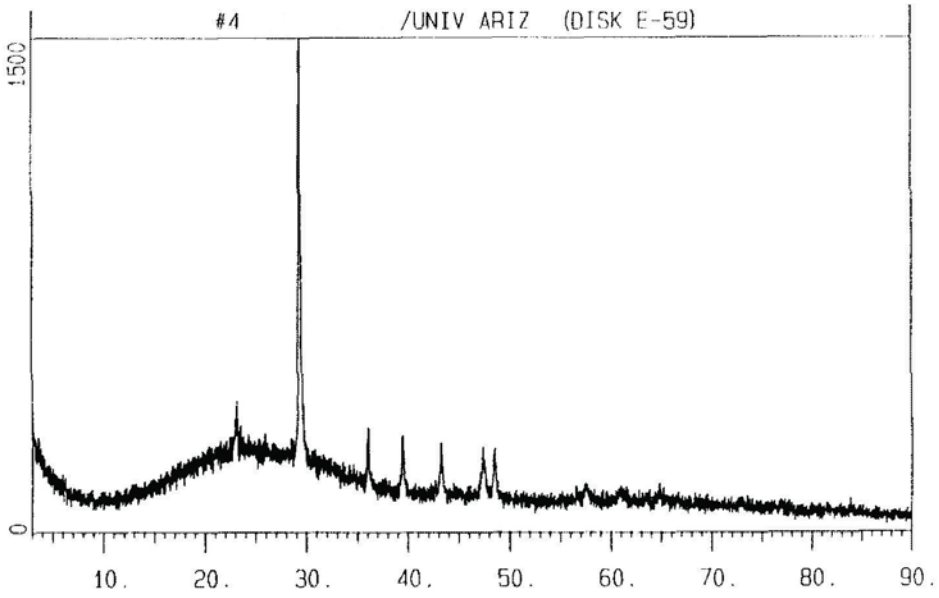

Figure 6.2 XRD spectra of crystals from the agarose gel set up.

The corresponding d space data is as follows and indicates calcite is the mineral in question.

Table 6.1 The d spacing for diffraction pattern of sample versus reference calcite.

2θ	d/A^o	reference calcite d/A^o	
23.02	3.860	3.860	medium
23.94	3.714		
24.48	3.633		
25.04	3.553		
26.56	3.353		
29.36	3.040	3.035	strong
33.70	2.657		
35.80	2.506		
35.98	2.494	2.495	medium
39.36	2.287	2.285	medium
39.54	2.277		
43.14	2.095	2.095	medium
47.18	1.925		
47.48	1.913	1.913	medium
48.48	1.876	1.875	medium

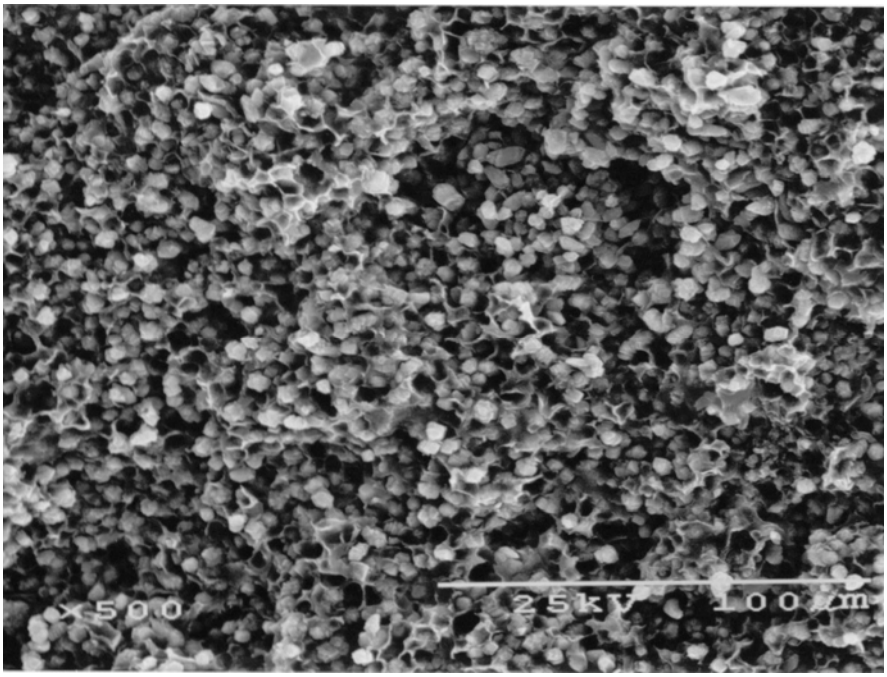

Figure 6.3 SEM micrograph of calcite in agarose gel section

6.1.3.3 Rings of Inhibition Measurement

As was previously mentioned, the gels in which the organic modifier/inhibitor have an effect a ring of inhibition is apparent. Initially the ring diameter is measured and the area of inhibition is measured. After all the diameter measurements were completed the data is then normalized by measuring the depth of penetration of the crystal growth and hence the volume inhibition data is obtained. The inhibition is presented in several forms, including diameter/area of inhibition as well as in volume of inhibition.

6.2 Series 1 Results and Analysis

The first series of data as reported a previous chapter 5 was intended as somewhat of conceptual proof of concept of the gel mineralization assay approach. With that understanding it is important to note that the certain parameters were not taken into account to the fullest context. The rings of inhibition measurements were done with an element of precision in terms of measuring the ring of inhibition that is formed. Following this the area of inhibition is easily obtained and hence is a direct result of a fairly evident measurement. However, the volume measurements are made based on the depth of penetration of the crystal formation. Within the given time constraints allowing for diffusion of the precipitating salts the depths vary throughout the gel. This issue was evident in both the Series 1 and is also evident in Series 2(to be illustrated and discussed in Chapter 7). However, that being said, it is always possible to derive some form of trend in most experiments. The following pages illustrate the data that were collected and calculated for the Series 1 of the gel mineralization assay. Some general trends are

apparent. It is also worth noting that in the first series a somewhat arbitrary concentration regime was used, once again as a conceptual illustration of the experimental setup. The salt concentrations used were 0.01, 0.05, 0.075, 0.5, 0.75 and 1.0 M solutions of calcium chloride and subsequently sodium bicarbonate. It is apparent in some of the data that the illustration of inhibition is not well applied in situations of such low concentration. The data appear far more scattered than in the higher concentration regimes.

The Series 1 data was completed with 2.2% agarose gel composition with the indicated calcium chloride, pH 10.3, concentrations included in the gel. The gels are then developed with a correspondingly equal concentration of sodium bicarbonate, pH 10.3. The quantities of inhibitor/modifier are also mentioned. The concentrations of inhibitor are indicated as 1%, 0.1% but this was based more on dispensing equal amounts of COOH groups with each aliquot. The use of 1% and 0.1% is close enough to actual amounts and is also used for ease of illustration and discussion.

It is also noted that initially in Series 1 the primary effect of inhibition is indicated primarily for the polyacrylic acid and not much effect is noted for either acrylic acid or EDTA. It is shown with a little more analysis that this is not apparent throughout. As with experimentation in general, new results often illustrate varying effects, and that is shown more so in Series 2.

The graphs below show the data that was plotted in several forms in order to attempt to detect a trend in terms of the potential impacting factors. Several trends are intuitive in terms of adding more inhibitor will usually increase the amount of inhibited area and volume. Other trends are not readily indicative in this series. A large number of

graphs are shown here and in the subsequent chapters. This is to show the thorough nature of data collection but also the consistency in being unable to spot highly noticeable trends. Error bars are not included for clarity sake. In this chapter the number of samples utilized per data point was limited to 3-4 measurements per point. In subsequent series a more thorough approach of 8-10 measurements per data point was used.

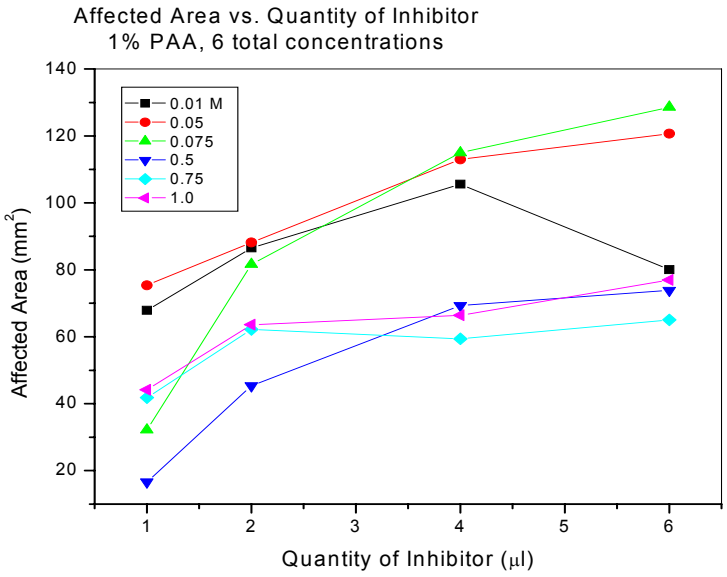

Figure 6.4 Affected area(mm^2) of gel vs. quantity of inhibitor injected for 1% PAA at six different concentrations.

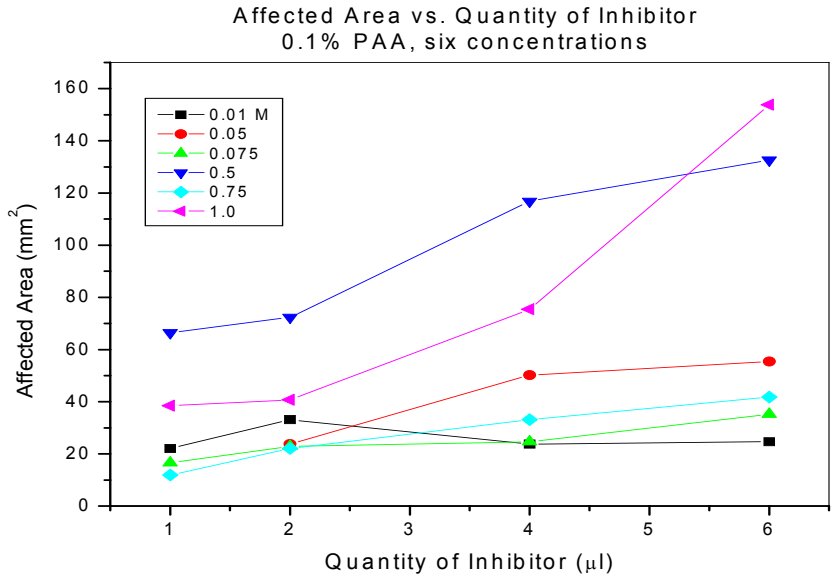

Figure 6.5 Affected area(mm^2) vs. quantity of inhibitor for 0.1% PAA at six different concentrations.

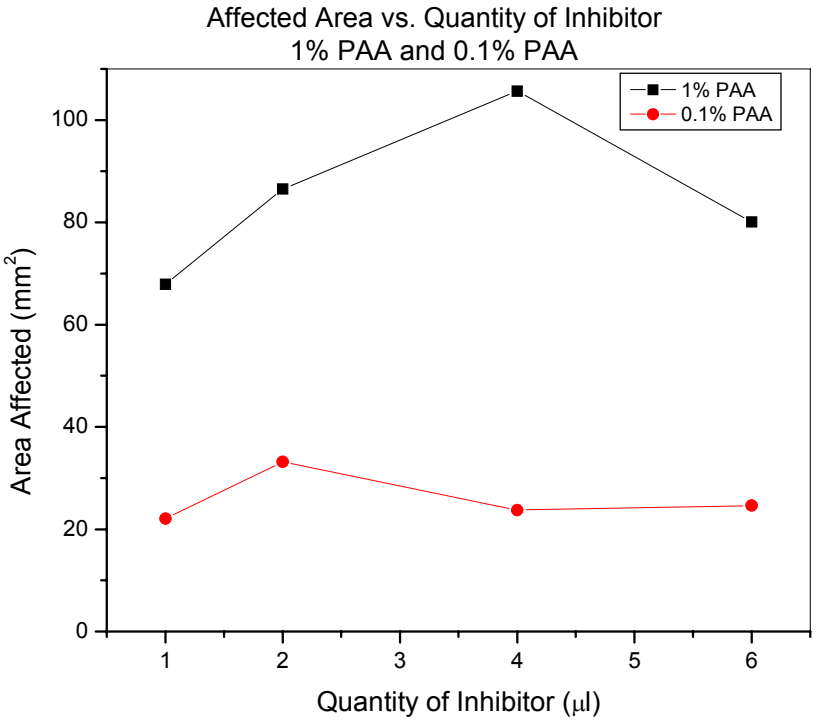

Figure 6.6 Affected area(mm^2) of gel vs. quantity of inhibitor. Plots are for 1% PAA injections and 0.1% PAA injections.

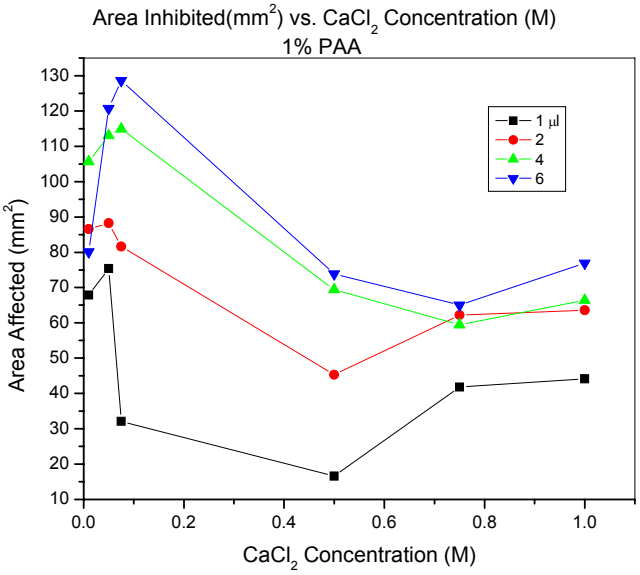

Figure 6.7 Area inhibited/affected(mm^2) vs. the calcium chloride concentration(M) for 1% PAA at 1,2,4,6 µl quantities. Data is from low calcium chloride concentration and a higher concentration regime, with a gap in concentration progression.

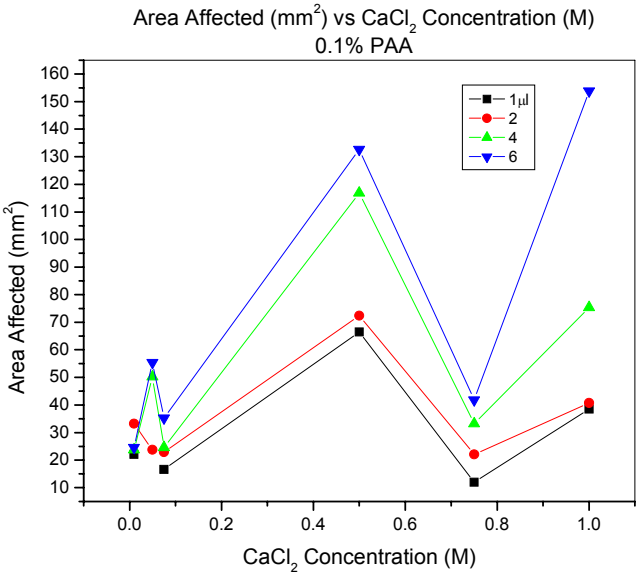

Figure 6.8 Area inhibited/affected(mm^2) vs. calcium chloride concentration(M) within gel for 0.1% PAA at 1,2,4,6 µl quantities. Note inconsistencies inhibition versus the Calcium chloride concentration.

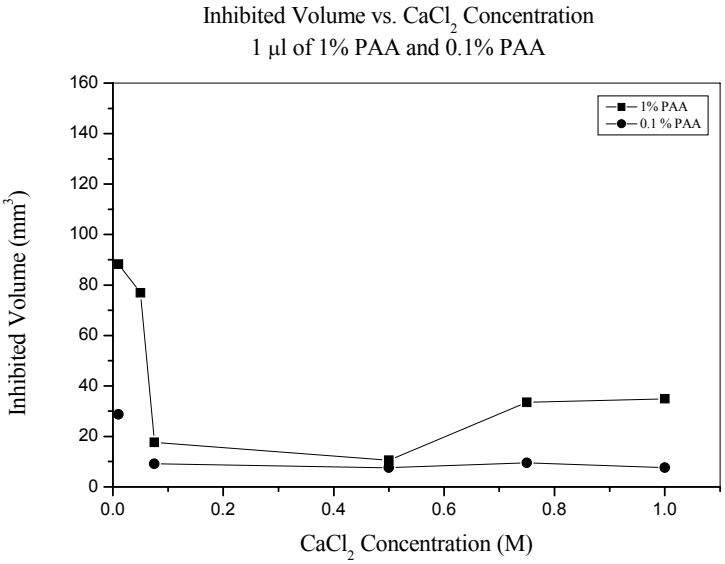

Figure 6.9 Inhibited volume of gel(mm^3) vs. calcium concentration (M). 1 µl each of 1% PAA and 0.1% PAA was injected. Note some consistency with 1% PAA showing greater overall effect than 0.1% PAA.

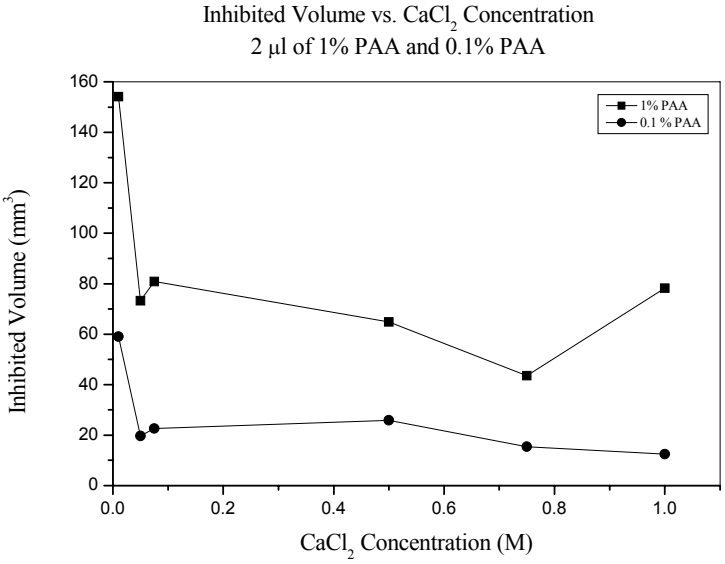

Figure 6.10 Inhibited volume of gel(mm^3) vs. calcium chloride concentration(M). 2 µl each of 1% PAA and 0.1% PAA was injected.

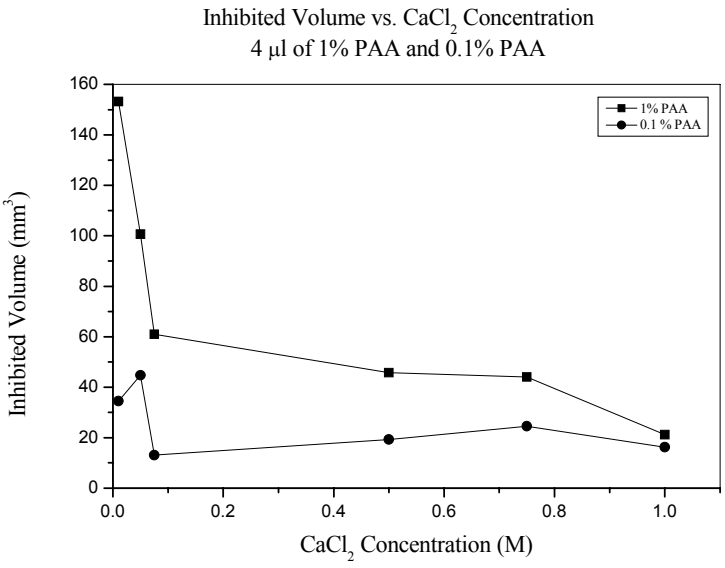

Figure 6.11 Inhibited volume(mm^3) vs. calcium chloride(M). 4 µl each of 1% PAA or 0.1% PAA into the gel before measurements were made.

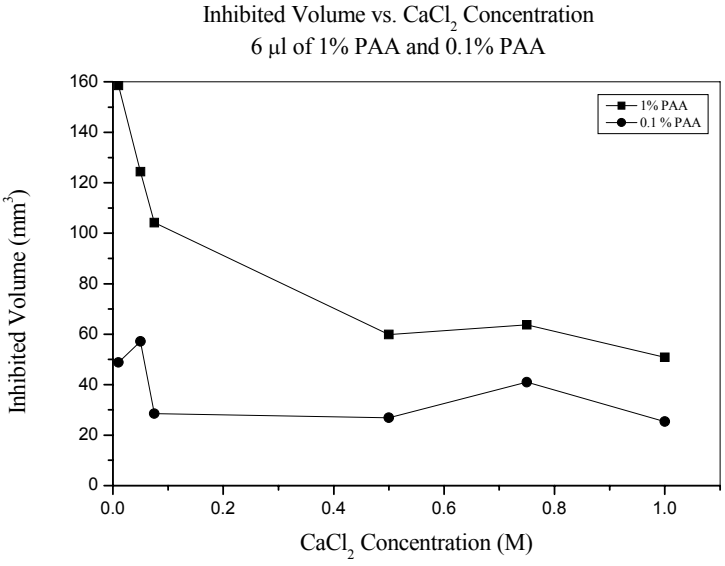

Figure 6.12 Inhibited volume(mm^3) vs. calcium chloride concentration(M). Data at 4 µl injection quantities of 1% PAA and 0.1% PAA. Note that at 6 µl the data is more consistent that at the lower injection quantities, especially at higher Calcium Chloride concentrations.

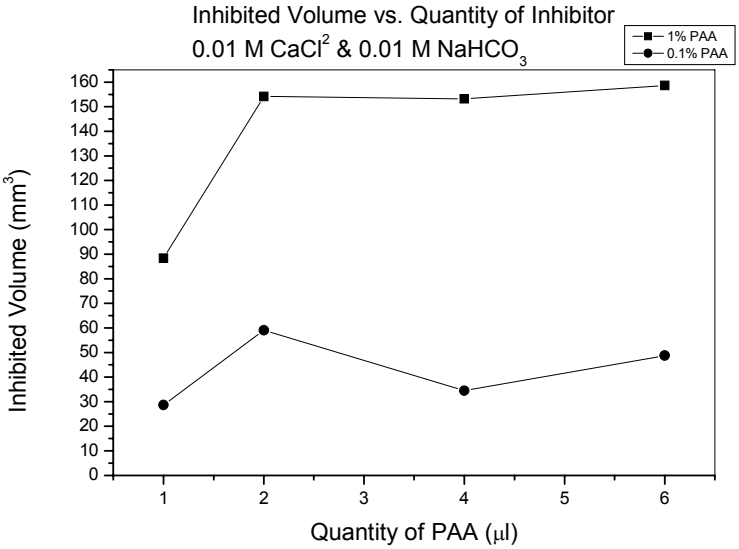

Figure 6.13 Inhibited volume (mm^3) vs. quantity of inhibitor(1,2,4,6 µl). At concentrations of 0.1 M calcium chloride/sodium bicarbonate. 1% PAA and 0.1% PAA data is shown.

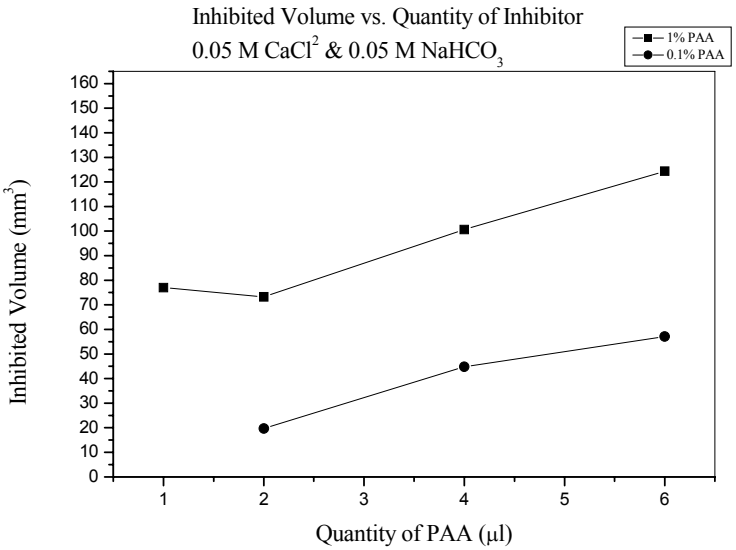

Figure 6.14 Inhibited volume (mm^3) vs. quantity of inhibitor(1,2,4,6 µl). 0.05 M concentration point of calcium chloride/sodium bicarbonate. 1% PAA and 0.1% PAA injection quantities are shown.

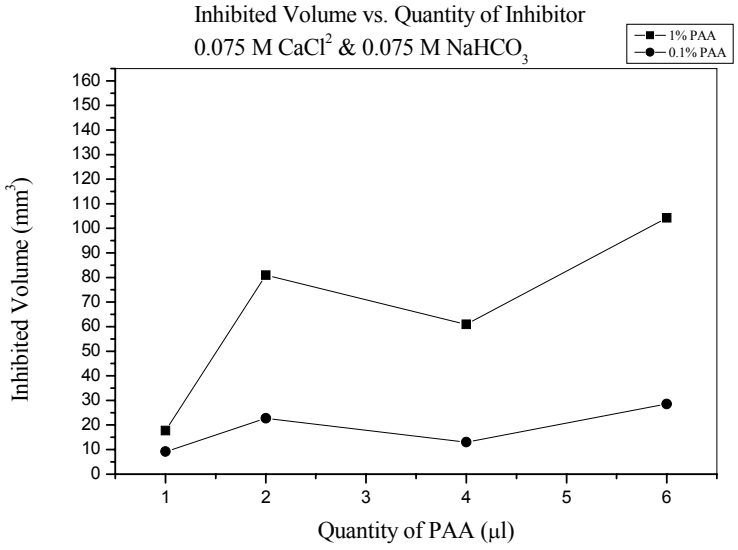

Figure 6.15 Inhibited volume (mm^3) vs. quantity of inhibitor(1,2,4,6 µl). The results are for 0.075 M calcium chloride and sodium bicarbonate. 1% PAA and 0.1% PAA injection quantities are shown.

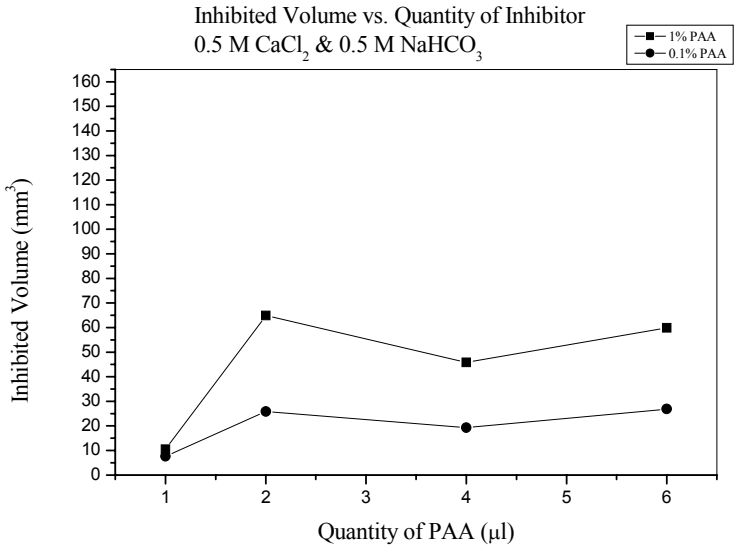

Figure 6.16 Inhibited volume(mm^3) vs. quantity of inhibitor for 0.5 M calcium chloride/sodium bicarbonate gels. The following injection quantities (1,2,4,6 µl) were utilized. The regime shows the results for 1% PAA and 0.1% PAA additives.

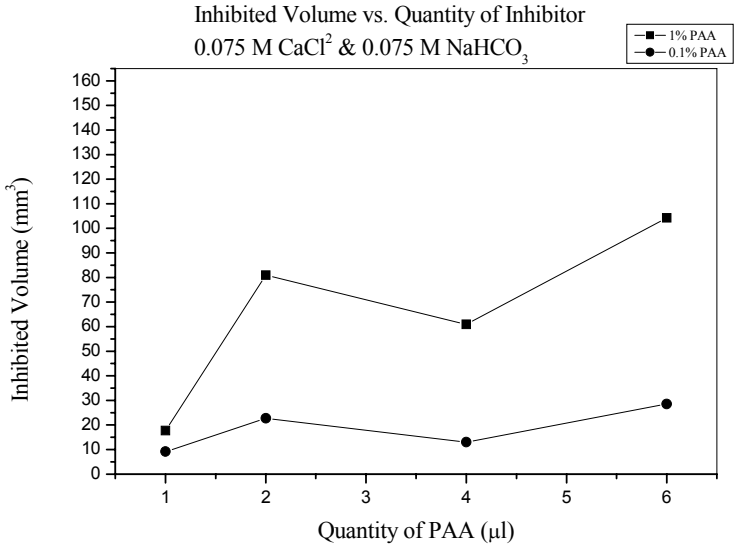

Figure 6.17 Inhibited volume(mm^2) vs. quantity of inhibitor for 0.075 M calcium chloride/sodium bicarbonate at the following injection quantities(1,2,4,6 µl). 1% PAA and 0.1% PAA data is shown. Note an overall general consistency, as expected, of 1% PAA increased effect over the 0.1% PAA.

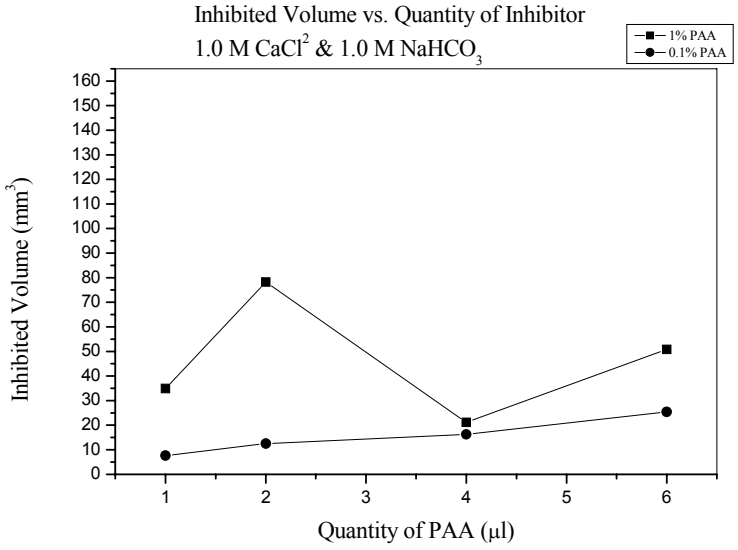

Figure 6.18 Inhibited volume (mm^3) vs. quantity of inhibitor for 1.0 M calcium chloride/sodium bicarbonate gels. Data is show for the 1%PAA and 0.1% PAA injections into the gel at the following quantities(1,2,4,6 µl).

6.3 Discussion and Conclusions

This chapter provided a more thorough analysis of the data presented in Chapter 5. The results of Chapter 5 are confirmed; however it is apparent that a more systematic approach to inhibitor concentrations is required to pinpoint general trends of the observed phenomena. The gel mineralization approach is confirmed to be a viable approach to studying effects of organic molecules on formation of calcium carbonates but a somewhat specific quantitative result is still desired. In order to facilitate comparisons the data sets of Chapter 5 and Chapter 6 are referred to as Series 1.

7.0 GEL MINERALIZATION: SERIES 2 MINERALIZATION DATA

This chapter presents a more thorough approach to the gel mineralization data of the previous chapters. This set of experiments was labeled as Series 2 for a more simplified way of reference. A concentration regime of precipitating salts was chosen in equal increments from 0.1 M to 1.0 M of calcium chloride and sodium bicarbonate. The pH is 10.3 and the agarose gel concentration is 2.2%(these conditions are identical to what was used in the work represented in previous chapters). In this series it is apparent that the chosen inhibitors/modifiers exhibit an inhibitory effect. However, at one concentration regime of 0.1 M the data were not consistent in terms of showing an apparent effect. This is somewhat consistent with what was indicated in Series 1.

Additional importance was given to determining depth of penetration of precipitates. The penetration depths were measure in several places throughout the gels. It is noted that the penetration depths were measured in purely uninhibited areas. The nature of setting up the gel assay in Petri dishes readily lends itself to large areas of testing as well as maintaining control sample areas. Additionally, several control plates were also developed in order to ensure no diffusional contamination and then subsequently measuring the depths of penetration. These measured depths were well matched to those measurements in the active Petri dishes. It is also noted that even in control plates there were indications of inconsistent penetration depths. These values were averaged and then used to determine inhibited volume.

The data are plotted out much like in Series 1 with the understanding that Series 2 was developed to provide a more thorough analysis of the gel mineralization assay. The

primary goal was to determine the feasibility of using this as a screening methodology. That has been illustrated in Series 1, albeit mildly. In Series 2 the experimentation was far more meticulous with a goal of furthering accuracy of the gel mineralization assay. An additional goal was to provide some form of consistent quantifiable data for use in a wider range of applications instead of as a screening only method.

The data are presented in order of first showing effects of the Polyacrylic acid molecule, followed by acrylic acid and finally EDTA all were set for equimolar concentration equivalents of COOH ions of 0.139 M. The affected area vs. quantity of inhibitor are shown, followed by affected area vs. salt concentrations(0.1 -1.0M) , then inhibited volume vs. quantity of inhibitor, which is followed by inhibited volume vs. salt concentration. After presenting data sets for each modifier/inhibitor additional data is included for comparing various aspects of all the inhibitors against quantities of inhibitor, concentrations and leads to a more in depth study of attempts to quantify COOH/Ca ion ratios. As all these three molecules provide COOH groups in varying confirmations it is relevant to provide some analysis. An additional goal of this series of measurements was to attempt to develop some other form of model for the behavior. However, as is indicated in the graphs it is difficult to determine any wholly consistent patterns. As mentioned in previous chapters the error bars are not indicated in the graphs to ease clarity of reading. Although intuitive trends are not readily apparent the data was quite consistent in terms of repeatability as each data point is a representation of 8-10 individual ring measurements. For ease or readability the error bars are not shown.

7. 1 Polyacrylic Acid Series

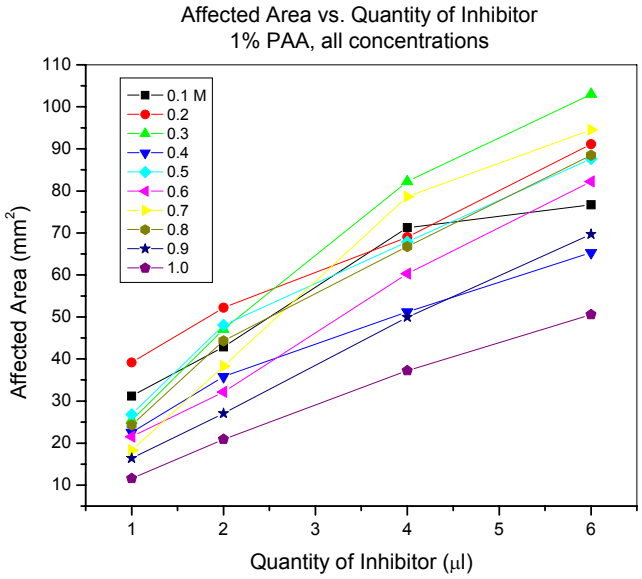

Figure 7.1 Affected area (mm^2) vs. quantity of inhibitor(1,2,4,6 µl). The concentration range is 0.1 M to 1.0 M calcium chloride/sodium bicarbonate gels. 1% PAA additive/inhibitor. Note consistent increases of affected area with increased quantity of inhibitor injection. However, some anomalous behavior at the 0.3 M concentration point.

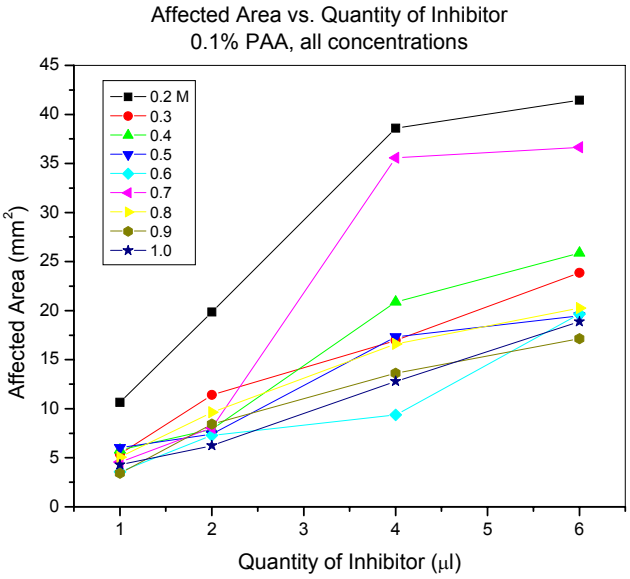

Figure 7.2 Affected area (mm^2) vs. quantity of inhibitor (1,2,4,6 µl) for 0.1 % PAA. Corresponding salt concentrations of calcium chloride/sodium bicarbonate ranges from 0.1M to 1.0M. It is seen here that 0.2 M concentrations result in greatest area of inhibition. With 1%PAA the 0.3 M concentration point showed greatest affected area.

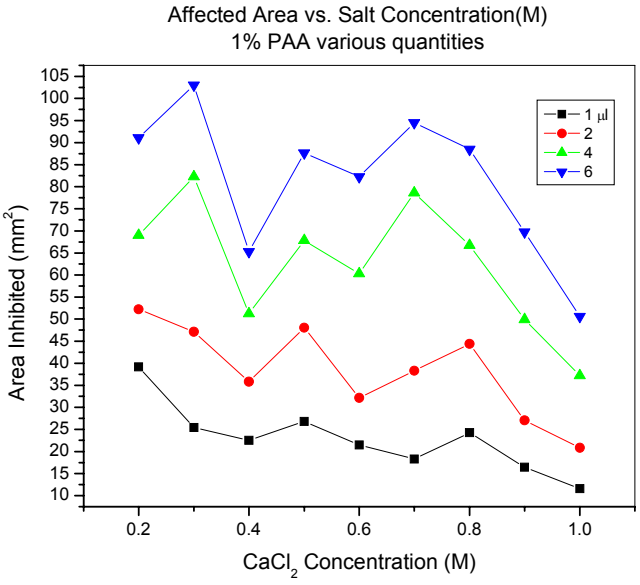

Figure 7.3 Affected area(mm^2) of gel vs. the salt concentrations(M). Presented at the various injection quantities (1,2,4,6 µl). 1% PAA. The behavior here is consistent in terms of greater quantities of inhibitor but not a linear progression that is expected. This shows in a different nature the spike associated with the 0.3 M concentration point.

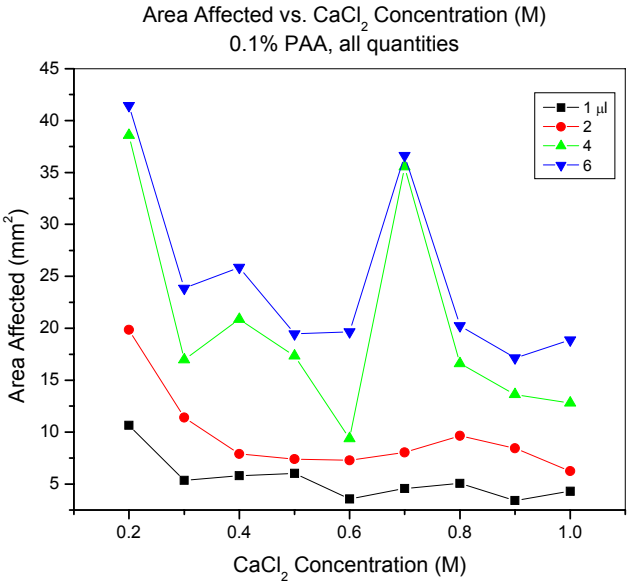

Figure 7.4 Affected area (mm^2) vs. calcium chloride concentration(M). Data shown for 0.1% PAA molecules injection at following quantities of injection(1,2,4,6 µl). Data indicates the limited consistency of greater quantity inducing greater affected areas but no linear or general trend is detected.

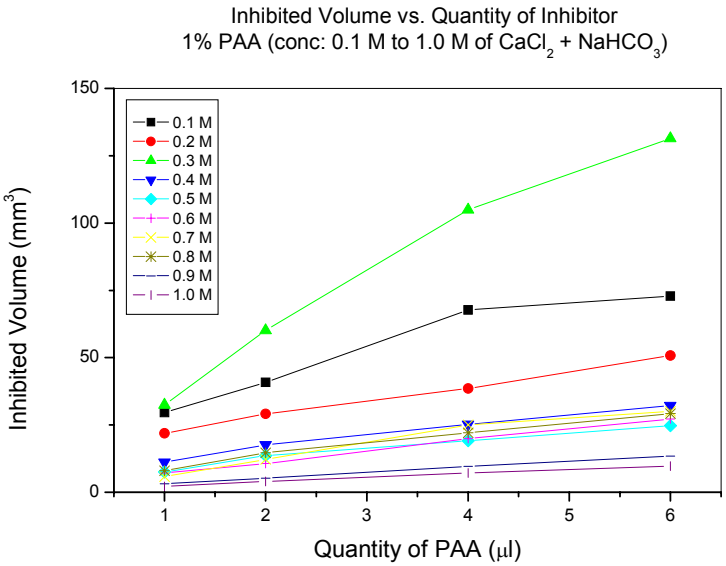

Figure 7.5 Inhibited volume (mm^3) vs. the quantity of inhibitor(1,2,4,6 µl) at the range of calcium chloride/sodium bicarbonate concentrations. As per the affected area graph that was shown earlier the 0.3 M concentration point indicates highest volumes of inhibition.

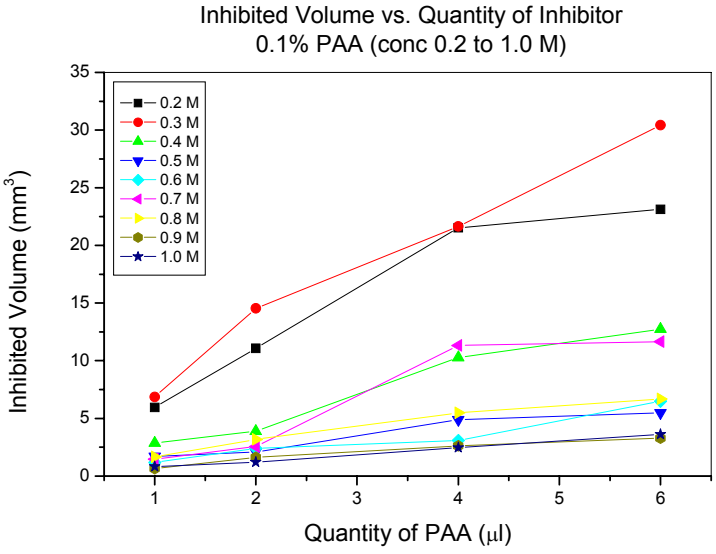

Figure 7.6 Inhibited volume(mm^3) vs. quantity of inhibitor(1,2,4,6 µl) for 0.1% PAA. Note that at 0.1 M salt concentrations there was no inhibitory effect of crystal growth and hence no data shown.

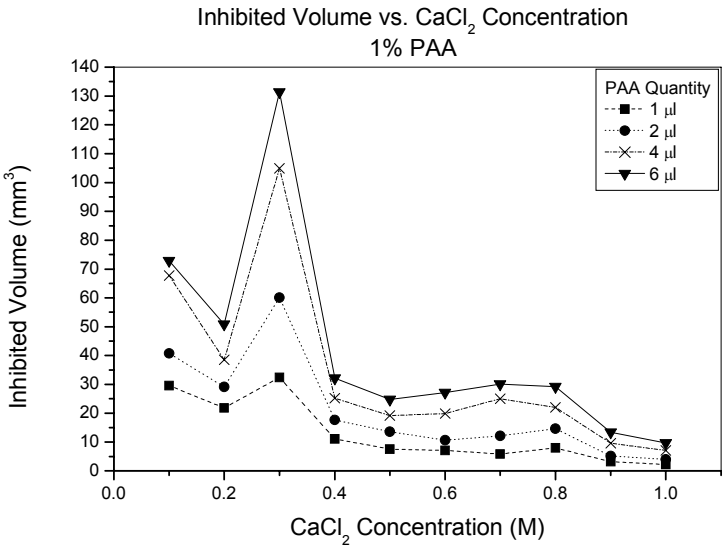

Figure 7.7 Inhibited volume (mm^3) vs. calcium chloride(M). 1% PAA at following quantities(1,2,4,6 µl). Once again the 0.3 M concentration point is notable.

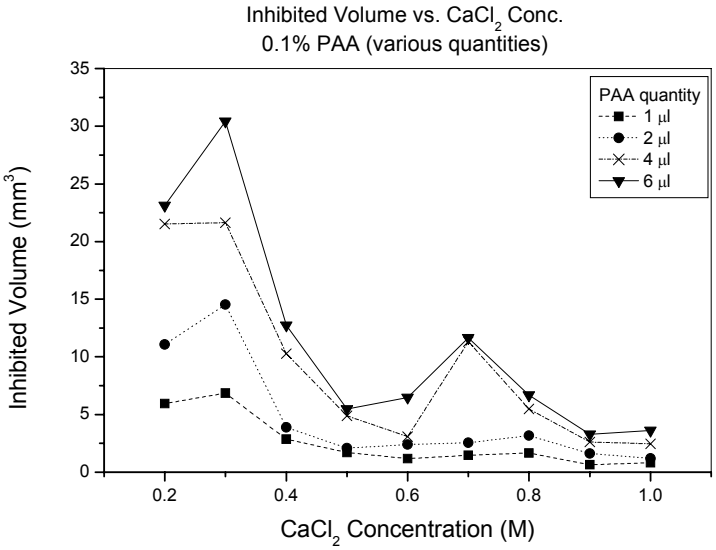

Figure 7.8 Inhibited volume (mm^3) vs. calcium chloride(M). 0.1% PAA at following quantities(1,2,4,6 µl). Once again it noted that at the lower concentration of 0.3 M there is a noticeable peak of inhibited volume.

7.2 Acrylic Acid series

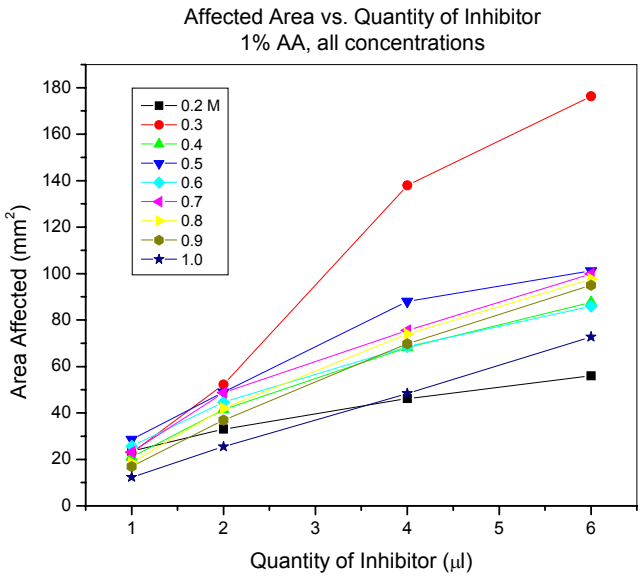

Figure 7.9 Acrylic acid(AA). Affected area(mm^2) vs. quantity of inhibitor(1,2,4,6 µl). Concentration range of 0.2-1.0 M calcium chloride/sodium bicarbonate. Any effect at 0.1 M is negligible and not shown. It is worth noting that once again a peak effect is apparent at the 0.3M calcium chloride concentration point.

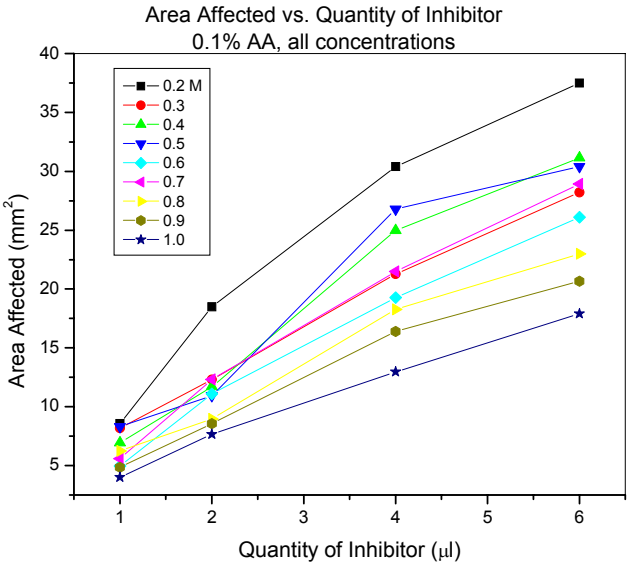

Figure 7.10 Affected area(mm^2) vs. quantity of inhibitor(1,2,4,6 µl) for 0.1% AA. 0.2-1.0 M concentration range of the calcium chloride/sodium bicarbonate. Somewhat anomalous behavior again as at 0.2 M concentration point the greatest inhibitory effect is shown as opposed to the 0.3 M point with 1% AA.

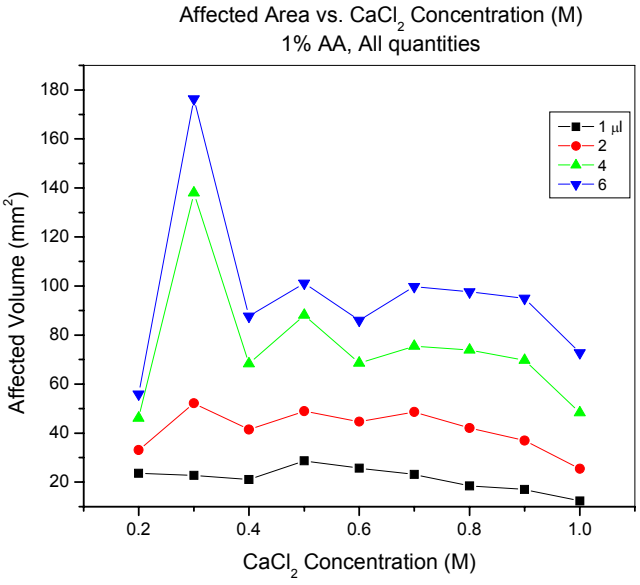

Figure 7.11 Affected area (mm^2) as plotted vs. the corresponding concentration of calcium chloride in the gel and the subsequent addition of equimolar concentration of sodium bicarbonate. Although there is consistency in greater quantities inducing greater affected areas at given concentration points there is no linear relationship. Again the notable points of interest are the 0.3 M concentration point. Quantities of AA inhibitor are in the range of (1,2,4,6 µl).

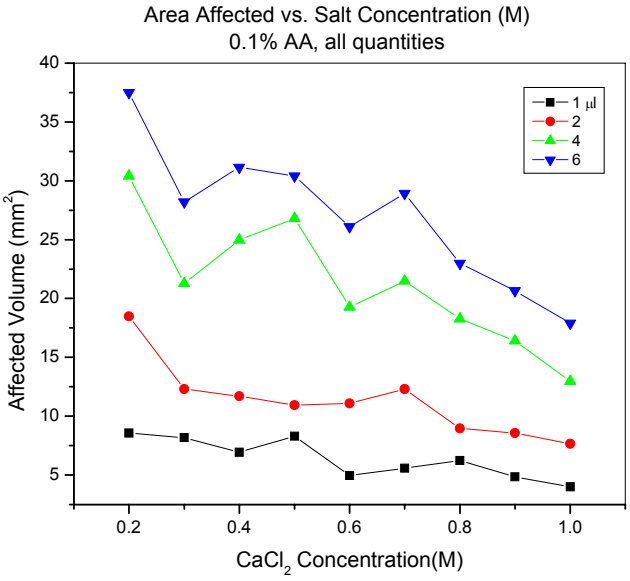

Figure 7.12 Affected area (mm^2) vs. calcium chloride/sodium bicarbonate concentration (M). From 0.2 to 1.0 M concentration range. For quantities of 0.1% AA of ranging in the following quantities(1,2,4,6 µl). The affected area decreases as the salt concentration increases.

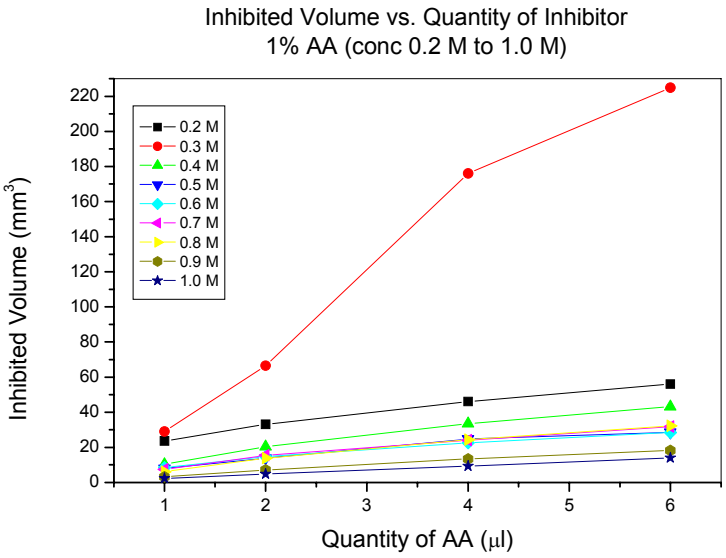

Figure 7.13 Inhibited volume(mm^3) vs. quantity of inhibitor(1,2,4,6 µl) at full concentration regime of calcium chloride/sodium bicarbonate(0.2-1.0M) for 1% AA. Once again as the data is calculated from the affected area the spike at 0.3 M is apparent. As is described in the text it is more consistent to look at the area measurements as opposed to the volume. The depth of penetration of crystal growth measurements is not as consistent and easily measured as the affected/inhibited diameter from the point source.

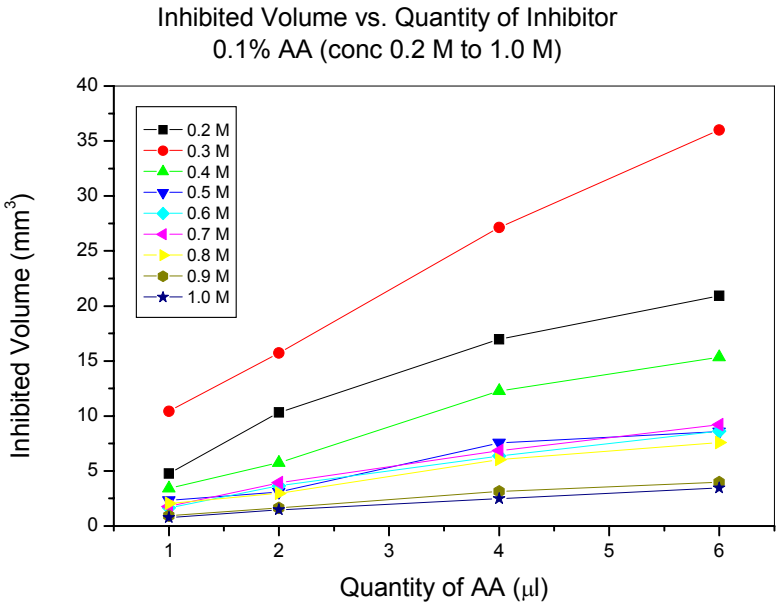

Figure 7.14 Inhibited volume(mm^3) vs. quantity of inhibitor(1,2,4,6 µl) for the 0.1% AA additive. The concentration regime of 0.2 -1.0 M of calcium chloride/sodium bicarbonate is shown. As is mentioned in the previous figure the spike is seen for 0.3 M as the calculation results from the area measurements.

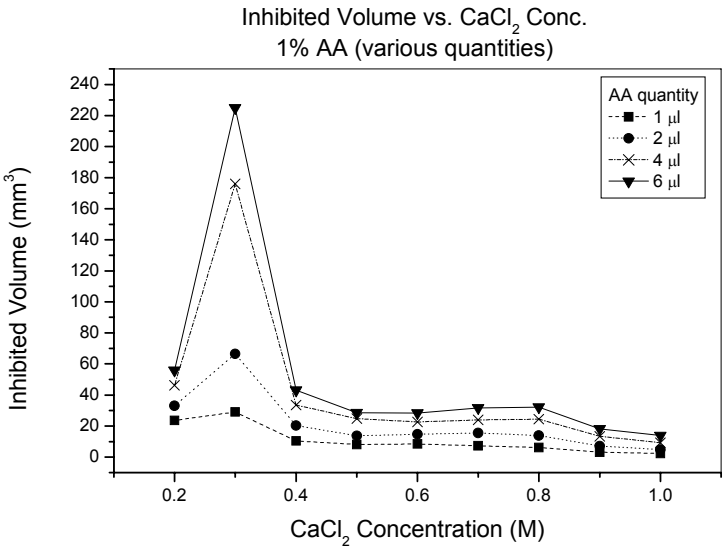

Figure 7.15 Inhibited volume (mm^3) vs. calcium chloride/sodium bicarbonate concentration(M). For 1% AA injections at quantities in range of (1,2,4,6 µl). The important observation is the consistency of increased inhibition with greater injection quantities. From 0.4 M to 1.0 M concentrations the profile is very consistent with an almost steady inhibition.

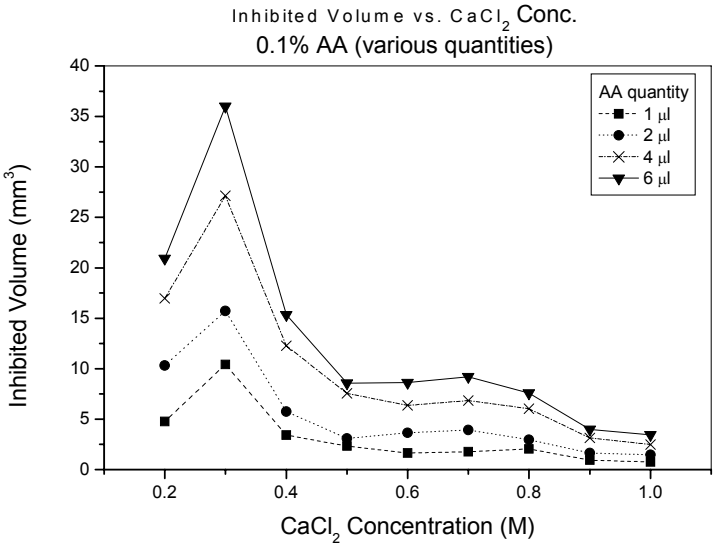

Figure 7.16 Inhibited volume(mm^3) vs. calcium chloride/sodium bicarbonate. This data is for the 0.1% AA injected at specific quantities(1,2,4,6 µl). The data here is fairly consistent with that of the 1% AA with the 0.4-1.0 M concentrations indicated somewhat linear behavior in inhibited volume.

7.3 EDTA Series

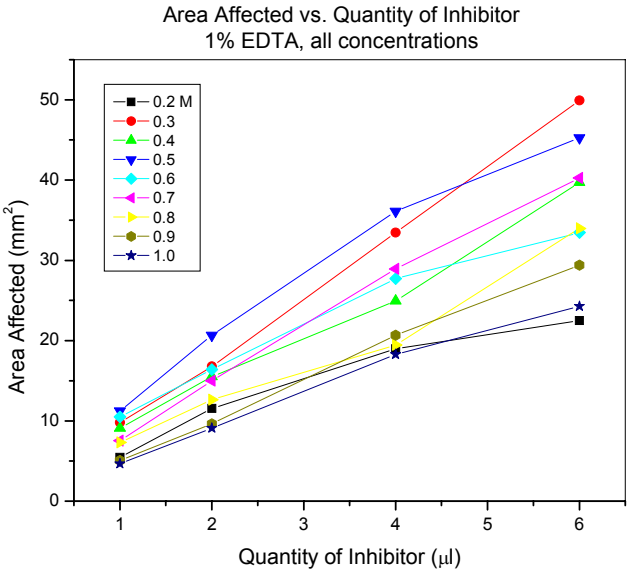

Figure 7.17 Area affected(mm^2) vs. quantity of inhibitor(1,2,4,6 µl) for 1% EDTA additive. Concentration range of calcium chloride/sodium bicarbonate from 0.2-1.0M as there is no reportable effect at 0.1 M. It is important to note that in these graphs and subsequent graphs the calcium chloride shown is equivalent to the sodium bicarbonate concentration with which the gels were developed to form crystals. Once again it is worth noting the spike in inhibition at the 0.3 M concentration point.

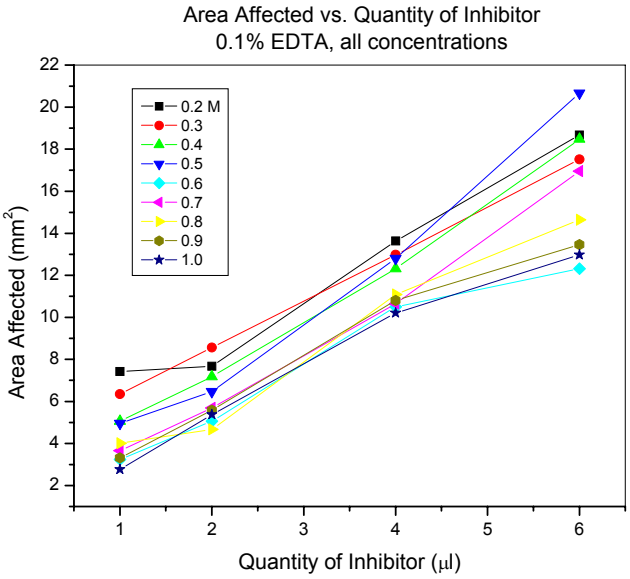

Figure 7.18 Area affected (mm^2) vs. quantity of inhibitor(1,2,4,6 µl) at full concentration regime for 0.1% EDTA additive. Indicates overall consistency but shows higher affected area at the 0.5 M concentration point while the 0.3 M point was noteworthy in other results.

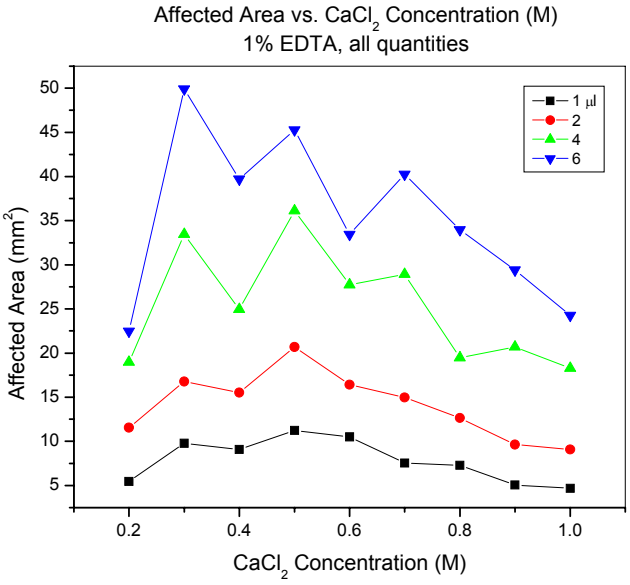

Figure 7.19 Affected area(mm^2) vs. calcium chloride/sodium bicarbonate concentration(M). 1% EDTA at the following quantities of injection(1,2,4,6 µl). Greater injection quantities show greater affected areas. However, at lower injection quantities the inhibited area is more controlled.

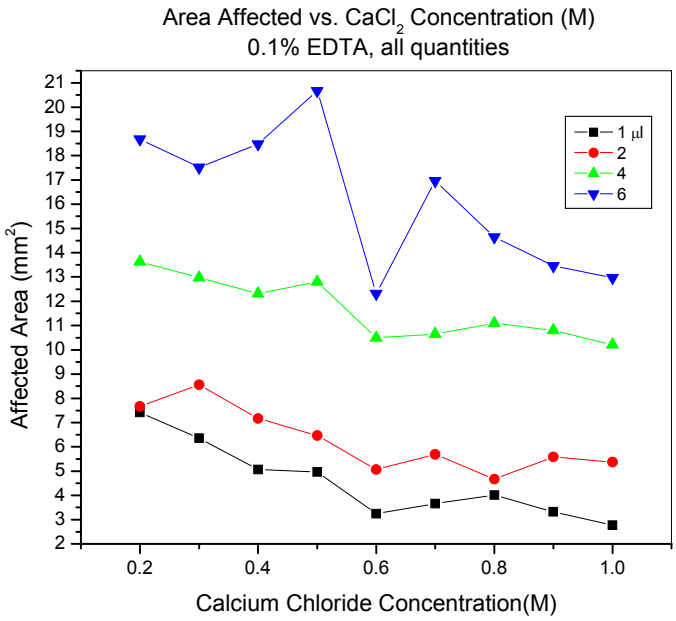

Figure 7.20 Area affected(mm^2) vs. calcium chloride/sodium bicarbonate concentration(M). Data is for 0.1% EDTA injected at the microliter quantities(1,2,4,6 µl). Some noteworthy observations include that at some concentration points such as 0.5 M the effect of 2µl vs. the 4 µl presents a nearly linear progression with just about double the affected area for 4 µl versus the 2 µl. The inhibited area for the 6 µl point at 0.5 M presents nearly triple the value as for 2 µl. Such behavior is not present throughout the concentration regimes however.

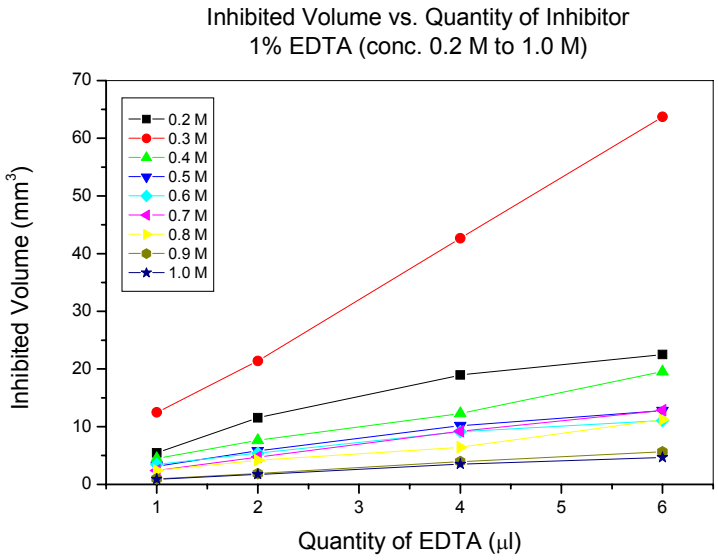

Figure 7.21 Inhibited volume(mm^3) vs. quantity of inhibitor(1,2,4,6 µl). 1% EDTA data for calcium chloride/sodium bicarbonate concentrations from 0.2 M to 1.0 M.

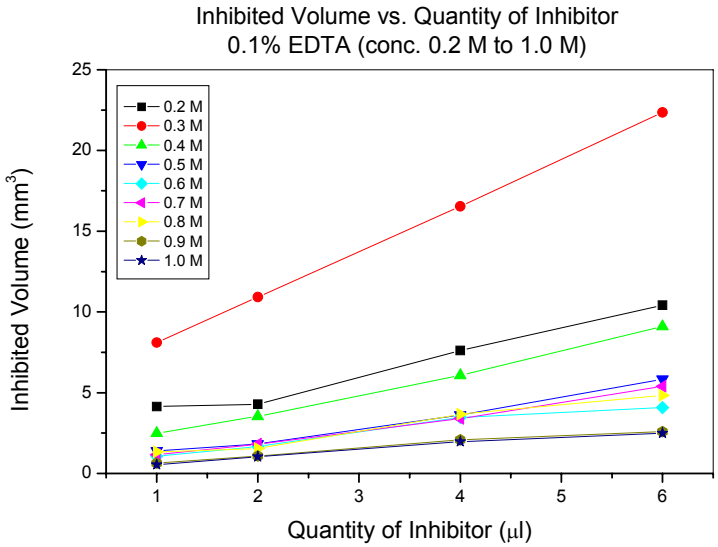

Figure 7.22 Inhibited volume (mm^3) vs. quantity of inhibitor(1,2,4,6 µl). 0.1% EDTA and calcium chloride/sodium bicarbonate concentrations of 0.2 - 1.0M.

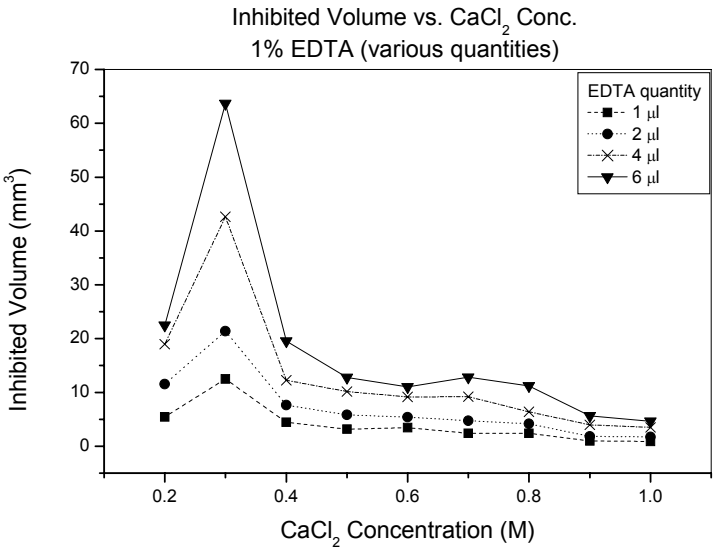

Figure 7.23 Inhibited volume (mm^3) vs. calcium chloride/sodium bicarbonate concentration(M). For 1% EDTA added at (1,2,4,6 µl) quantities. Once again as the volume calculations are based on the area calculations the 0.3 M spike is noted. Additionally, the behavior from the 0.4-1.0M concentration range is somewhat linear with slight decreases in inhibited volume even as increased quantities are injected.

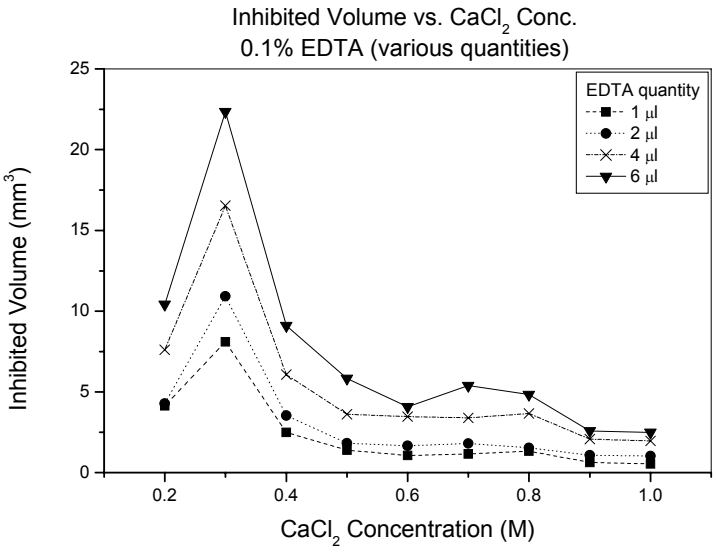

Figure 7.24 Inhibited volume (mm^3) vs. calcium chloride/sodium bicarbonate concentration(M) . 0.1% EDTA addition in following quantities (1,2,4,6 μl). Salt concentration range is from 0.2 M 0 1.0 M. Behavior is somewhat consistent with 1% EDTA with the exception that with lower concentration of EDTA the inhibited volumes are smaller in value.

7.4 Comparisons of PAA, AA and EDTA

The following series of graphs shows a comparison of inhibited volumes versus the quantity of inhibitor injected for each additive, PAA, AA, EDTA and throughout the whole concentration regime. The graphs are shown with direct comparisons of the additives thus allowing for a correlation in using a particular additive that results in a known inhibitory value of area or volume. This allows for potential selection of the additive in a freeform fabrication method in which select quantities of inhibitor are desired in order to influence a controlled area in which crystal growth may not result. In this case the inhibited volumes are shown as opposed to the inhibited area. One reason is in subsequent discussion and calculation a potential correlation between the number of

Ca^{+2} ions versus the numbers of $COOH^{-}$ ions is analyzed. However, it is maintained that the measurement of the area of inhibition remains the more accurate and repeatable measurement of inhibitor/modifier effect.

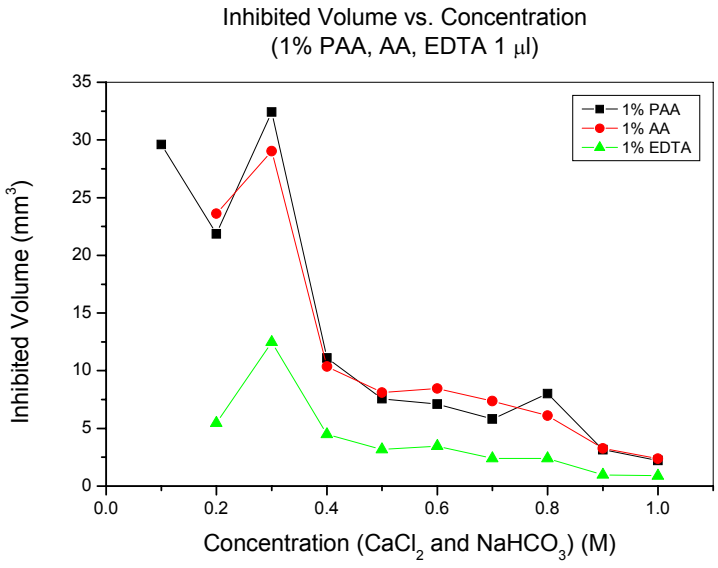

Figure 7.25 Comparison of 1% PAA, AA and EDTA simultaneously and resulting inhibition of crystal growth in gel volume. It is noted that the 1% PAA and 1% AA do not show marked differences when applied in 1 μl quantities. All three show somewhat linear behavior from the 0.4 to 1.0 M calcium chloride/sodium bicarbonate concentrations. Slight decreases in inhibited volume result as the concentration moves towards 1.0M.

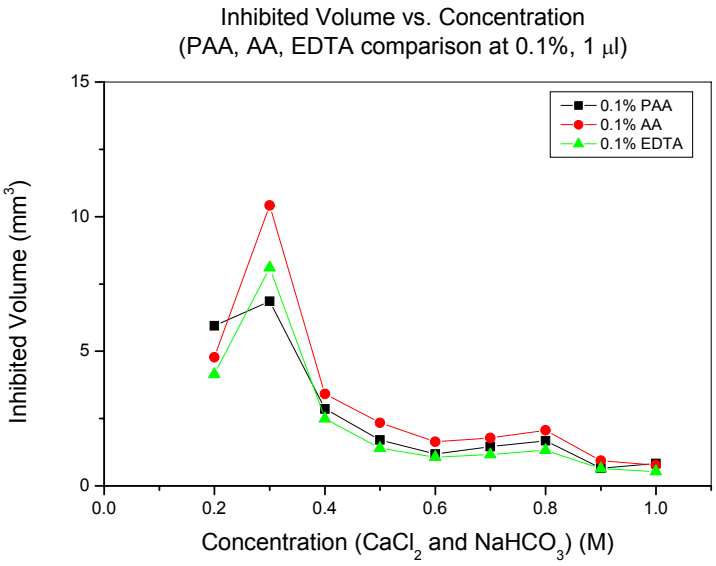

Figure 7.26 Comparison of 0.1% PAA, 0.1% AA, and 0.1% EDTA in quantities of 1 μl. Plotted as inhibited volume (mm^3) vs. calcium chloride/sodium bicarbonate concentration from 0.2 -1.0 M. Once again the spike at 0.3 M is noted for all three cases. Additionally a rather controlled trend is detected from 0.4M to 1.0M salt concentrations. The magnitude of volume appears to be the same regardless of the additive.

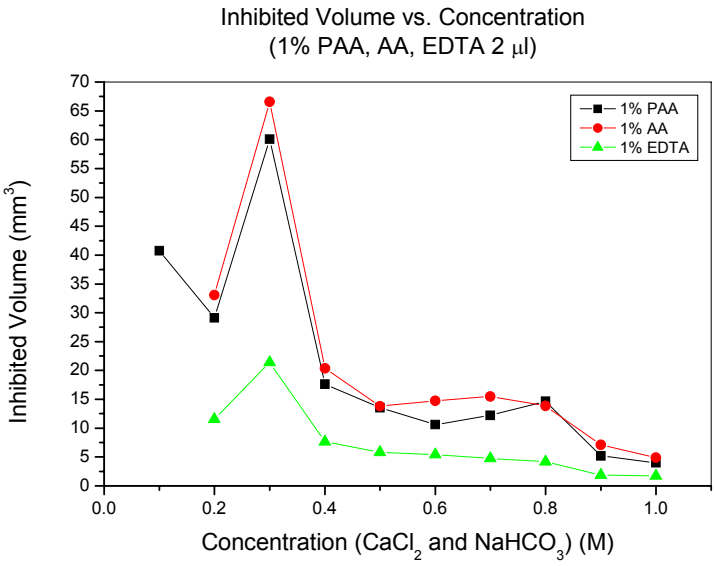

Figure 7.27 2 µl injections of 1% PAA, 1% AA and 1% EDTA. Concentration of salt solutions, calcium chloride/sodium bicarbonate, is from 0.2 M to 1.0 M. Note the spike in inhibition at the 0.3 M concentration point for all three of the inhibitors/modifiers.

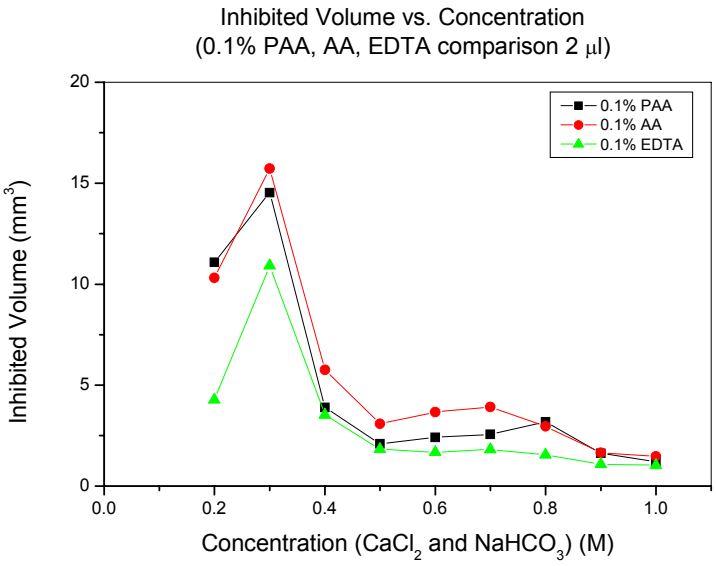

Figure 7.28 2 µl injections of 0.1% PAA, 0.1% AA and 0.1 % EDTA comparison in volume inhibition.

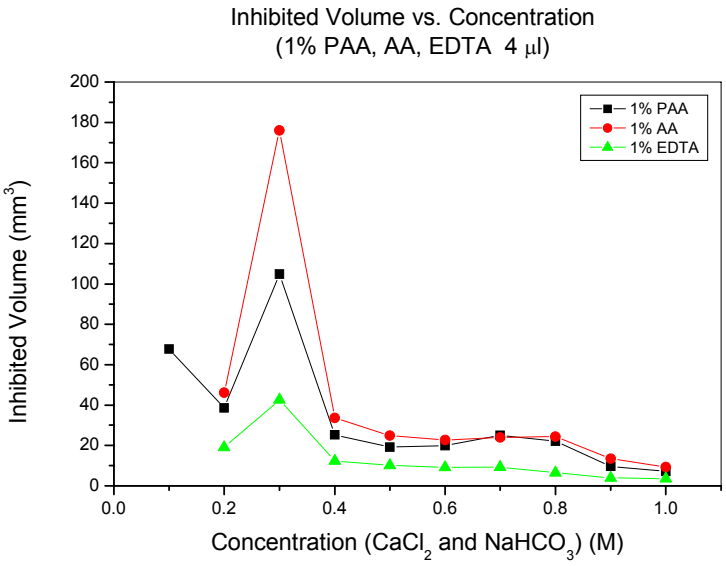

Figure 7.29 Inhibited volume comparison of 1% PAA, 1% AA and 1% EDTA at 4 µl injection quantities. Full concentration regime of calcium chloride/sodium bicarbonate 0.2 M- 1.0 M. Once again the 1% PAA and 1% AA show similar effects, primarily in the 0.4 – 1.0M concentration range.

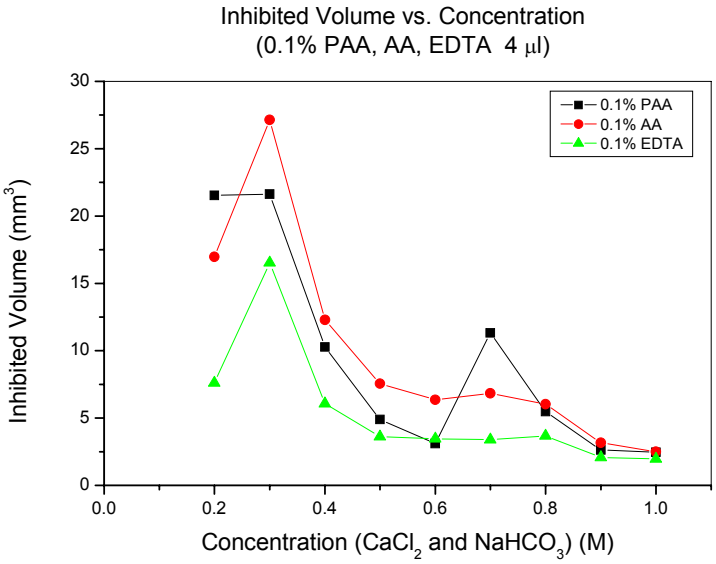

Figure 7.30 Inhibited volume comparison for 0.1% PAA, 0.1% AA and 0.1% EDTA at 4 µl injection quantity for 0.2 to 1.0 M concentration range of calcium chloride/sodium bicarbonate. Less consistent inhibition volumes in higher concentration range.

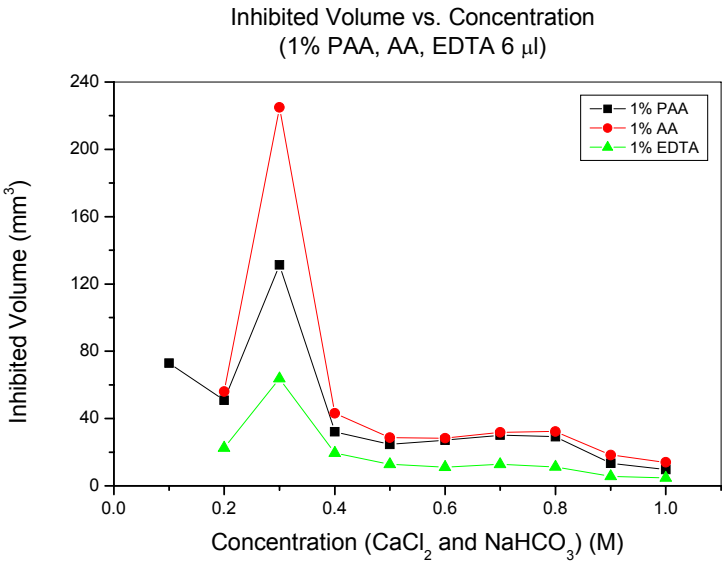

Figure 7.31 Inhibited volume comparison for 6 µl injection quantities of 1% PAA, 1% AA and 1% EDTA. As per previous results this injection quantity shows consistency from 0.4 M -1.0M concentration range. Once again, the spike at 0.3 M is apparent.

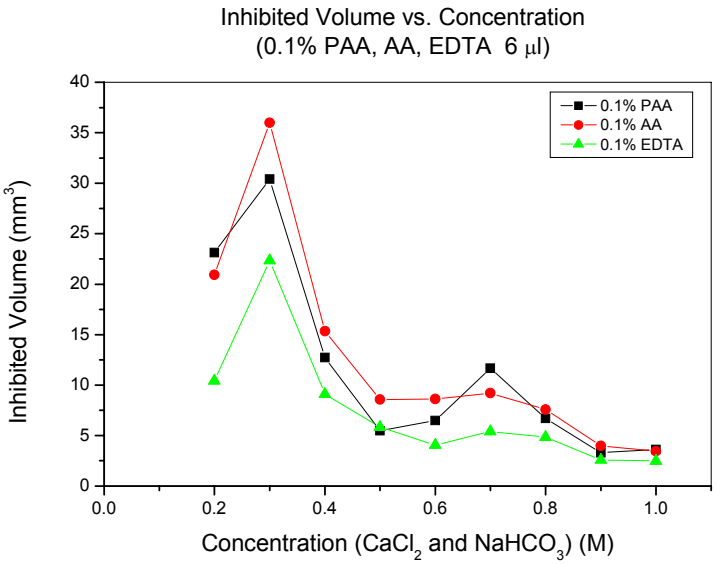

Figure 7.32 Inhibited Volume comparison for 6 µl injection quantity of 0.1% PAA, 0.1% AA and 0.1% EDTA. Some inconsistencies in the higher concentration range once again. The PAA and AA effects over EDTA are not as pronounced.

7.5 Discussion and Analysis

As mentioned some of the indicate general trends but other data sets do non. There is an inconsistency in the concentration regimes at 0.3 M which is notable. In all modifiers this area and corresponding volume of inhibition is not consistent with other data. No immediate explanation is apparent.

One aspect to analyze in this case is the COOH/Ca ion ratio in given areas and volumes. As the agarose gels are made with a known concentration of calcium chloride the numbers of Ca ions may be calculated per given volume based on the concentrations used. Based on this the following data is presented. It is assumed that COOH groups inhibit the growth of calcium carbonate by binding to the Ca ions growth front. Based on this the higher ratios of COOH/Ca should be responsible for highest areas and volumes of inhibition but this is not shown with consistency.

Certain trends are noticeable. For example the 0.2 M concentration regime as plotted in quantity of inhibitor versus area inhibited. The area inhibited is expected to increase with larger quantities of inhibitor. This is generally indicated. Additionally, when comparing 0.2 M versus the 1.0 M with identical inhibitor quantities it is noted that there is greater area of inhibition in the 0.2 M regime than in the 1.0M regime. As the COOH adsorbs onto the Ca ion growth front it is predicted that with fewer Ca ions to bind the inhibitor diffuses further outward in order to satisfy the binding numbers of COOH:Ca.

Much of the data presented so far has been in the form of inhibited areas and volumes as the additive of PAA, AA or EDTA are diffused radially outward from a point source. However it is important to also note any effects the additives have on the resulting $CaCO_3$ sizes. The table below is a brief analysis of the resulting particles sizes in the 2.2% agarose gel regimes. As per previous experimental mention this regime was done with a full concentration regime of 0.1 -1.0 M salt solutions. The pH of the salt solutions was adjusted to 10.3.

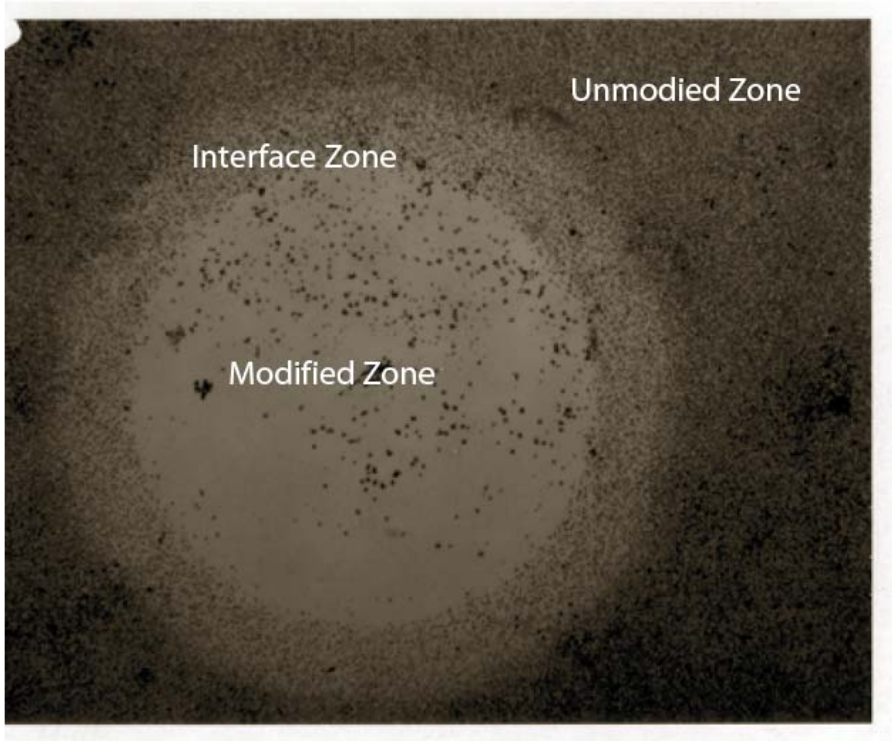

Figure 7.33 The various zones of crystal growth in gel mineralization assay. Unmodified is inhibitor/additive free. The interface zone is where the effects of the inhibitor/additive are decreasing and the modified zone is where the inhibitor/additive has played a critical role in inhibition/modification. The diameter of the modified zone is on the order of 5 mm.

The data were obtained by analysis of SEM micrographs as true particle size analysis was unavailable at the time. The resulting crystal sizes are presented in a range of sizes for each region. The regions are defined as follows. There is unmodified area in which no inhibitor/additive was present. These numbers are obtained from specific areas where it is known that the inhibitor had no effect and were compared to a control gel in which no additives were ever added and only the precipitated salts were present. The interface zone is that in which an interface results where the additive's effect is ended and the unmodified zone begins.

Table 7.1 Crystal size results for 0.5 and 1.0 M $CaCl_2$ + $NaHCO_3$ concentrations at pH 10.3 in 2.2% agarose.

	0.5 M $CaCl_2$+$NaHCO_3$			1.0 M $CaCl_2$+$NaHCO_3$		
Additive	Modified Zone	Interface Zone	Unmodified Zone	Modified Zone	Interface Zone	Unmodified Zone
1% PAA	2-3 μm	6-8 μm	16-20 μm	2-4 μm	5-7 μm	16-20μm
1% AA	5-7 μm	8-10 μm	16-20 μm	4-6 μm	7-10 μm	16-20 μm
1% EDTA	5-7 μm	8-10 μm	16-20 μm	4-6 μm	8-11 μm	16-20 μm

The crystal size data was not acquired for all the sample concentration ranges but the two significant results were obtained for the 0.5 M and 1.0 M concentration regimes. As is seen from the table the resulting calcite crystals were rather significant in size, ranging from 16-20 μm in the unmodified area and as was noted this was compared to the

resulting sizes in control gels without inhibitors/additives. The crystals in the interface zone showed some decrease in particle size primarily in the 7-10 μm range. In the modified area there were very few crystals, if any, that were detectable. However, some basic particle size analysis via SEM micrograph analysis was done. The numbers indicate significantly smaller crystal sizes. The crystal sizes were as much 3x smaller than in the unmodified zones.

The influence of the additives on the crystal size is an important factor in overall functionality of the gel mineralization assay systems. In the case of these aforementioned additives, PAA, AA and EDTA the important factor is the presence of the COOH functionality.

In terms of general crystal nucleation and growth of calcium carbonate crystals the effects of molecular containing carboxylic(COOH) functional groups are noteworthy. The formation of calcium carbonate in solution from calcium chloride and sodium bicarbonate is described as follows:

$CaCl_2 + NaHCO_3 \rightarrow CaCO_{3\,(s)} + H^+$

Because of this mechanism there are instances in which the formation of the calcium carbonate can be monitored by drift in the pH, known as the pH drift method. The pH decreases as the crystallization proceeds[151, 152]. Another method of monitoring the crystallization of the calcium carbonate is the constant composition method developed by Nancollas et al[153]. This method entails the used of seed crystals with a known surface area that are added to metastable solutions. The seeds will then grow immediately upon contacting the solution and hence there is an induction time but really no way of

measuring the actual effects on nucleation but the growth rate is estimated[154]. The gel mineralization assay may also be used to monitor such details as induction time and other nucleation effects. However, the method used here is more pertinent to understanding and interpreting the end result of whether or not the crystals are grown and the effects of the organic inhibitors/additives.

The initial experimentation of the gel mineralization assay, as mentioned in Chapter 5, was done in order to obtain conceptual proof that agarose gel charged with a calcium chloride solution would provide a suitable matrix to study the effects of inhibition of various organic molecules possessing a COOH functionality in both single molecule and chain molecule confirmations. Amongst the first data sets obtained was a preliminary crystal counts based on the numbers of resulting calcium carbonate crystals in uninhibited/unmodified control gels versus the relative numbers that may or may not be detected in the inhibited/modified areas. Initial data indicated that PAA was far more effective an inhibitor based on preliminary crystal counts. Based upon this experimentation the gel mineralization system was tested with Polyacrylic acid (PAA), acrylic acid (AA) and Ethylenediamine tetra acetic acid (EDTA).

Table 7.2 Crystal count numbers in unmodified (control) regions versus inhibited/modified areas.

Sample Label	Count/$mm^{2.}$ Area of injected modifier	Count/mm^{2}. Unmodified(plain) area
P1	6±2	117±8
P2	8±3	108±9
P3	39±4	83±9
A1	97±9	89±8
A2	86±8	83±12
A3	67±9	75±10
E1	128±15	133±21
E2	133±19	139±18
E3	125±14	114±15

As the experimentation and data collection progressed it was determined that crystal count numbers were somewhat impractical to obtain for large numbers of samples. Hence the protocols were altered to measure inhibited areas and subsequent inhibited volumes of the inhibition, by measuring depth of penetration of crystal growth within the gels, and attempt to develop some quantitative parameters measuring the effects of the COOH molecules on the development of calcium carbonate crystals. The data below illustrates the broad range of parameters that are obtained from the raw data collection, beginning with measurements of inhibited areas in the gels that represent the absence of calcium carbonate crystals.

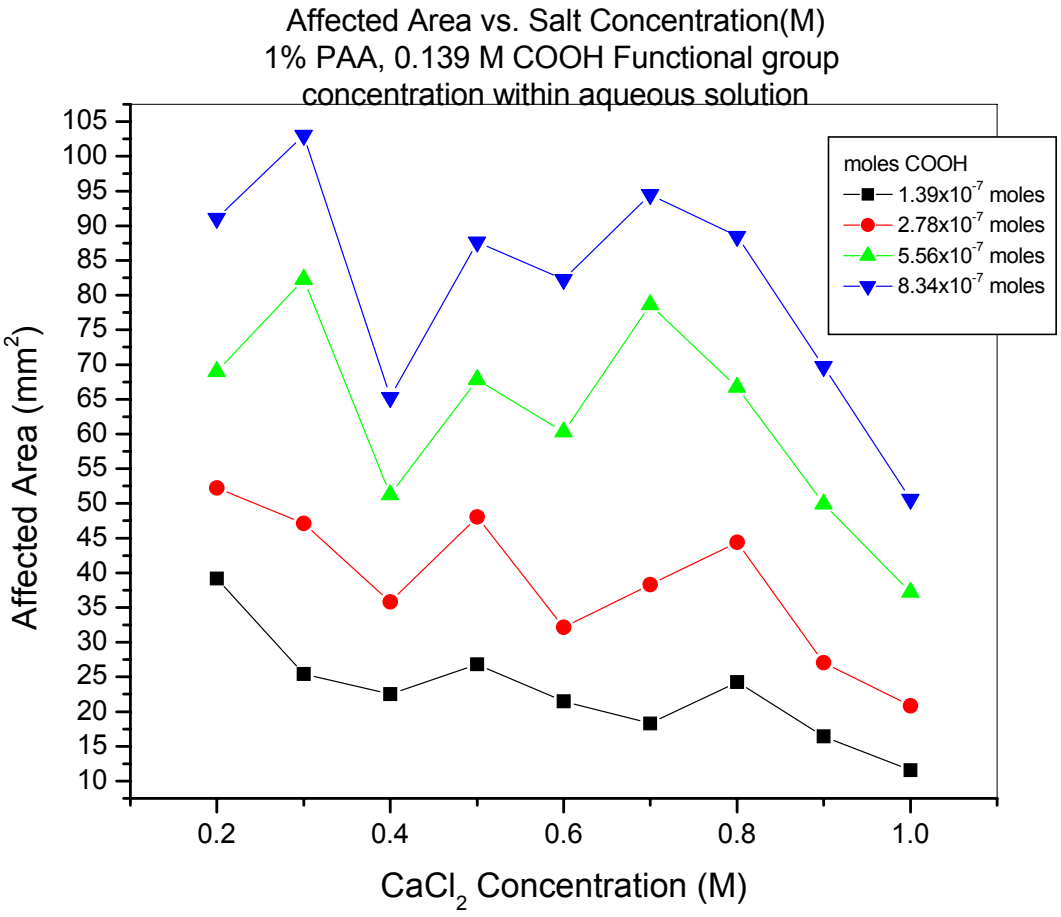

Figure 7.34 Affected area versus the Calcium chloride/Sodium bicarbonate concentration (from 0.2 M to 1.0 M). Area quantities represent regions of inhibited crystal growth of calcium carbonate.

Figure 7.34 shows the data for the full precipitating salt concentration regime of 0.2 to 1.0 M. It is important to note that the three inhibitors chosen for observation in this series of experiments are shown as 1% w/v solutions of polyacrylic acid, acrylic acid and EDTA. The number of moles of COOH dispensed corresponds to a dispensing quantity of 1, 2, 4 and 6 µl, respectively. As was mentioned in chapter 5 the 1% is used more as a

convenient representation as the goal was to dispense equal amounts of the COOH functional groups to the Ca^{+2} ion molar concentration that was present in the aqueous solution incorporated into the gels. The 1% is very close to the equivalent molar concentrations and is used for simpler labeling reasons. Each of the candidate inhibitor solutions was formulated such that they had equal molar concentrations of COOH groups. This enabled the direct comparison of their efficacy in inhibiting the crystallization of $CaCO_3$ within the gels.

Table 7.3 Quantity of inhibitor in microliters and the equivalent quantity of moles COOH dispensed at each point.

Quantity in µl of inhibitor injected (PAA, AA or EDTA)	Moles COOH in present solution
1 µl	$1.39x10^{-7}$
2 µl	$2.78x10^{-7}$
4 µl	$5.56x10^{-7}$
6 µl	$8.34x10^{-7}$

After determining the inhibited volume several other comparisons can be made. These include the relative or effective molarities, of the inhibitors (COOH functional group molecules) in the gel once diffusion has completed and comparing that to the molarities of the calcium chloride-sodium bicarbonate salt solution concentrations. The initial motivation is to determine ratios of COOH groups to that of the Ca^{+2} ion concentrations. It is believed that the COOH concentration can be correlated to the calcium ion concentration and hence related to the relative amounts of inhibition.

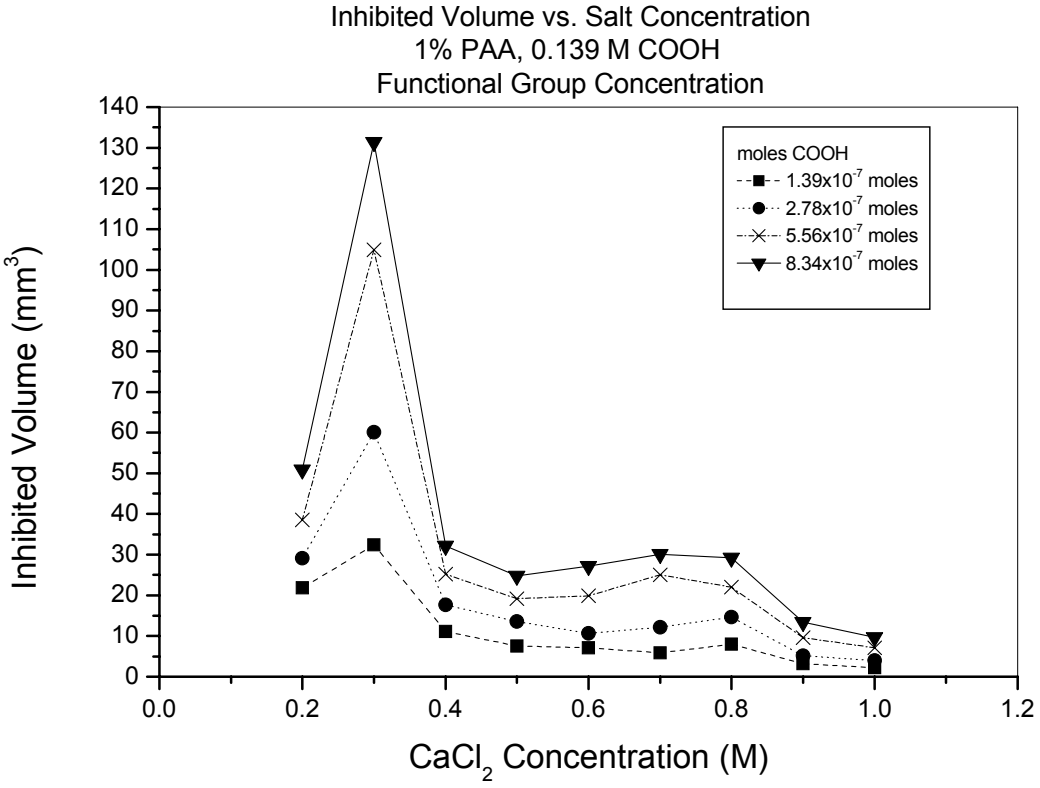

Figure 7.35 Inhibited volume in mm^3 versus the calcium chloride-sodium bicarbonate salt concentrations (0.2 – 1.0 M). The 1% PAA is equivalent to 0.139 M COOH functional group concentration. Inhibited volume data are representative of gel portions in which no calcium carbonate crystals were observed.

Figure 7.35 shows the data for the volume of inhibition in (mm^3 or ml) that corresponds to the area inhibited from figure 7.34. The inhibited volume is representative of the volume of the gel in which calcium carbonate crystals are absent as compared to the remaining portions of the gel. As the injected quantities of moles of COOH are known and correspond to this measured volume within the gel, the effective molarity of the COOH group functionality can be calculated. This resulting effective

molarity of CCOH functionality is then compared to the calcium chloride molar concentration and a ratio is obtained providing some element of comparison of COOH concentration to the calcium chloride, and subsequent calcium ion concentration. A few representative tables will be shown here for selected concentration points of the calcium chloride-sodium bicarbonate concentrations.

Table 7.4 Calcium Chloride-Sodium bicarbonate at the 0.4 M concentration point. Data present for injected COOH moles, area and volume inhibited, effective molarity of COOH in inhibited volume zone and finally the COOH/Ca ion molar ratio.

0.4 M calcium chloride
1% PAA

Quantity of Inhibitor (µl)	moles COOH dispensed	Area Inhibited (mm^2)	Volume Inhibited (ml)	Effective COOH Molarity(M)	Molar Ratio COOH/Ca ions
1	1.39E-07	22.55	11.099	1.25E-05	3.13E-05
2	2.78E-07	35.83	17.639	1.58E-05	3.94E-05
4	5.56E-07	51.21	25.210	2.21E-05	5.51E-05
6	8.34E-07	65.27	32.130	2.60E-05	6.49E-05

Table 7.4 is representative of the data that is collected and calculated. First of all, as was previously mentioned the quantity of moles of COOH is known and the area of inhibition is the first data set collected. From that point the volume of inhibition is calculated based on the depth of penetration of the crystal growth and hence inhibition. From this point the new effective molarity of the COOH ion groups is obtained. The primary assumption is that since the area of inhibition is confined to the measured area and, hence the volume, all the injected COOH molecules are present in that volume. This leads to the calculation of the effective molarity of the COOH ions. Since the concentration of the calcium chloride for the entire gel is known, a direct comparison of

the effective molarity of the COOH ions and the Ca ions may be calculated. This molar ratio is presented in the last column of the table. Since the calcium is a divalent cation and the COOH group is monovalent anionic, stoichiometry dictates that two COOH groups are capable of binding/reacting with the cation.

There is a sharp peak in terms of inhibited volume that occurs at the 0.3 M concentration point. This spike appears for all three regimes of PAA, AA and EDTA at 0.3 M calcium chloride-sodium bicarbonate salt concentrations. A salting-out effect of the precipitating salts within the agarose gel is believed to be responsible for the observed behavior and is addressed in greater detail later in the chapter.

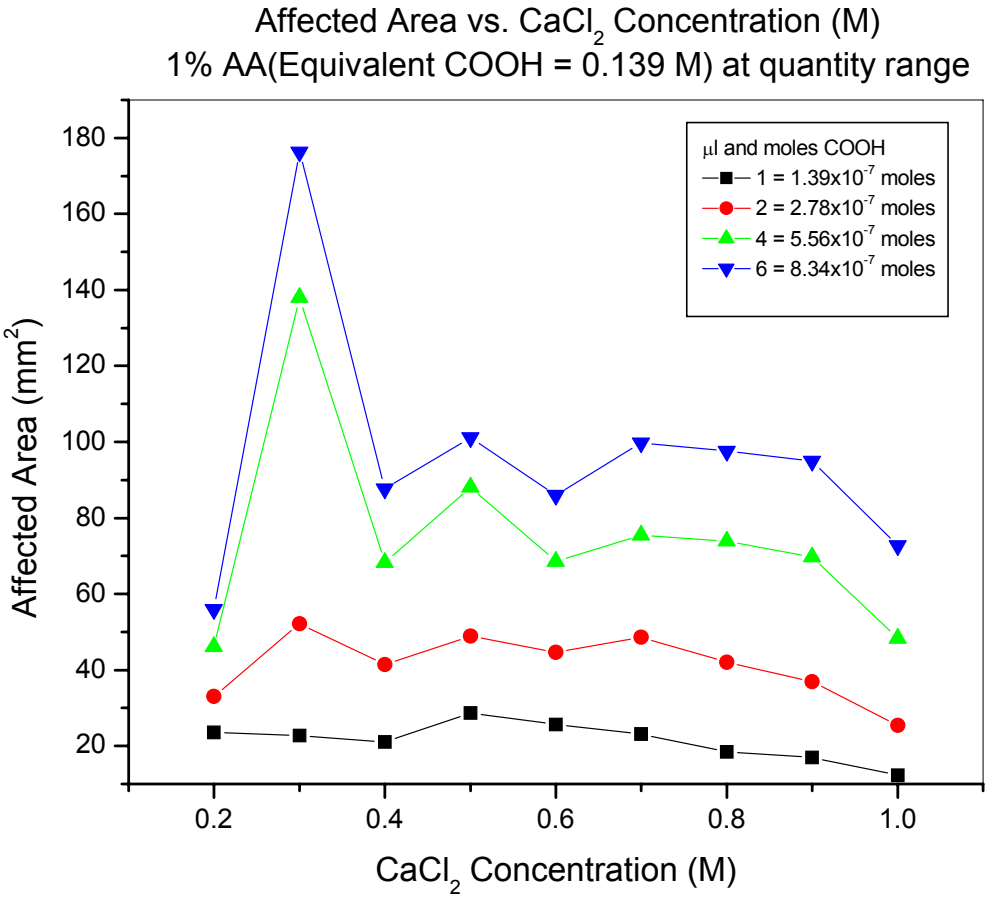

Figure 7.36 Inhibited area vs. calcium chloride-sodium bicarbonate concentration (0.2 M -1.0 M). Shown for various quantities of injected 1% AA (0.139 M COOH groups). The legend shows the equivalent numbers of moles COOH ions injected at each quantity.

From the data presented in figure 7.36 additional data is calculated, first is the corresponding inhibited volume data for the same concentration regime.

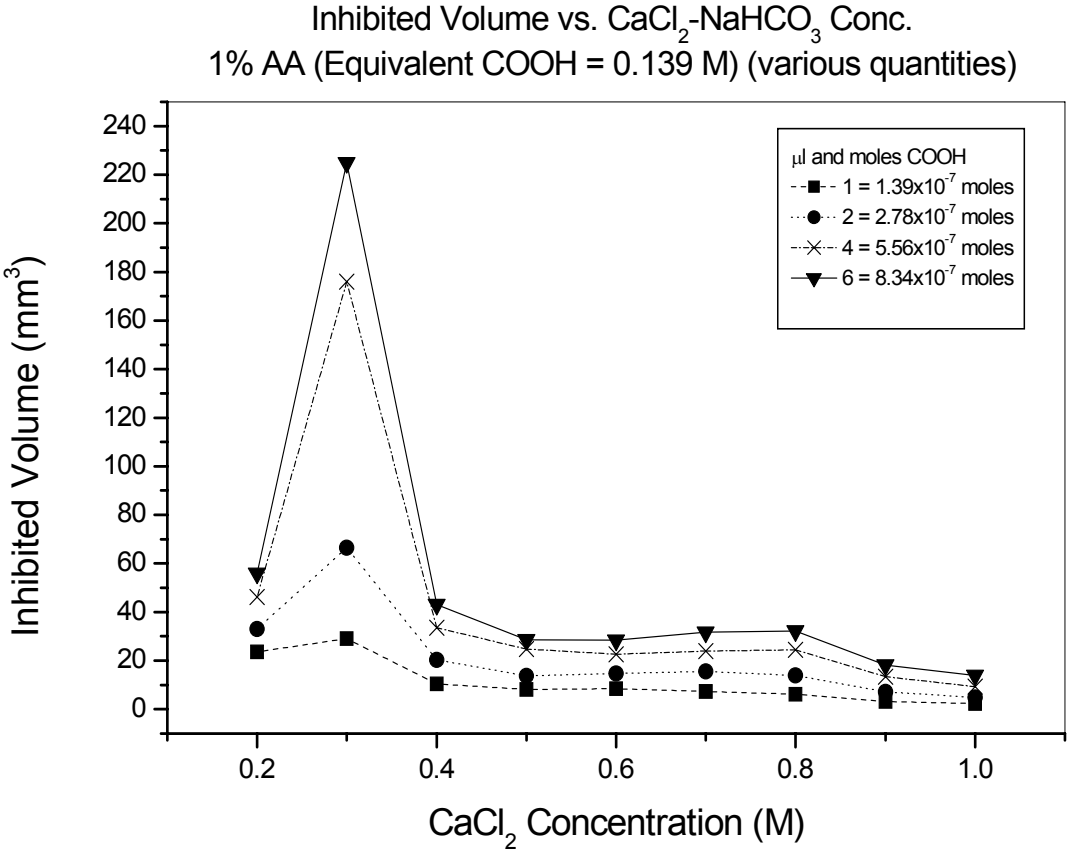

Figure 7.37 Inhibited volume at the various calcium chloride-sodium bicarbonate concentrations. Data obtained at 1% AA (0.139 M COOH groups). The legend shows the corresponding numbers of moles of COOH dispensed at each quantity.

As was seen with the 1% PAA data regime figure 7.37 allows for calculation of the effective molarity of the COOH groups and the molar ratios of COOH to calcium ions. Data table is shown for a representative concentration point.

Table 7.5 Calculated values for 0.4 molar concentration point of calcium chloride and subsequently the sodium bicarbonate concentration.

0.4 M calcium chloride
1% AA

Quantity of Inhibitor (µl)	moles COOH dispensed	Area Inhibited (mm^2)	Volume Inhibited (ml)	Effective COOH Molarity(M)	Molar Ratio COOH/Ca ions
1	1.39E-07	21.08	10.375	1.34E-05	7.76E-05
2	2.78E-07	41.43	20.392	1.36E-05	9.10E-05
4	5.56E-07	68.21	33.578	1.66E-05	1.13E-04
6	8.34E-07	87.64	43.143	1.93E-05	1.07E-04

Table 7.5 shows data ranging from area inhibited to volume inhibited as well as the effective molarity of the COOH ions and the resulting molar ratio of COOH to Calcium ions. Note that despite the somewhat significant inhibited volumes the molar ratios are not indicative of excess of COOH binding to free calcium ions. As originally hypothesized, the COOH ions may not be acting as nucleating inhibitors but rather growth inhibitors. Additional, discussion of this point is presented following additional data for the EDTA regime.

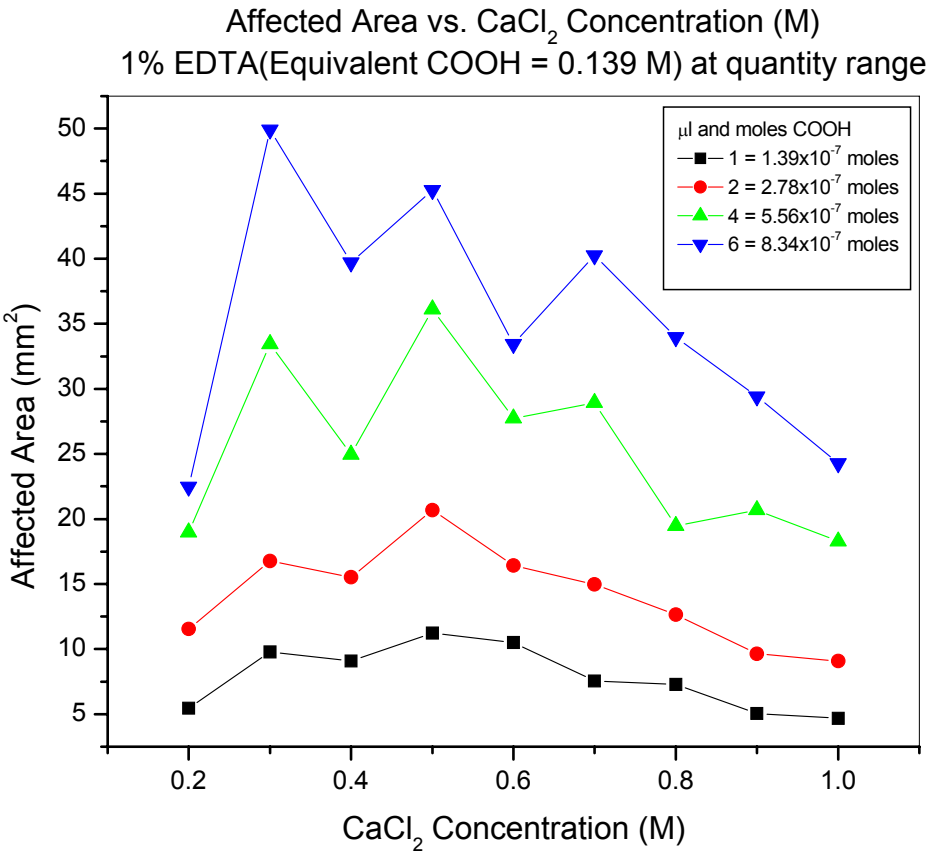

Figure 7.38 Inhibited area vs. molar concentration of calcium chloride-sodium bicarbonate solutions (0.2 M to 1.0M). Data collected at 1% EDTA (0.139 M COOH) regime. The legend shows equivalent moles COOH dispensed for each microliter scale quantity of EDTA.

Figure 7.38 shows the data for area of inhibition versus the calcium chloride-sodium bicarbonate molar concentrations. As with the PAA and AA regimes this leads to the inhibited volume calculation with the other parameters of the graph remaining the same.

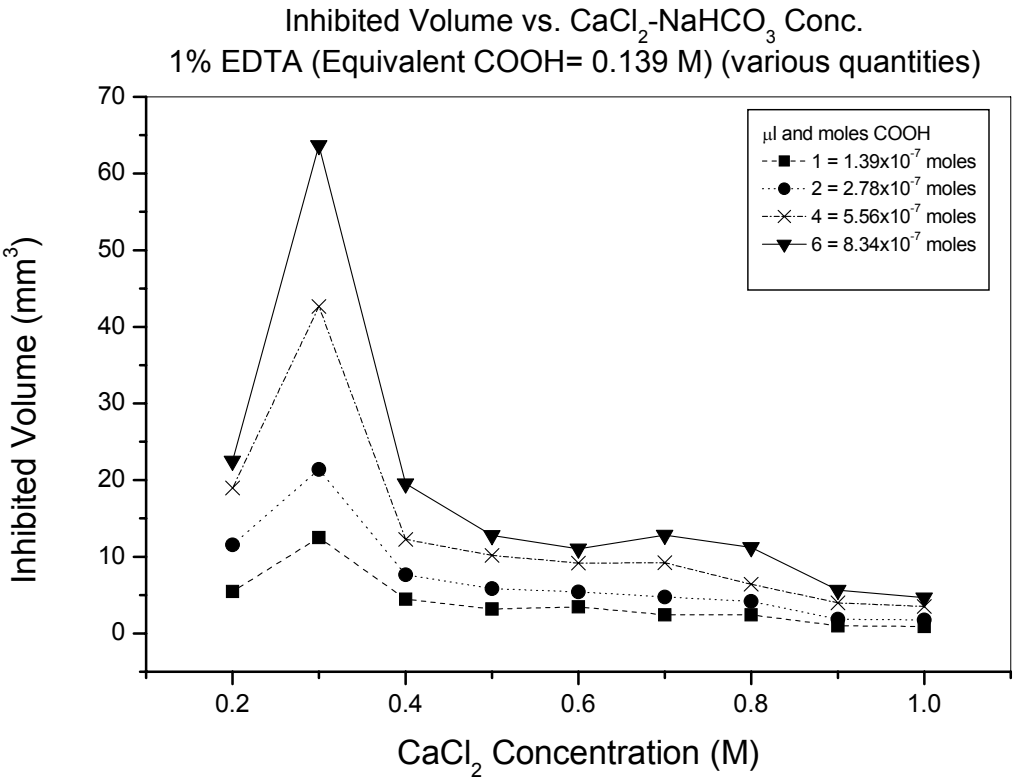

Figure 7.39 Inhibited volume vs. the molar concentrations of calcium chloride-sodium bicarbonate (0.2 M to 1.0M). Data is present for 1% EDTA (0.139 M COOH groups) at various injection quantities. The legend shows the equivalent numbers of COOH moles injected at each point.

Figure 7.39 provides the basis for the calculation of effective COOH molarity and the subsequent comparison to the molar quantities of calcium ions. Table 7.5 shows the calculated data for the 0.4 M concentration point for 1% EDTA.

Table 7.6 Table of 1% EDTA data at the 0.4 M concentration point of calcium chloride and sodium bicarbonate. Resulting data for moles COOH dispensed, area inhibited, volume inhibited, effect molarity of COOH and molar ratios of COOH/Ca ions.

0.4 M calcium chloride
1% EDTA

Quantity of Inhibitor (µl)	moles COOH dispensed	Area Inhibited (mm^2)	Volume Inhibited (ml)	Effective COOH Molarity(M)	Molar Ratio COOH/Ca ions
1	1.39E-07	9.09	4.476	3.11E-05	7.76E-05
2	2.78E-07	15.51	7.635	3.64E-05	9.10E-05
4	5.56E-07	24.96	12.287	4.53E-05	1.13E-04
6	8.34E-07	39.71	19.545	4.27E-05	1.07E-04

As was mentioned previously, in all the regimes, PAA, AA and EDTA, the resulting molar ratios of COOH/Ca ions represented an important data parameter. If initial hypotheses were correct the numbers of COOH to Ca ions should provide a direct comparison as to degree of inhibition of calcium carbonate crystals. However, it is seen that the molar ratios are highly in favor of the calcium ions. It is important to take into account the valency requirements for the calcium plus-2 ions versus the negative-1 net charge of the COOH ion group. With a 2:1 requirement of COOH:Ca ions the effective concentration of COOH ions is reduced further.

It is important here to explore in brief detail some of the mechanisms involved in the inhibition of the calcium carbonate growth. Such an explanation readily lends itself to understanding the processes of calcium carbonate crystal growth inhibition that is shown in the gel mineralization work.

Although initially the inhibition was expected via binding of the $COOH^-$ to Ca^{+2} ions the true mechanism may be a bit different. Work has been put forth both experimentally[155] and via atomistic simulations[156] that indicates that the COOH ions may not be inhibiting via direct binding of Ca^{+2} but more due to OH^- groups within the COOH functionalities binding to calcium carbonate crystals and interfering with growth. This suggests that the COOH is not a nucleation inhibitor but more of a growth inhibitor. However, the growth is inhibited in such a way that the calcium carbonate nucleates but then upon growth the COOH functionalities bind to the developing crystal and then inhibit or modify the growth. The developing crystals that don't reach the critical cluster size are not visible to the microscopic techniques that were used. The additives with the COOH functionality essentially reduce the number of active growth sites via adsorption on the crystal surfaces. This also leads to increases in induction times defined as the time required for initial nuclei formation[157]. The induction times were not measured in the gel mineralization studies.

In atomistic simulations[156] it is shown that various additives, of COOH groups and other molecules with OH^- groups, the additive functional groups indicate a preferred adsorption on the step edges of the growing calcium carbonate crystal. The stronger attachments between the calcium carbonate cluster and the adsorbate occur in positions where the organic molecules can form multiple interactions with the surface species, especially if it allows for a bridge between two calcium ions from and edge to a terrace below[156]. The carboxylic acids are good growth inhibitors, as was shown in the gel mineralization assays, as they effectively replaces the water at the experimental growth

steps and hence block the sites preventing further addition of calcium carbonate material. If the =O and OH- groups are spread over two carbons the interaction is enhanced and hence a bridging interaction occurs between a step and terrace[156].

This analysis indicates that in the current gel studies the $COOH^-$ is not just binding to available free calcium ions and inhibiting the nucleation. However, it does support recent work based on atomistic and experimental analysis that the COOH groups function as inhibitors by interfering with calcium carbonate growth as opposed to nucleation. The calcium carbonate clusters are formed but before reaching the critical clusters sizes the COOH groups adsorb onto the growth fronts, including the terraces and steps of the developing calcium carbonate clusters [156, 158].

It is interesting to note that determining general trends of inhibition is rather difficult to pinpoint. All three regimes show spikes initially where the calcium carbonate and sodium bicarbonate concentration are low e.g. specifically at the 0.2-0.3 M range. However, from the 0.4 M to the 1.0 M range of concentrations the behavior is slightly more consistent with a somewhat slight decline as the precipitating salt concentration increases and approaches the 1.0 M point.

7.5.1 Salting out effect in agarose gels

The previous section showed plots of the inhibited area and volume as affected by injections of quantities of PAA, AA, and EDTA. These molecules were dispensed such that 0.139 molar equivalents of COOH functional groups were dispensed at various selected quantities. The results indicated an effect of inhibition throughout a

concentration regime of calcium chloride-sodium bicarbonate precipitating salts. However, it was interesting to note that the 0.3 M concentration point the effect of inhibition peaked and the subsequent higher concentrations (0.4 -1.0 M concentrations of calcium chloride-sodium bicarbonate) had little variation in inhibited area and volume. Initial thoughts were that an issue with the concentrations of the salts and inhibitors were the primary contributors but additional analysis indicates that the contributing factor is most likely the fact that the calcium chloride was incorporated into the agarose/water mixture. It is important to analyze the potential effects of the calcium chloride on the agarose gel to explain the limitations of effects of the inhibitors at the higher concentrations of the precipitating salts. Figure 7.40 illustrates the basic structure of the agarose molecule.

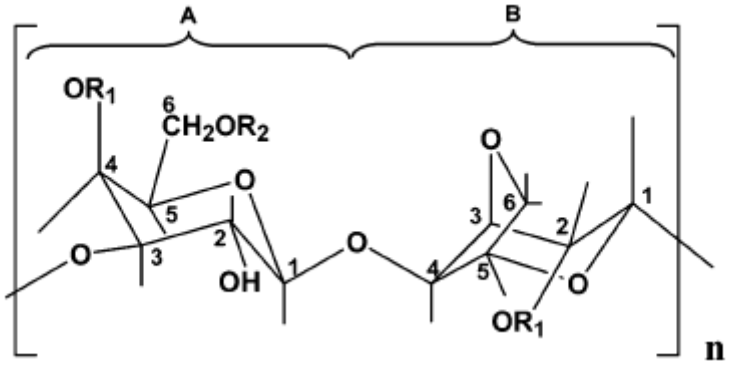

Figure 7.40 An idealized AB repeat unit of agarose. (A) 1,3 linked β-D galactose residue (B) 1,4 linked 3,6-anhydro-α-L-galactose residue. In native agarose $R_1=R_2=R_3=H$. Adapted from Xiong et al [120].

The agarose gelation mechanism may be described in three distinct stages (Figure 7.41): induction stage, gelation stage and the pseudoequilibrium stage and can be briefly

represented in the schematic in figure 7.41 [120]. Agarose gelation is initiated by a nucleation and growth mechanism and the kinetics of the gelation are determined by the formation of nuclei of polymer-rich phases, aggregation of agarose chains with the polymer-rich phase and the local coagulation of the polymer-rich phases [120].

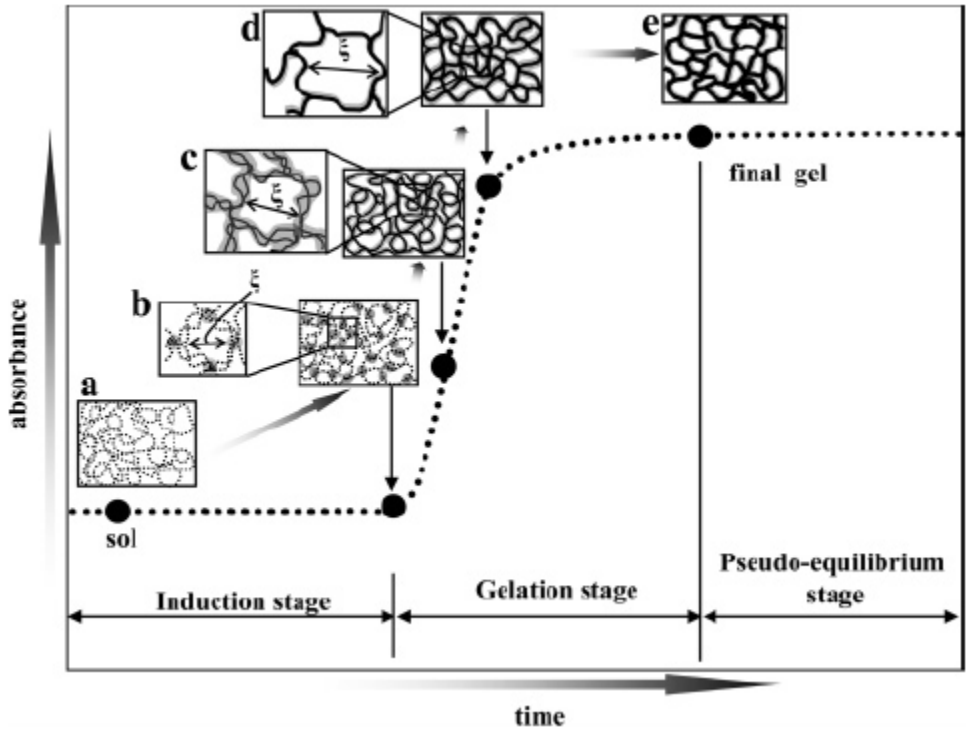

Figure 7.41 A schematic representation of the gelation mechanism of agarose gel[120].

It is within the gelation stage that the presence of calcium chloride may play a role in altering the resulting properties of the agarose gel. Figure 7.42 shows the effects of a low concentration (6.8 mM) of $CaCl_2$ on the dynamic modulus of agarose (0.08%). There is a significant variation in dynamic modulus of the plain agarose as compared to the agarose with $CaCl_2$ as the $CaCl_2$ contributes to an order of magnitude increase. As the

temperature increases the general behavior of the plain agarose is similar to that with $CaCl_2$, however the difference in the dynamic modulus remains an order of magnitude different[159]. This is attributed to the salting-out effect, which likely occurs due to an increase in rigidity of the molecular chains that is increase by intra- and inter-molecular hydrogen bonds of the anhydro-α-L-galactosyl residues[159, 160]. The influence of the

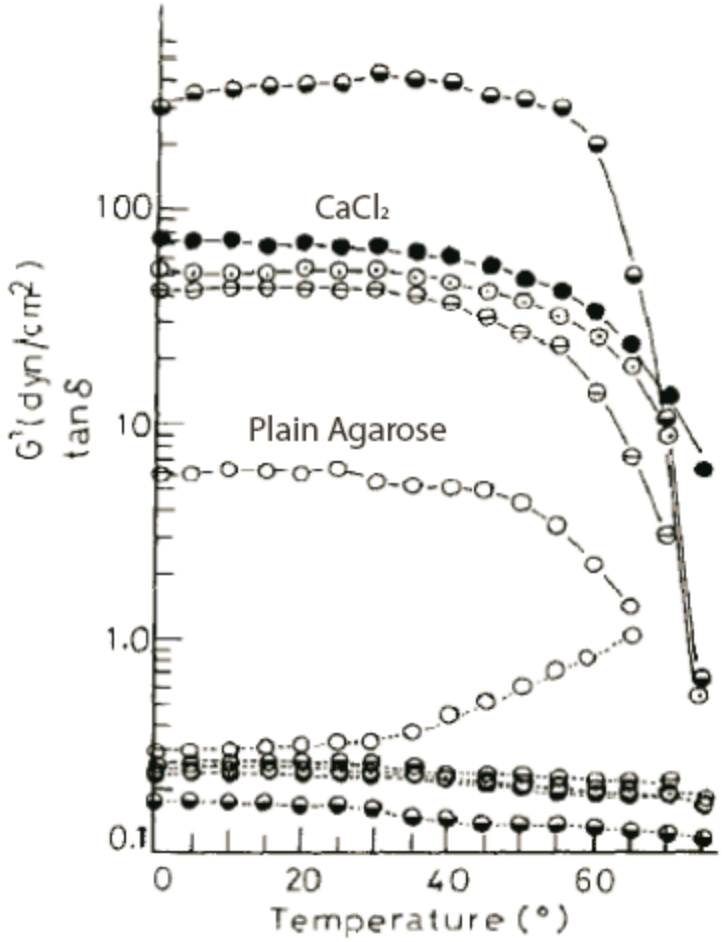

Figure 7.42 The graph shows the effects of temperature on the dynamic modulus for a 0.08% solution of agarose (○ – open circle). The data set of interest is represented by the addition of 6.8 mM $CaCl_2$ represented by the solid (● - filled circles). The solid lines between the points refer to the dynamic modulus and the broken lines refer to the tan δ. The tan δ values differ for the plain agarose versus that with the calcium chloride. However, in the graph, the data points are overlapping at the bottom and hence are difficult to see. Adapted from Tako[159].

$CaCl_2$ likely provides a change in the gelation behavior and transport properties of the resulting gel due to effects between the calcium and the OH^- groups of the agarose gel. The resulting gel is stable and did not inhibit the precipitation of the calcium carbonates

via the subsequent addition of sodium bicarbonate, however, the diffusion of the carbonates and inhibitors may have been affected. The solubility product constant, $K_{sp,}$ of $CaCO_3$ is 3.36×10^{-9} and hence if the transport properties within the gel are affected this may contribute to reduced calcium carbonate growth. This may explain the limited volume of inhibitions due to limited diffusion of the carbonates and inhibitors into the gel depth. The concentrations of both the calcium chloride and the agarose were significantly higher in the gel mineralization assay and hence the salting out effect was likely more pronounced. Additionally, the salting out effect accounts for particular observations that at first may appear to be counterintuitive regarding the EDTA influence on the calcium carbonate inhibition. The stability constant of the EDTA-Ca ion complex is 10.70, indicating a very strong and stable complex[161]. The limitations on the diffusion organic molecules throughout the agarose likely contribute to the limited effect of EDTA to calcium ion binding and hence limit the effect of inhibition by EDTA on the resulting calcium carbonate growth.

With this in mind it is noteworthy to look at its relevance once again as pertaining to the visible differences in the zones in the gel mineralization pictures(Fig. 7.33 as repeated below). Since the effect of the inhibitor is dependent on the diffusion of the molecules throughout the gel media the salting-out-effect likely plays a role. The expected diffusion profile would likely result in zones that are not as clearly defined e.g. current data show sharp cutoff/transition points and there would likely be zones in which the modified/inhibited zone would slowly transform into the unmodified zone but with more and more crystals slowly appearing and giving a gradual change.

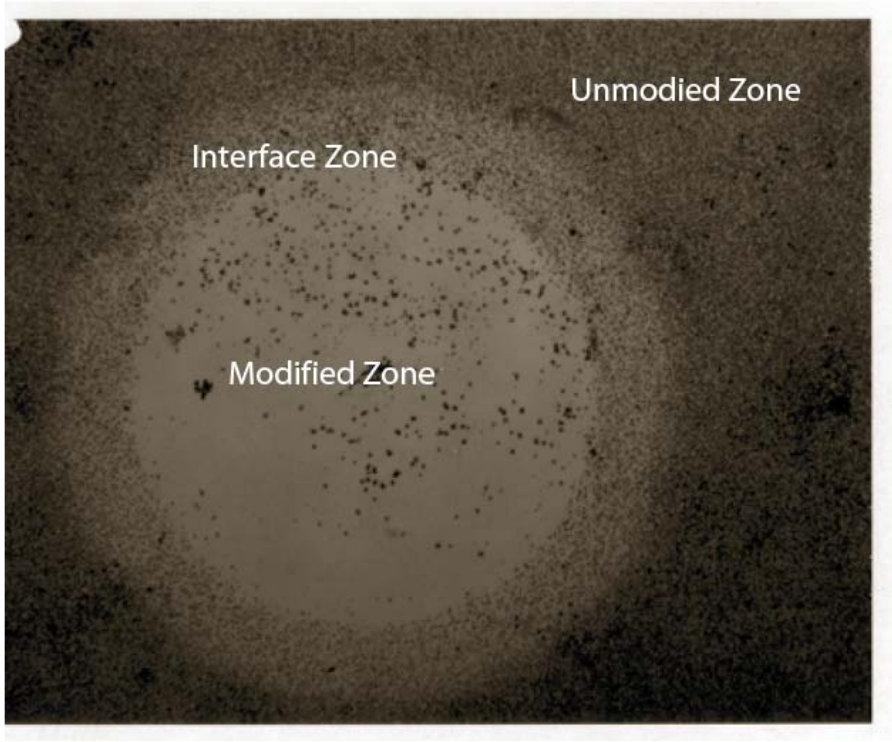

Figure 7.42 The image(also figure 7.33) showing the various zones in the gel mineralization assay. The modified zone diameter is on the order of 5 mm.

In this case it appears there appears to be an abrupt change thus indicating that there some threshold concentration at which point when the inhibitor concentration falls below this the salting out effect likely contributes to the limited diffusion once the concentration of the inhibitor falls below the presumed threshold value. A more thorough analysis of the diffusional aspects of the gel mineralization assay are critical to future success and application of the assay.

7.6 Future Work in the Salting-out effects analysis

In order to better understand the salting out effects in the agarose further experimentation and characterization is required. Initially, a concentration range around 0.2-0.4 molar for the calcium chloride would be necessary. Selecting much smaller

concentration intervals would give a more accurate point at which a noticeable effect takes place in terms of an inhibited volume plateau point.

Additionally, in order to more thoroughly characterize the gels, small angle x-ray scattering would provide insight towards the structural variations induced by calcium chloride concentrations.

7.7 Conclusions

Series 2 confirms that the gel mineralization approach is a viable method for screening of organic molecules that exert an inhibitory effect on the growth of calcium carbonate minerals. However, several inconsistencies do arise. Although quantitative data are extensive no definite trends are notable. Somewhat anomalous behavior arises at the 0.3 M concentration regime showing a spike in terms of inhibited areas and volumes.

The controlling factor does not appear to lay purely in the COOH/Ca ion ratios where it was thought that increasing the number of COOH groups per calcium ion groups will have direct influence on inhibiting calcium carbonate growth. In regards to a quick analysis the low COOH/Ca ratios should indicate higher overall inhibition. The ratios in all the regimes do not fully support the expectations. In several cases, including the PAA regime the COOH/Ca do not vary much when compared to quantities of the inhibitor yet a large difference in inhibited areas and volumes is detected.

As was mentioned in the discussion section the COOH functional groups appear to act not by binding directly to the free calcium ions but to the calcium carbonate clusters of which many may not reach the critical cluster size, and those that do will be

inhibited in further growth due to COOH group adsorption onto the growth fronts. Additionally, a salting-out effect of the agarose gel inhibits diffusion processes after certain concentration levels of the precipitating salts are achieved. Although the salting-out effect presents some limitations the gel mineralization assay is still a viable method for screening effects of organic molecules on the growth of calcium carbonate.

Additionally, as was mentioned in a previous section the overall future success and application of the gel mineralization assay would be strengthened by detailed studies of the diffusional dynamics of the system, in regards to the modifier/inhibitor as well as the precipitating salts.

8.0 GEL MINERALIZATION SERIES III

8.1 Introduction

In this chapter the continuing experimentation with the gel mineralization assay is performed. Previous work in Series 1 and Series 2 proved to be conclusive in terms of further proving the utility of the gel assay. However, neither one has provided strong enough results to provide solid footing for consistent predictable behavior.

In this Series 3 of the gel mineralization the overall setup is similar with several changes made to the setup. Calcium chloride is incorporated into the gel setup and subsequently developed with sodium bicarbonate following inhibitor addition. Previous experiments were done with 2.2% agarose and corresponding pH 10.3 for the precipitating salt solutions and in this chapter some comparisons are done with 1.1% agarose to see any effects of the gel concentration on area/volume of inhibition.

One of the primary goals of the gel mineralization assay was to develop a screening method to determine the effects of various organic molecules and functional groups on the formation of important biominerals such as calcium carbonate and potentially other calcium based biominerals. Additionally, once particular molecules are chosen the methodologies may be readily applied to such applications as free form fabrication of mineralized parts. Such uses lend themselves to simplified processing and hence altering the gel mineralization process for speedier execution may be desired.

In the previous experiments polyacrylic acid was shown to be an able inhibitor in a wide range of concentration regimes and quantities. Inhibition was seen throughout the

tests. Polyacrylic acid has abundant numbers of –COOH groups and has been shown to effect modification in calcium based mineral formation. Additionally, it has been shown that particular pyrophosphates are active in vivo and in vitro in terms of affecting calcium based mineralization.

8.1 Test Setup and Conditions

This Series 3 of data indicates experimentation with Tetrasodium Pyrophosphate(TSPP) along with comparison tests with polyacrylic acid. However, particular changes were made in terms of the final conditions. To improve in overall processing time as pertaining to potential applications in freeform fabrication particular steps were taken to speed processing. The precipitating salts of calcium chloride and sodium bicarbonate are no longer adjusted to pH 10.3 and instead are mixed as is at given concentrations. Such conditions still resulted in formation of calcium carbonate crystals with no detectable variation in final form. XRD patterns match up with the previously mentioned XRD data.

In addition to altering the pH conditions a new agarose gel concentration was added, 1.1% agarose and 2.2% agarose are used. The pH adjustments were also made in order to help determine if any of the data in previous Series may show significant change when pH is changed. The alterations in gel concentration were incorporated simply to determine effects of the gel concentration in terms of its diffusion as interpreted through the relative areas and volumes of inhibition.

As per previous work the concentration of salt solutions ranged from 0.1 M to 1.0 M, the quantities of inhibitor that were deposited are 1, 2, 4, 6 µl. The remainder of the setup and procedures are identical.

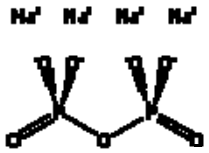

Figure 8. 1 Chemical Structure of tetrasodium pyrophosphate(TSPP). $Na_4O_7P_2$ - Note the confirmation of the molecule and directionality of the oxygen groups.

8.2 Results and Discussion

The data are now presented for the PAA and TSPP systems. It is interesting to note that while PAA was shown to be highly effective in the pH 10.3 regime its effect was greatly diminished and almost negligible in this case. In the 1.1% agarose system the effects were not even reported as they were highly inconsistent and sporadic. The no pH adjusted 2.2% agarose regime provides a direct comparison to the 2.2% pH 10.3 series and with no pH adjustment the effect of PAA is greatly altered. As with the previous systems the area and volume of inhibition increase as greater quantities of inhibitor are added yet at 1 µl for the regime without pH adjustment there is no consistent effect. However, as the area and volume inhibited effect are analyzed as the salt concentrations are increased an opposite effect is detected. The area and volume

inhibited decrease as concentration was increased. At concentrations higher than 0.5 M there was no consistently detectable inhibition effect.

The TSPP samples indicate a more consistent inhibitory effect. However, the quantities of the volumes and areas inhibited are of smaller magnitude. No significant changes were detected as 1.1% agarose in comparison to 2.2% agarose.

8.2.1 PAA data

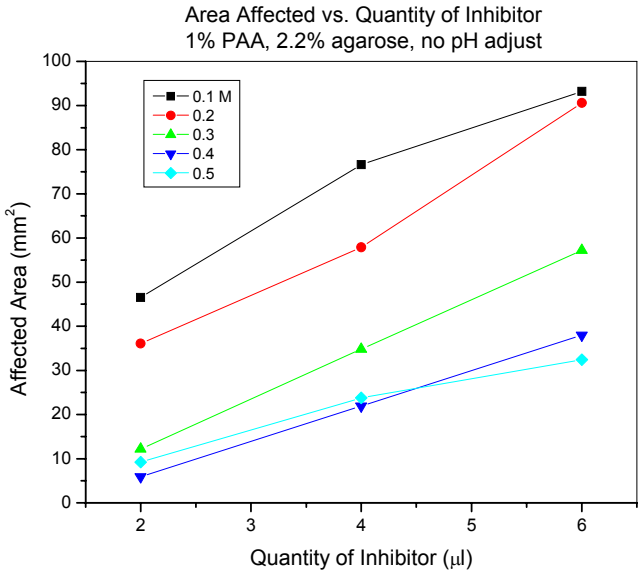

Figure 8.2 Area affected(mm^2) vs. Quantity of inhibitor, 1% PAA injection quantities of 1,2,4,6 µl. A concentration regime for calcium chloride/sodium bicarbonate or 0.1 M - 1.0 M was used however there was no observable effect of inhibition for concentrations above 0.5 M.

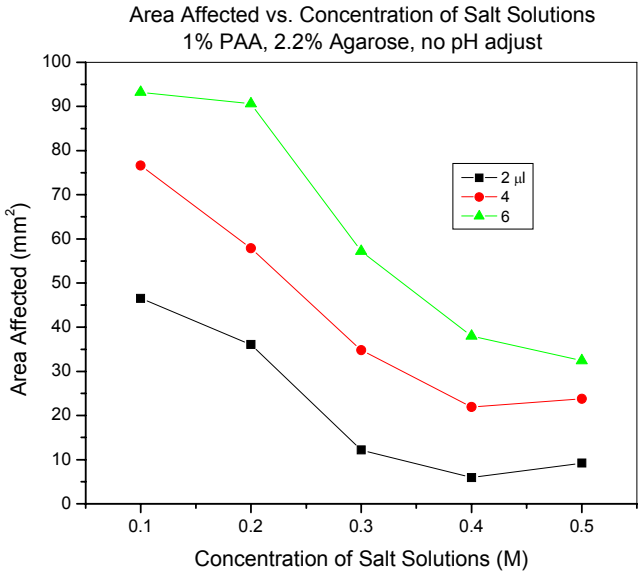

Figure 8.3 Affected area(mm^2) vs. Concentration of Calcium chloride/sodium bicarbonate(0.1 -0.5 M). For 1% PAA injections into the gel. No observable effect at injection quantity of 1 µl but observable effect is present for injection quantities of 2,4,6 µl. Note the greatest inhibition occurs at low salt concentration and slowly decreases. Appears to be proportional effect based on the quantity of injection.

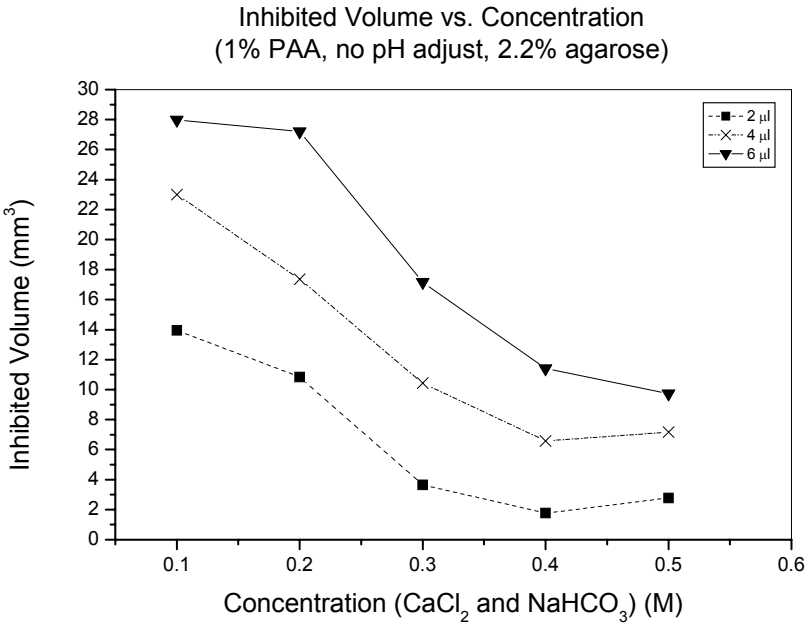

Figure 8.4 Inhibited volume (mm^3) vs. Concentration of calcium chloride/sodium bicarbonate(M). Concentration range of 0.1 M to 0.5 M. As expected the data trends similarly to the area affected presented in the previous graph.

This series of testing PAA with no pH adjustment of the precipitating ion salts present behavior contrary to the pH 10.3 series of data. The PAA effect is negligible in the higher solution concentrations after 0.6 M. No immediate explanation is found. The behavior amongst the lower concentrations is somewhat analogous to the high pH 10.3 series of the previous chapters but the disappearance of the effect after 0.5-0.6 M concentrations is inconclusive.

8.2.2 TSPP data, 1.1% agarose

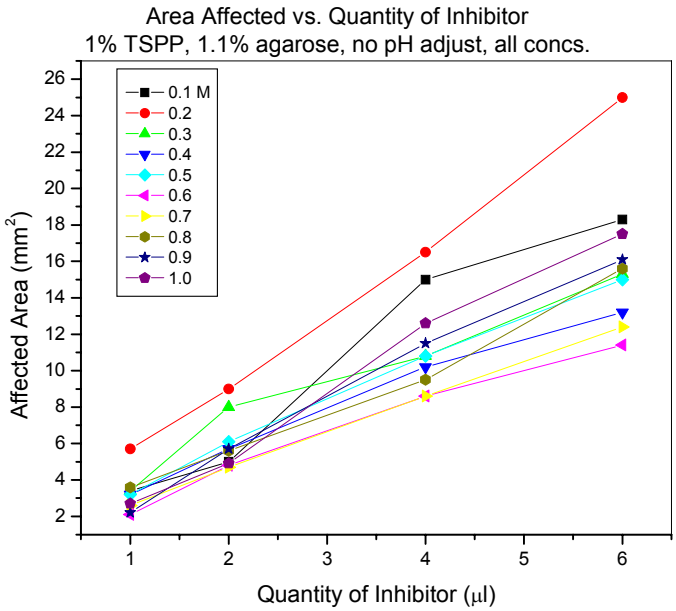

Figure 8.5 Affected area(mm^2) vs. Quantity of Inhibitor(1,2,4,6 µl) of 1% TSPP with 1.1% agarose gel concentration. Somewhat anomalous behavior is apparent in the 0.2 M range instead of 0.3 M in previous series. Data is shown for full range of calcium chloride/sodium bicarbonate concentrations of 0.1 -1.0M solutions. The pH of the precipitating salts was not adjusted.

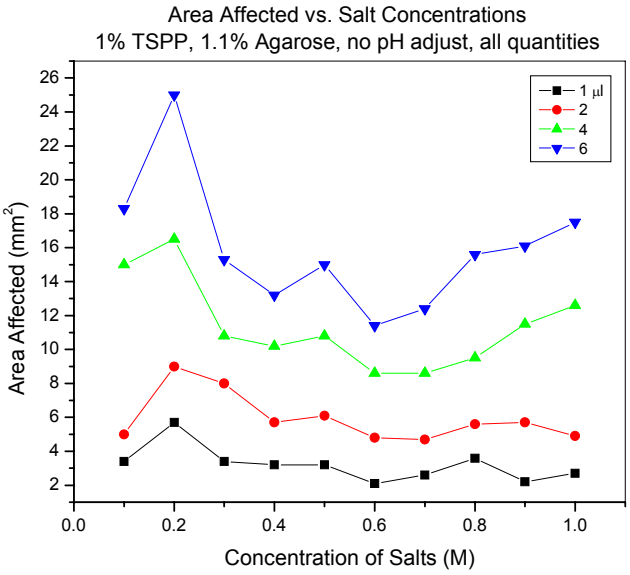

Figure 8.6 Area affected (mm^2) vs. Precipitating salt concentrations of calcium chloride/sodium bicarbonate. Concentration range from 0.1 M to 1.0 M. For 1% TSPP injections of (1,2,4,6 µl). Note that somewhat analogous to previous pH adjusted regimes the inhibition is somewhat more 'controlled' at the lower quantities of 1 and 2 µl and at the higher injection quantities there is less consistency. Once again it is noted that there is a peak of inhibition at the 0.2 M concentration point. Previously this occurred with a the pH of each salt at 10.3 and in this case there was no pH adjustment and is also with a different inhibitor.

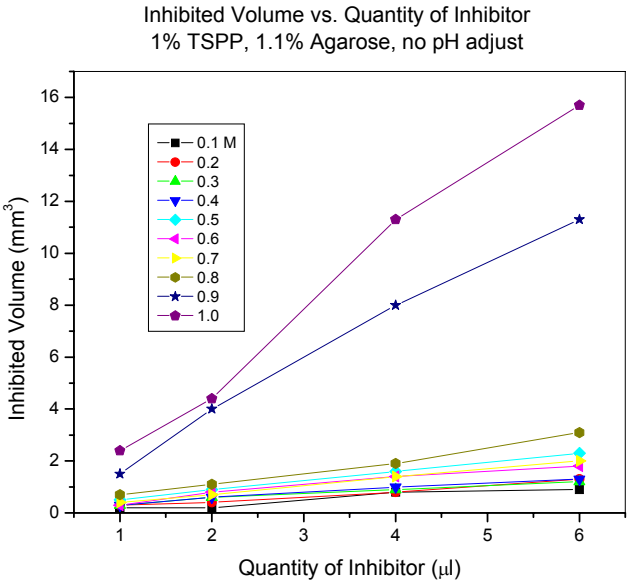

Figure 8.7 Inhibited volume (mm^3) vs. Quantity of inhibitor(1,2,4,6 µl) of 1% TSPP. Shown for concentrations of 0.1 M – 1.0 M calcium chloride/sodium bicarbonate without any pH adjustment. The highest inhibition is shown at 1.0M and 0.9 M concentrations. That important note again is that the volume measurement provides less overall consistency as the depth of penetration of the crystal growth presents inconsistencies and average depths are taken.

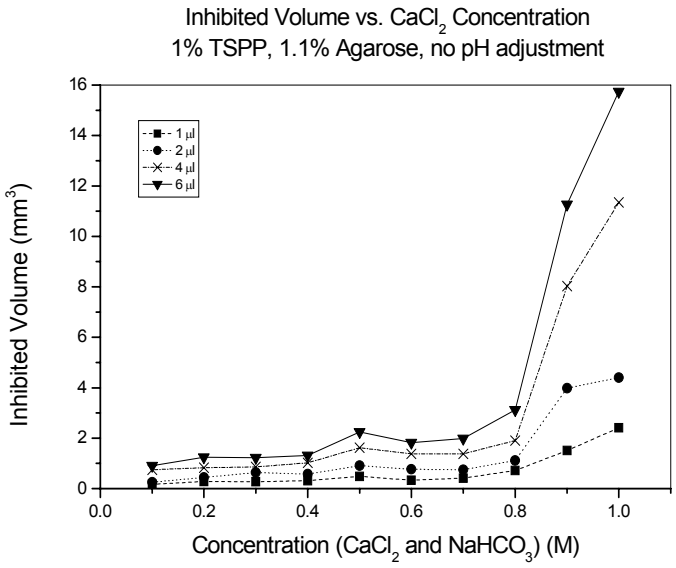

Figure 8.8 Inhibited volume (mm^3) vs. calcium chloride/sodium bicarbonate concentration ranging from 0.1 – 1.0 M. Quantity of 1% TSPP inhibitor in the following quantities(1,2,4,6 µl). Greater inhibition is seen at higher concentrations somewhat nearly contrary to the pH 10.3 results.

8.2.3 TSPP data, 2.2% Agarose

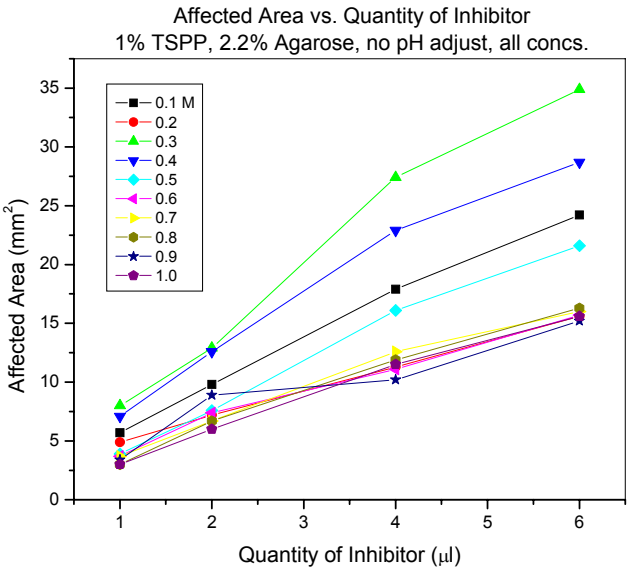

Figure 8.9 Affected area(mm^2) vs. Quantity of inhibitor(1,2,4,6 µl) for 1% TSPP. Data is shown for full concentration range of 0.1 M – 1.0 M of calcium chloride/sodium bicarbonate precipitating salts. As was seen with the previous tests with 1% PAA, 1% AA and 1% EDTA in pH 10.3 adjusted solutions there is a spike here at the 0.3 M concentration point. It suggests that the gel concentration being the only static variable plays a determining role at the 0.3 M concentrations.

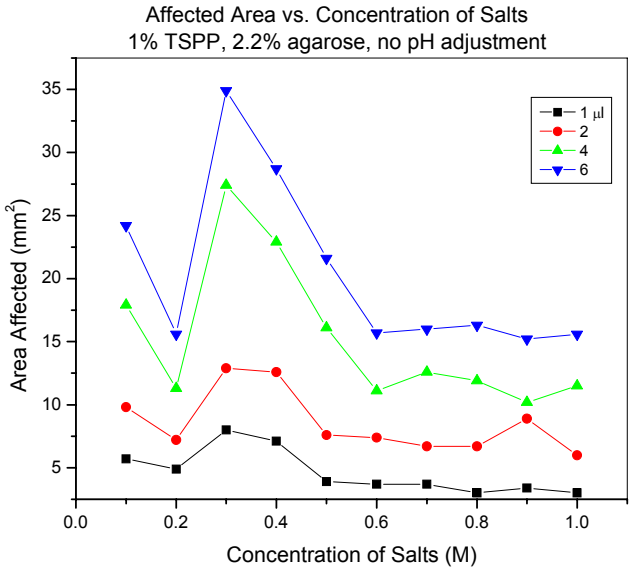

Figure 8.10 Affected area(mm^2) vs. Concentration of calcium chloride/sodium bicarbonate from 0.1 M to 1.0 M. For 1% TSPP injection quantities of (1,2,4,6 µl). Once again the spike at 0.3 M is apparent. At the lower quantities of inhibitor injection the spike is not as steep as with the 4 and 6 µl quantities.

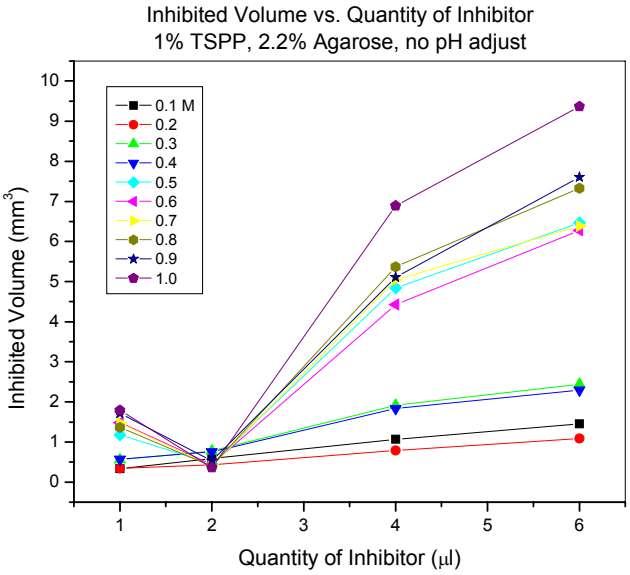

Figure 8.11 Inhibited volume (mm^3) vs. Quantity of inhibitor for (1,2,4,6 µl) of 1% TSPP. Data is shown for full concentration regime of 0.1 – 1.0 M calcium chloride/sodium bicarbonate solutions. Note the higher inhibition at the higher injection quantities. However the sheer quantities are much smaller than with the pH 10.3 regimes of the previous chapters.

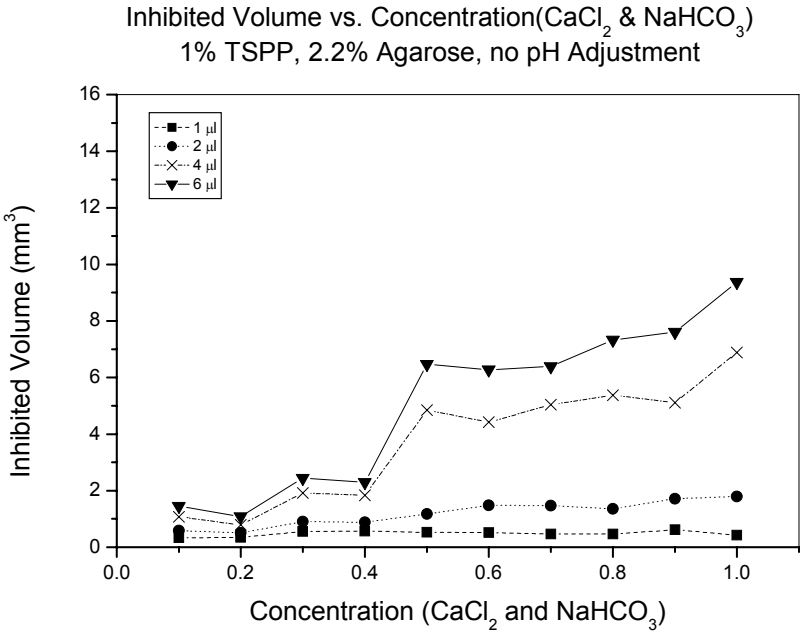

Figure 8.12 Inhibited volume(mm^3) vs. concentration of calcium chloride/sodium bicarbonate from 0.1 M to 1.0 M. For injection quantities of (1,2,4,6 µl). Note a fairly consistent volume inhibition is apparent for the lower injection quantities. The salient point is that there is some general trending of inhibition. However the overall absolute quantities of inhibition are far less than with the regime of pH 10.3 adjusted samples.

8.3 Conclusions

Series 3 shows once again that the gel mineralization assay is a viable protocol for the screening of organic molecules to determine their effects on formation of calcium minerals. The data in this Series show that TSPP is a viable inhibitor and appears to offer some form of predictability and control. However, no clearly apparent quantification is made. In Series 2 it was shown that particular, perhaps anomalous, spikes in inhibited area/volume occurred at the 0.3 M concentrations. In Series 3 this was once again

apparent with the TSPP but not with the PAA which showed this behavior in Series 2. This TSPP behavior was only shown in the 2.2% agarose setup much like in Series 2. Despite the fact that there were no pH adjustments both Series indicate this behavior at 0.3 M salt concentrations. Although the pH adjustments were not made in this regime the salting-out effect, as was previously mentioned in Chapter 7, may be playing a role.

Figure 8.8 (1.1% agarose) and figure 8.12 (2.2% agarose) show provide interesting comparisons. In both regimes there is a somewhat consistent behavior in which greater inhibitor quantities provide greater volumes of inhibition. In the 1.1% agarose system a significant jump occurs at 0.8 M solution concentrations while the 2.2% agarose shows somewhat of a jump at 0.6 M. The 2.2% system provides a denser gel network to perhaps provide a limit to diffusional distance.

The most definitive conclusion of these results is that the gel mineralization proves useful in identifying potential molecules that will inhibit calcium carbonate growth.

9.0 ORGANIC MOLECULE SCREENING IN GEL MINERALIZATION ASSAY

In the continuing efforts to gain more utility from the gel mineralization assay a somewhat qualitative approach is taken. This section describes efforts to utilize the agarose gel system to make rapid determinations of organic molecule effects on formation of calcium carbonates. One of the initial goals was to determine a method for making biocomposite-biomineralized parts via free form fabrication methodologies. The previous chapters described in more quantitative details the effects of the inhibitors. In practice there may be instances in which the end parts are subject to varying chemical environments in vivo or in vitro. In certain cases a with free form fabrication application lines may be written in media with chemical entities that may or may not be detrimental to precipitation of calcium carbonate crystals. The approach in this section is to select various organics, in some cases even arbitrarily, to determine what effects these organics will have on the ultimate calcium carbonate formation.

9. 1 Organic Molecule Selection

A range of organic molecules were chosen in a somewhat systematic nature and several were chosen essentially at random. This provides more a qualitative illustration the a gel mineralization assay may be easily executed to find molecules of importance or interest. The motivation behind such a selection method was to illustrate the utility of the mineralization assay as well as it being based on choosing functional groups, such as COOH groups that have previously shown to be active in modifying growth and development of Calcium salts [63, 77, 162]. In chapter 6 it was illustrated that molecules

possessing the COOH functionalities in a chain form, notably PAA vs AA showed a marked difference in overall inhibition/modification of resulting calcium carbonate. The selected molecules include the following (note: not all tested molecules are included) Polydiethyldimethyl ammonium chloride, 1-vinyl-2-pyrrolidinone, polystyrenesulfonic acid-maleic acid sodium salt, polysodium-4-styrene sulfonate, poly(allylamine hydrochloride), polyvinylphosphonic acid, alginic acid, caffeine, Tetrasodium pyrophosphate(TSPP). This is in addition to the previously tested and more thoroughly analyzed polyacrylic acid, acrylic acid and EDTA. The table below provides a quick look at these particular molecules and a remark on whether or not an inhibitory effect had taken place. There are indications that certain molecules play a limited role in affecting the resulting areal crystal formation however few show well defined interfaces.

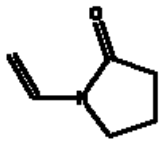

Figure 9.1 Chemical structure of 1-vinyl-2-pyrrolidinone. (C_6H_9NO)

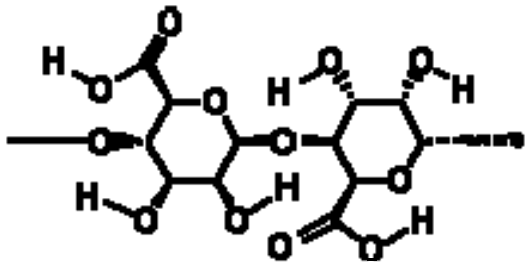

Figure 9.2 Chemical structure of alginic acid. $(C_6H_8O_6)_n$ Note the abundance of COOH-groups. From previous experience it is known that the COOH groups play an inhibitory role in regards to calcium carbonate growth.

Table 9.1 Summary of Modifier and subsequent effect on crystal growth

Identifier/ Code	Molecule Name	Inhibitory/Modified Effect
M1	Polydiethyldimethyl ammonium chloride	No
M2	1-vinyl-2-pyrrolidinone	No
M3	polystyrenesulfonic acid-maleic acid sodium salt	No
M4	polysodium-4-styrene sulfonate	No
M5	poly(allylamine hydrochloride)	Limited effect
M6	polyvinylphosphonic acid	No
M7	alginic acid	Yes
M8	caffeine	No
M9	tetrasodium pyrophosphate	Yes

9.2 Results

Ultimately it was once again proven that the COOH functionality played a major role in the resulting precipitation of calcium carbonate. Alginic acid is a molecule comprised of carboxyl group functionality. Additionally, as was illustrated in a previous chapter tetrasodium pyrophosphate also proved to have an influence.

The results of this phase of the gel mineralization screening assay are presented in the form of images taken via optical microscope and images were taken with an attached

digital CCD camera. Magnifications are on the order of 50x. The images show uninhibited/unmodified areas as compared to areas in which selected molecules were injected into the gel. Visual inspection of the resulting images provides indications of relative areal coverage of crystals. Although a qualitative analysis is the ultimate approach the regime of concentrations was very thorough. The gel concentrations varied were set at either 1% agarose or 2% agarose. Within each agarose concentration regime calcium chloride-sodium bicarbonate salt concentrations were in a range of 0.1 M to 1.0 M. As expected from previous experiments higher areal coverage and areal density of crystals is present at higher concentrations. The variations in the images are noted as per control images where no external organic was added hence providing an area of pure calcium carbonate formation. A large number of pictures were taken but only representative ones are presented here. For ease of comparison only select images from the 0.5 M concentration ranges are presented and agarose concentration is either 1.1% or 2.2%.

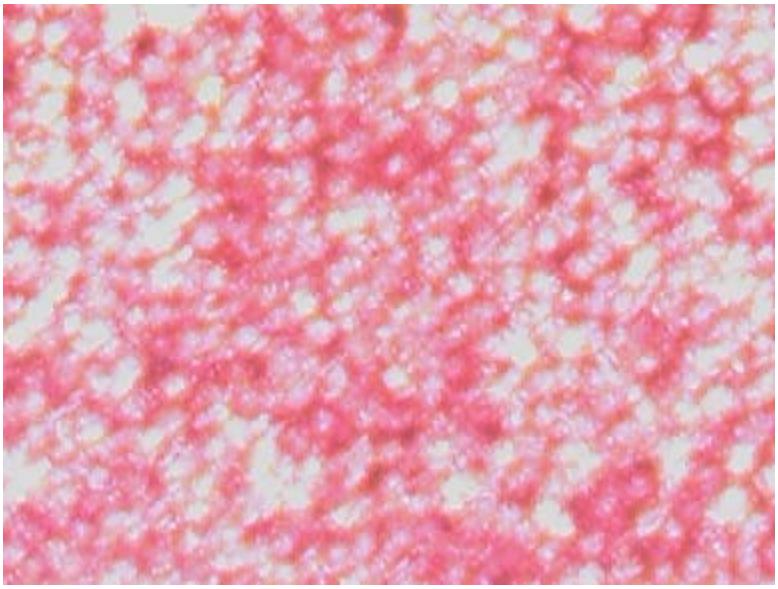

Figure 9.3 Picture shows agarose gel with calcium carbonate crystals as result of calcium chloride/sodium bicarbonate precipitation. No inhibitors/modifiers were added hence picture serves as a control image for comparison. Transmission mode is used. 0.5 M salt solutions. 1.1% Agarose.

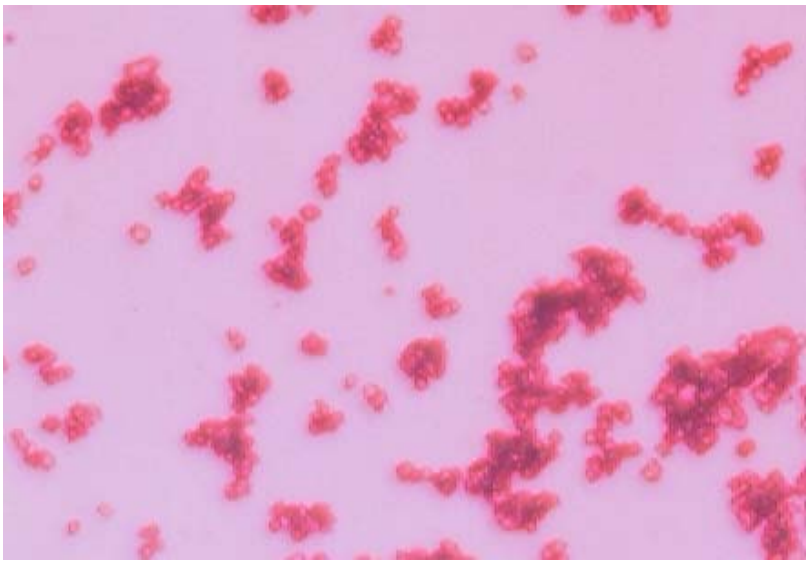

Figure 9.4 Image indicating inner portion of ring of inhibition. 1% PAA injected area. Note, as compared to Figure 9.1 there is significant reduction of crystals in terms of areal coverage.

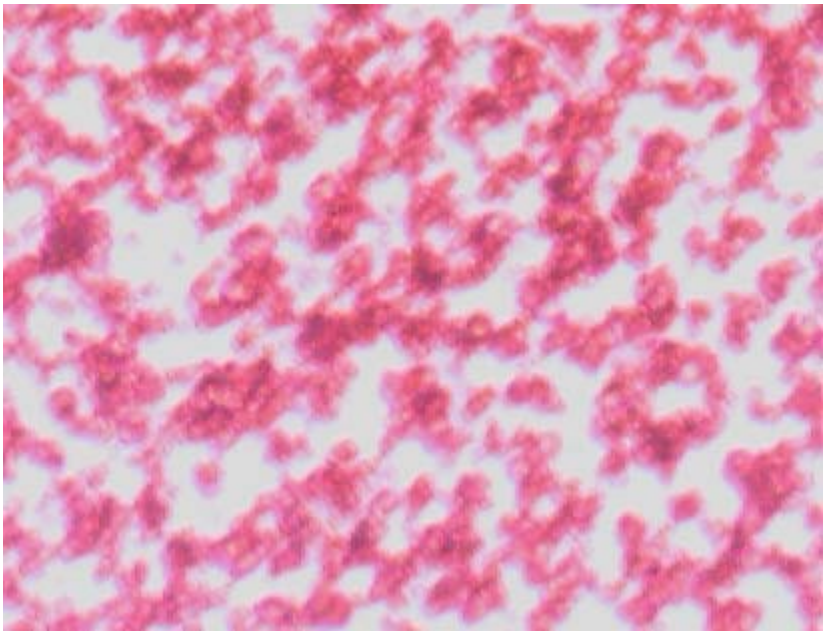

Figure 9.5 Image shows an outer ring area in which polyacrylic acid was injected. Shown as a comparison to indicate the near complete lack of crystals as per inhibition induced by polyacrylic acid. 0.5 M salt solutions. Somewhat apparent to see less areal coverage of crystals.

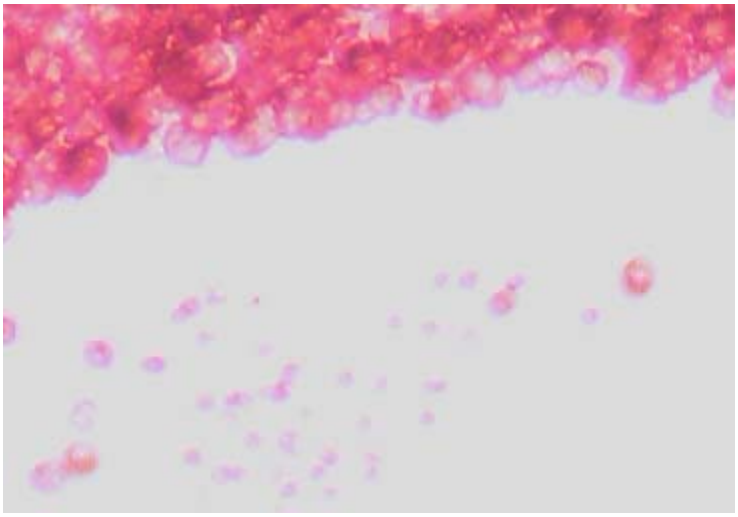

Figure 9.6 Image showing effects of alginic acid. Presence of COOH groups. This shows a well defined interface of crystal formation versus inhibition.

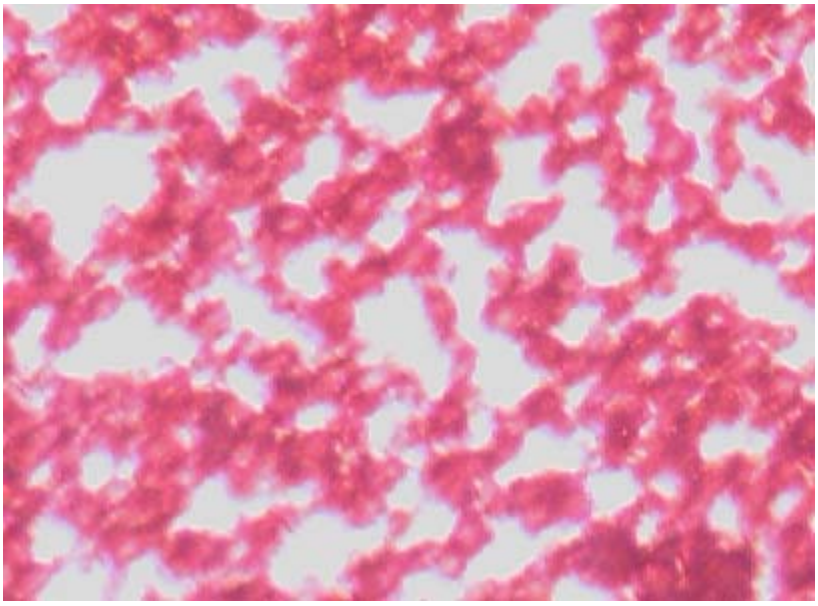

Figure 9.7 Image shows effect of molecule M5(poly(allylamine hydrochloride)) from above table. Inspection of the image indicates some inhibitory effects as the areal coverage of crystals is less than that of the control image/test.

9.3 Conclusions

This chapter concludes that utilizing a gel mineralization assay as a screening method for determining effects of various organic and inorganic molecules on the effects of calcium carbonate formation. With additional resources a more high throughput method may be developed with a greater emphasis on quantification.

10.0 GEL MINERALIZATION AND CALCIUM PHOSPHATES: A QUALITATIVE ANALYSIS

10.1 Introduction

Calcium phosphates are one of the most important inorganic components of all biological hard tissues. When they are carbonate and the form of hydroxyapatite(HA) they are a primary component of bone, teeth and tendons. They provide stability to these entities and also provide hardness and function[163]. Although in nature calcium phosphates may be found in such instances as mineral deposits in occasionally extreme conditions of high pressure and temperature the biological forms of calcium phosphates result in far more mild conditions. In biological organisms the calcium phosphate crystals often form in ambient conditions and are frequently in the nanosize realm[164].

Due to the importance of calcium phosphate growth one of the long term goals of the research was to develop a method for the synthetic formation of calcium phosphate parts. Much like the efforts with calcium carbonate the end goal was to develop biomimetic parts with an emphasis on using a free form fabrication method and understanding the influence of various organic additives on the formation and development of calcium based biominerals, in this case calcium phosphates.

As was mentioned in the original introduction part of the importance of biomimetics is the ultimate development of biologically functional materials synthesized by biological analogous methodologies. Calcium base biominerals such as calcium carbonate and calcium phosphates are very important minerals of numerous biological

organisms. The development of artificial analogues or synthetically produced substitutes is an ultimate goal. With this motivation in mind and the utility of free form fabrication the original effort was to incorporate gel mineralization with free form fabrication. The previous chapters showed success in utilizing the gel mineralization to provide some element of control of calcium carbonate formation in agarose gel systems. This chapter extends the practice and protocols towards the development of calcium phosphates. The calcium phosphates, in hydroxyapatite form, are the primary components of bones and teeth in biological organisms. Hence an effort was made to develop calcium phosphate based minerals in agarose gel systems.

The results that are presented below do not represent in depth analyses of inhibition and modification. For the calcium phosphate system study a more qualitative approach was necessitated.

10.2 Experimental Approach

The initial goal was to develop a thorough agarose gel system to analyze the formation of calcium phosphate minerals and also investigate effects of low molecular weight organic and inorganic molecules on the formation of the phosphate based minerals. However, due to limitation of resources a less thorough and somewhat more qualitative approach was achieved. Calcium phosphate was synthesized with calcium chloride incorporated into the gel and developing ion solutions ammonium phosphate monobasic $(NH_4)_2HPO_4$ at pH 10.3 and also with potassium phosphate monobasic and

pH 10.3. The resulting crystals appeared to be consistent with the hydroxyapatite XRD pattern but certain cases provided the brushite phase of calcium phosphates as well.

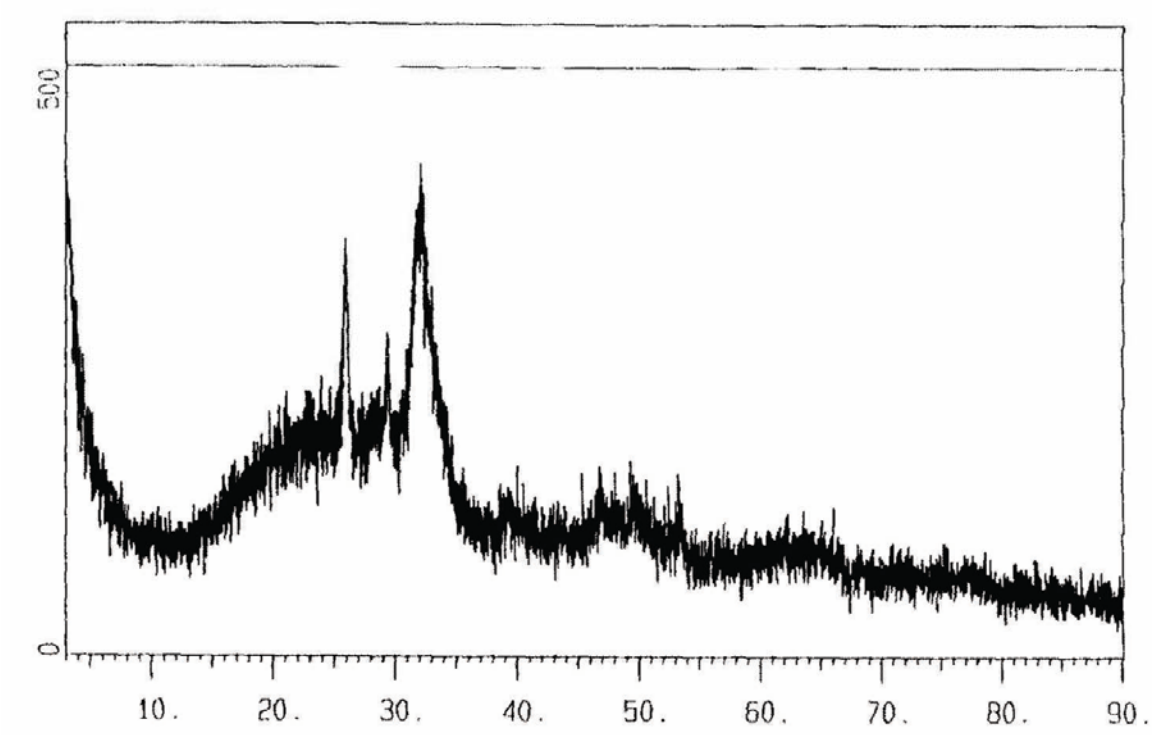

Figure 10.1 XRD pattern calcium phosphate crystals that were grown within and on the gel.

2θ	d/A^o	Reference HA d/A^o	
25.90	3.437	3.440	strong
28.36	3.145	3.170	
29.40	3.036	3.080	medium
31.80	2.812	2.814	strong
32.10	2.786	2.778	strong
32.90	2.720	2.720	strong
34.30	2.612	2.631	medium
39.22	2.295	2.262	medium
41.80	2.159		
45.10	2.009		
46.78	1.940	1.943	medium
48.00	1.894	1.890	medium
50.66	1.800		
53.24	1.719	2.495	medium

Figure 10.2 d-space values for hydroxyapatite reference

10.3 Results and Discussion

The inhibitor/additive molecules of choice included PAA, AA, EDTA , TSPP as per previous experimentation with calcium carbonate gel mineralization studies. Qualitative analysis indicates that the gel mineralization assay may be applied to understanding inhibitory effects of organic molecules on the formation of calcium phosphate crystals. The gel mineralization assay proves to be a viable experimental method to furthering the understanding of calcium phosphate formation. Applications of the work include advancement in developing bone substitutes utilizing biomimetic techniques.

11.0 APPLICATIONS AND FUTURE WORK

The gel mineralization assay proved to be an effective tool for the exploration of understanding the influence or organic molecules on the nucleation and growth of calcium carbonate. There was and observed effect on the formation of calcium phosphates but the results presented were not in such detail as to provide any quantification although via optical microscopy and observation there were apparent differences in the resulting calcium phosphate crystals including variation of the polymorphs including brushite. The end goal would be to develop hydroxyapatite crystals to emulate synthetic bone formation.

Hence it can be said that the gel mineralization assay may be used to determine inhibitory effects of organic molecules. It can be used to directly measure and quantify data such as nucleation rates, including induction times, and growth rates. With more work and more resources the experimental protocols can easily be extended to measure many more type of data. Additionally, with some knowledge of the effects on of the additives on the resulting crystal sizes the gel mineralization method may be used to attempt to grow large numbers of crystals of somewhat uniform size. Uniformity in crystal size may prove highly useful in ceramic processing in which incorporation of uniform sized particle in slurry could lead to improved mechanical properties and enhance functionality of the parts.

11.1 Gel Mineralization and Small Parts Development

In regards to developing parts, one of the initial goals was to utilized the gel mineralization data in developing mechanical parts via solid freeform fabrication. Solid freeform fabrication(SFF) is a methodology for the development or manufacture of parts that is considered one of several methods that fall under the category of rapid prototyping. Although there are numerous methods all conform to the principal of converting a solid or liquid into a singular, somewhat monolithic, structure. The building process is carried out in a layer by layer method until a final part results. The build rates in a typical SFF setup may exceed one layer per minute and have resolutions and layer thickness of 0.1 – 1 mm. SFF is primarily used in manufacture of small scale parts and prototypes and provides an efficient and quick way to develop new parts. Though SFF can be considered for manufacture perhaps its greater strength lies in the production of of limited numbers of highly specialized parts.

Solid freeform fabrication was used to write, synthesize, several test bars using calcium based minerals. The initial work was done with agarose with calcium chloride and subsequent addition of sodium bicarbonate to precipitate the calcium carbonate crystals. The procedures were identical to the gel mineralization assay. However, instead of developing the gels in the Petri dishes the gel-calcium chloride mixture was deposited via the heated syringe in the solid freeform apparatus. Original test bars were made in which 0.5 M each of calcium chloride/sodium bicarbonate and 1.0 M each of calcium carbonate/sodium bicarbonate. The agarose-calcium chloride was written with the SFF machine and after several layers was removed and allowed to cool and gel and then was

developed with an equimolar concentration of sodium bicarbonate solution and allowed to sit for 12-16 hours. Upon expected completion of precipitation the test bars were measured for weight percent of mineral. The 0.5 M regime resulted in 55 wt% mineral while the 1.0 M regime resulted in 58 wt%. These results are favorable as per developing parts with some mechanical integrity.

Preliminary data on mechanical properties indicates a modulus E of approximately 45 Gpa and a strength of approximately 80 MPa. Elastic modulus was in the 5 GPa range. These bars were tested after heating to 200 ºC to ensure water removal and allow some strengthening of the parts. The data presented is considered preliminary as only a limited number of samples were developed and hence any true standard deviation and statistical analysis were unavailable.

The correlation between the solid freeform fabrication development of the parts and the gel mineralization is that they can be used together. The goal in joining the two process is in developing a consistent quantitative analysis of inhibition areas using the organic additives of the gel mineralization assay and incorporating them into mechanical property analysis. Once a more thorough analysis of mechanical properties is achieved and all the parameters are optimized to achieve desirable values then the gel mineralization data comes into the process. In order to emulate true biomimetic functional parts some flexibility of parts is desirable. The potential exists to introduce small amounts of a desired organic molecular inhibitor/modifier into the gel as it is being written in the freeforming process to have localized modification of the wt% of mineral hence providing some flexibility within the final parts.

The gel mineralization assays combined with freeform fabrication of gel based biomineral parts shows great potential in advancing biomimetic materials processing.

12.0 CONCLUSIONS

Molecular imprinting was successfully illustrated in film form. The original goal was to develop a methodology utilizing the selective recognition of molecular imprinting and showings its viability in film form. There are several advantages to the success of molecular imprinting in film form. By utilizing a film it is increases potential applications toward a greater number of situations as it may be used in filtration systems and as selective recognition coatings. Additionally, the methodology that has been illustrated lends itself to a simpler form of processing as the film may be directly dipped in and out of solutions and reasonably extract various imprint molecules.

A gel mineralization assay has successfully been shown as a useful method for the screening of organic molecules as applied to their importance in biomineralization. The results indicate that COOH groups, in polyacrylic acid, and pyrophosphates are able to inhibit growth of calcium carbonates and in limited cases may inhibit calcium phosphate growth.

The work here successfully illustrates progress in the field of biomimetic materials processing and lays a solid groundwork for future experimentation.

13.0 REFERENCES

1. Mosbach, K., Vlatakis, G., Andersson, L. I., Muller, R., *Drug Assay Using Antibody Mimics Made by Molecular Imprinting*. Nature 361, 645 (1993).
2. Ansell, R. J., Ramstrom, O., Mosbach, K., *Towards artificial antibodies prepared by molecular imprinting*. Clinical Chemistry 42, 1506 (1996).
3. Weiner, S., in *CRC Critical Reviews in Biochemistry* Lowenstam, Ed. (CRC, 1986), vol. 20, pp. 365-408.
4. Heuer A.H. *et al.*, *Innovative Materials Processing Strategies: A Biomimetic Approach*. Science 255, 1098 (1992).
5. Weiner, S., Moradian-Oldar, J., Frolow, F., Addadi, L., *Interactions Between Acidic Matrix Macromolecules and Calcium Phosphate Ester Crystals: Relevance to Carbonate Apatite Formation in Biomineralization*. Proceedings of the Royal Society of London, B 247, 47 (1992).
6. Ma, C. L. *et al.*, *Comparison of controlled crystallization of calcium phosphates under three kinds of monolayers*. J. Crystal Growth 173, 141 (1997).
7. Wulff, G., in *Polymeric Reagents and Catalysts* W. T. Ford, Ed. (American Chemical Society, 1986), vol. 308, pp. 186-230.
8. Mosbach, K., *Molecular Imprinting*. Trends in Biochemical Sciences 19, 9 (1994).
9. Wulff, G., *Molecular Imprinting in Crosslinked Polymers- The Role of the Binding Sites*. Mol. Cryst. Liq. Cryst. Sci. Technol. A 276, 1 (1996).
10. Sherrington, D. C., Steinke, J., Dunkin, I. R., *Imprinting of Synthetic Polymers Using Molecular Templates*. Adv. Polym. Sci. 123, 81 (1995).
11. Andersson, L. I., *Molecular Imprinting: developments and applications in the analytical chemistry field*. J. Chromatography B 745, 3 (2000).
12. Kempe, M., Mosbach, K., *Molecular Imprinting used for Chiral Separations*. Journal of Chromatography A 694, 3 (1995).
13. Adamson, A. W., in *Physical Chemistry of Surfaces*. (Wiley Publications, 1990) pp. 379-420.
14. Bartsch, R. A., Maeda, M., in *Molecular and Ionic Recognition with Imprinted Polymers* R. A. Bartsch, M. Maeda, Eds. (American Chemical Society, Washington D.C., 1998), vol. ACS Symposium Series 703, pp. 1-8.
15. Haupt, K., Mosbach, K., *Plastic Antibodies: developments and applications*. Trends in Biochemical Sciences??? (1999).
16. McNiven, S. J. *et al.*, in *Molecular and Ionic Recognition with Imprinted Polymers* R. A. Bartsch, M. Maeda, Eds. (American Chemical Society, Washington D.C., 1998), vol. 703, pp. 90-108.
17. Yano, K., Karube, I., *Molecularly imprinted polymers for biosensor applications*. Trends in Analytical Chemistry 18, 199 (1999).
18. Mosbach, K., Moradian, A., *Preparation of a Functional, Highly Selective Polymer by Molecular Imprinting. A Demonstration with L-p-*

Aminophenylalanine Anilide as a Template Molecule Allowing Multiple Points of Attachment. J. Molecular Recog. 2, 167 (1989).

19. Wulff, G., in *Bioorganic Chemistry in Healthcare and Technology* U. K. Pandit, Alderweireldt F.C., Ed. (Plenum Press, New York, 1991) pp. 55-68.
20. Shea, K. J., Dougherty, T. K., *Molecular Recognition on Synthetic Amorphous Surfaces. The Influence of Functional Group Positioning on the Effectiveness of Molecular Recognition*. J. Am. Chem. Soc. 108, 1091 (1986).
21. Kirsch, N., Alexander, C., Lubke, M., Whitcombe, M. J., Vulfson, E. N., *Enhancement of selectivity of imprinted polymes via post-imprinting modification of recognition sites*. Polymer 41, 5583 (2000).
22. Wulff, G., Schauhoff, S., *Racemic Resolution of Free Sugars with Macroporous Polymers Prepared by Molecular Imprinting. Selectivity Dependence on the Arrangement of Functional Groups versus Spatial Requirements*. Journal of Organic Chemistry 56, 395 (1991).
23. Wulff, G., Haarer, J., *Enzyme Analogue Built Polymers, 29. The Preparation of Defined Chiral Cavities for the Racemic Resolution of Free Sugars*. Makromol. Chem. 192, 1329 (1991).
24. Wulff, G., Sarhan, A., *Enzyme Analogue Built Polymers, 13. On the Introduction of Amino- and Boronic Acid Groups into Chiral Polymer Cavities*. Makromol. Chem. 183, 85 (1982).
25. Damen, J., Neckers, D. C., *On the Memory of Synthesized Vinyl Polymers for their Origins*. Tetrahedron Lett. 21, 1913 (1980).
26. Wulff, G., Best, W., Akelah, A., *Enzyme Analogue Built Polymers, 17. Investigations on the Racemic Resolution of Amino Acids*. Reactive Polymers 2, 167 (1984).
27. Wulff, G., Vietmeier, J., *Enzyme-analogue built polymers, 25: Synthesis of Macroporous Copolymers from alpha-amino acid based vinyl compounds*. Makromol. Chem. 190, 1717 (1989).
28. Wulff, G., *The Role of Binding-Site Interactions in the Molecular Imprinting of Polymers*. Trends in Biotechnology 11, 85 (1993).
29. Mosbach, K., Nicholls, I. A., Ramstrom, O., *Insights into the Role of the Hydrogen Bond and Hydrophobic Effect on Recognition in Molecularly Imprinted Polymer Synthetic Peptide Receptor Mimics*. Journal of Chromatography A 691, 349 (1995).
30. Fersht, A. R., *The Hydrogen Bond in Molecular Recognition*. Trends in Biochemical Sciences 12, 301 (1987).
31. Andersson, L. I., *Molecular imprinting for drug bioanalysis A review on the application of imprinted polymers to solid-phase extraction and binding assay*. J. Chromatography B 739, 163 (2000).
32. Mosbach, K., Glad, M., Norrlow, O., Sellergren, B., Seigbahn, N., *Use of Silane Monomers for Molecular Imprinting and Enzyme Entrapment in Polysiloxane-coated Porous Silica*. Journal of Chromatography 347, 11 (1985).

33. Mosbach, K., Arshady, R., *Synthesis of Substrate-selective Polymers by Host-Guest Polymerization*. Makromol. Chem. 182, 687 (1981).
34. Mosbach, K., Norrlow, O., Glad, M., *Acrylic Polymer Preparations Containing Recognition Sites Obtained by Imprinting with Substrates*. J. Chromatography 299, 29 (1984).
35. Sherrington, D. C., Dunkin, I. R., Lenfeld, J., *Molecular Imprinting of flat polycondensed aromatic molecules in macroporous polymers*. Polymer 34, 77 (1993).
36. Mosbach, K., Andersson, L., Sellergren, B., *Imprinting of Amino Acid Derivatives in Macroporous Polymers*. Tetrahedron Letters 25, 5211 (1984).
37. Mosbach, K., Andersson, L., Ekberg, B., *Synthesis of a New Amino Acid Based Cross-linker for Preparation of Substrate Selective Acrylic Polymers*. Tetrahedron Letters 26, 3623 (1985).
38. Mosbach, K., Sellergren, B., Ekberg, B., *Molecular Imprinting of Amino Acid Derivatives in Macroporous Polymers: Demonstration of Substrate- and Enantio-Selectivity by Chromatographic Resolution of Racemic Mixtures of Amino Acid Derivatives*. Journal of Chromatography 347, 1 (1985).
39. Mosbach, K., Sellergren, B., Lepisto, M., *Highly Enantioselective and Substrate-Selective Polymers Obtained by Molecular Imprinting Utilizing Noncovalent Interactions. NMR and Chromatographic Studies on the Nature of Recognition*. Journal of the American Chemical Society 110, 5853 (1988).
40. Mosbach, K., O'Shannessy, D. J., Ekberg, B., *Molecular Imprinting of Amino Acid Derivatives at Low Temperature (0 C) Using Photolytic Homolysis of Azobisnitriles*. Anal. Biochem. 177, 144 (1989).
41. Mosbach, K., O'Shannessy, D.J., Ekberg, B., Andersson, L.I., *Recent Advances in the Preparation and use of Molecularly-Imprinted Polymers for Enantiomeric Resolution of Amino Acid Derivatives*. Journal of Chromatography 470, 391 (1989).
42. Mosbach, K., Andersson, L. I., O'Shannessy, D. J., *Molecular Recognition in Synthetic Polymers: Preparation of Chiral Stationary Phases by Molecular Imprinting of Amino Acid Amides*. Journal of Chromatography 513, 167 (1990).
43. Mosbach, K., Andersson, L. I., Miyabayashi , A., O'Shannessy, D. J., *Enantiomeric Resolution of Amino Acid Derivatives on Molecularly Imprinted Polymers as Monitored by Potentiometric Measurements*. Journal of Chromatography 516, 323 (1990).
44. Mosbach, K., Andersson, L. I., *Enantiomeric Resolution on Molecularly Imprinted Polymers Prepared with only Non-covalent and Non-ionic interactions*. Journal of Chromatography 516, 313 (1990).
45. Shea, K. J., Sellergren, B., *Influence of Polymer Morphology on the Ability of Imprinted Network Polymers to Resolve Enantiomers*. Journal of Chromatography 635, 31 (1993).

46. Mosbach, K., Andersson, L. I., Hedborg, E., Winquist, F., Lundstrom, I., *Some Studies of Molecularly-imprinted polymer membranes in combination with field-effect devices*. Sensors and Actuators A 37-38, 796 (1993).
47. Karube, I. *et al.*, *Molecular Recognition in Continuous Polymer Rods Prepared by a Molecular Imprinting Technique*. Analytical Chemistry(Anal. Chem.) 65, 2223 (1993).
48. Mosbach, K., Ramstrom, O., Andersson, L. I., *Recognition Sites Incorporating Both Pyridinyl and Carboxy Functionalities Prepared by Molecular Imprinting*. J. Org. Chem. 58, 7562 (1993).
49. Mosbach, K., Fischer, L., Muller, R., Ekberg, B., *Direct Enantioseparation of Beta-Adrenergic Blockers Using a Chiral Stationary Phase Prepared by Molecular Imprinting*. J. Am. Chem. Soc. 113, 9358 (1991).
50. Shea, K. J., Spivak, D. A., Sellergren, B., *Polymer Complements to Nucleotide Bases. Selective Binding of Adenine Derivatives to Imprinted Polymers*. Journal of the American Chemical Society 115, 3368 (1993).
51. Wulff, G., *Molecular Imprinting in Synthetic Polymers. Models for the Receptor Site in Enzymes*. Makromol. Chemie., Macromol. Symp. 70/71, 285 (1993).
52. Wulff, G., Gross, T., Schonfeld, R., Schrader, T., Kirsten, C., in *Molecular and Ionic Recognition with Imprinted Polymers* R. A. Bartsch, M. Maeda, Eds. (American Chemical Society, Washington D.C., 1998), vol. 703, pp. 10-28.
53. Mosbach, K. (United States Patent Office, 1992) pp. 8.
54. Nicholls, I. A., *Towards the rational design of molecularly imprinted imprinted polymers*. J. Molecular Recognition 11, 79 (1998).
55. Ensing, K., de Boer, T., *Tailor-made materials for tailor-made applications: application of molecular imprints in chemical analysis*. Trends in Analytical Chemistry 18, 138 (1999).
56. Wulff, G., *Molecular Imprinting in Cross-Linked Materials with the Aid of Molecular Templates- A Way Towards Aritificial Antibodies*. Angew. Chem. Int. Ed. Engl. 34, 1812 (1995).
57. Sellergren, B., *Molecular Imprinting by Noncovalent Interactions: Tailor-made Chiral Stationary Phases of High Selectivity and Sample Load Capacity*. Chirality 1, 63 (1989).
58. Katz, A., Davis, M. E., *Investigations into the Mechanisms of Molecular Recognition with Imprinted Polymers*. Macromolecules 32, 4113 (1999).
59. Ye, L., Mosbach, K., *The Technique of Molecular Imprinting – Principle, State of the Art, and Future Aspects*. Journal of Inclusion Phenomena and Macrocyclic Chemistry 41, 107 (2001).
60. Dickert, F. L., Sikorski, R., *Supramolecular strategies in chemical sensing*. Materials Science and Engr. C 10, 39 (1999).
61. Ramstrom, O., Ansell, R. J., *Molecular Imprinting Technology: Challenges and Prospects for the Future*. Chirality 10, 195 (1998).

62. Mayes, A. G., Lowe, C. R., in *Drug Development Assay Approaches, Including Molecular Imprinting and Biomarkers* E. Reid, H. M. Hill, I. D. Wilson, Eds. (The Royal Society of Chemistry, Cambridge, UK, 1998), vol. 25, pp. 28-36.
63. Wulff, G., Heide, B., Helfmeier, G., *Enzyme-Analogue Built Polymers, 24. On the Distance Accuracy of Functional Groups in Polymers and Silicas Introduced by a Template Approach*. Reactive Polymers 6, 299 (1987).
64. Wulff, G., Minavik, M., Journal of Liquid Chromatography 13, 2897 (1990).
65. Wulff, G., Kirstein, G., *Measuring the Optical Activity of Chiral Imprints in Insoluble Highly Cross-linked Polymers*. Angew. Chem. Int. Ed. Engl. 29, 684 (1990).
66. Haupt, K., Mosbach, K., *Molecularly Imprinted Polymers and Their Use in Biomimetic Sensors*. Chemical Reviews 100, 2495 (2000).
67. Surugiu, I., Danielsson, B., Ye, L., Mosbach, K., Haupt, K., *Chemiluminescence Imaging ELISA Using and Imprinted Polymer as the Recognition Element Instead of Antibody*. Analytical Chem. 73, 487 (2001).
68. Wulff, G., Vietmeier, J., *Enzyme-analogue built polymers, 26: Enantioselective synthesis of amino acids using polymers possessing chiral cavities obtained by an imprinting procedure with template molecules*. Makromol. Chem. 190, 1727 (1989).
69. Lerner, R., Benkovic, S. J., Schultz, P. G., *At the Crossroads of Chemistry and Immunology: Catalytic Antibodies*. Science 252, 659 (1991).
70. Mosbach, K., Muller, R., Andersson, L. I., *Molecularly Imprinted Polymers Facilitating a Beta-elimination reaction*. Makromol. Chem. Rapid Commun. 14, 637 (1993).
71. Mann, S., *Molecular Recognition in Biomineralization*. Nature 332, 1988 (1988).
72. Mann, S. *et al.*, *Biomineralization: Biomimetic Potential at the Inorganic-Organic Interface*. MRS Bulletin 17, 32 (1992).
73. Simkiss, K., Wilbur, K. M., *Biomineralization: Cell Biology and Mineral Deposition* (Academic Press Inc., San Diego, 1989), pp. 337.
74. Kitano, Y., Hood, D. W., *The influence of organic material on the polymorphic crystallization of calcium carbonate*. Geochimica et Cosmochimica Acta 29, 29 (1965).
75. Kazmierczak, T. F., Tomson, M. B., Nancollas, G. H., *Crystal Growth of Calcium Carbonate. A Controlled Composition Kinetic Study*. J. Phys. Chem. 86, 103 (1982).
76. Mann, S., Heywood, B. R., *Template-Directed Nucleation and Growth of Inorganic Materials*. Adv. Materials 6, 9 (1994).
77. Weiner, S., Addadi, L., *Interactions Between Acidic Macromolecules and Structured Crystal Surfaces. Stereochemistry and Biomineralization*. Mol. Cryst. Liq. Cryst. 134, 305 (1986).
78. Wada, N., Yamashita, K., Umegaki, T., *Effects of Carboxylic Acids on Calcite Formation in the Presence of Mg^{+2} Ions*. J. Colloid & Interface Science 212, 357 (1999).

79. Addadi, L., Weiner, S., *Interactions between acidic proteins and crystals: Stereochemical requirements for biomineralization*. Proceedings of the National Academy of Sciences, USA 82, 4110 (1985).
80. Tiller, T. A., *The Science of Crystallization* (Cambridge University Press, Cambridge, 1991), pp.
81. Otsuki, A., Wetzel, R. G., *Interaction of yellow organic acids with calcium carbonate in freshwater*. 490 (1973).
82. Peterman, J., Broza, G., *Epitaxial Deposition of Metals on Uniaxial Oriented Semi-crystalline Polymers*. J. Mater. Sci. 22, 1108 (1987).
83. Wittman, J. C., Smith, P., *Highly Oriented Thin Films of Poly(tetrafluoroethylene) as a Substrate for Oriented Growth of Materials*. Nature 352, 415 (1991).
84. Wong, K. K. W., Mann, S., *Small-scale structures in biomineralization and biomimetic materials chemistry*. Curr. Opin. Colloid & Interf. Sci. 3, 63 (1998).
85. Wheeler, A. P., Sikes, C. S., *Regulation of Carbonate Calcification by Organic Matrix*. Amer. Zool. 24, 933 (1984).
86. Lowenstam, H. A., Weiner, S., *On Biomineralization* (Oxford University Press, New York, 1989), pp. 324.
87. Hunter, G. K., *Interfacial Aspects of Biomineralization*. Curr. Opin. Solid State & Mat. Sci. 1, 430 (1996).
88. Mann, S., in *Biomimetics: Design and Processing of Materials* M. Sarikaya, I. A. Aksay, Eds. (American Institute of Physics, Woodbury, New York, 1995) pp. 91-116.
89. Calvert, P., *Strategies for Biomimetic Mineralization*. Scripta Metallurgica et Materialia 31, 977 (1994).
90. Mann, S., Heywood, B. R., *Crystal Recognition at Inorganic-Organic Interfaces: Nucleation and Growth of Oriented $BaSO_4$ under Compressed Langmuir Monolayers*. Advanced Materials 4, 278 (1992).
91. Addadi, L., Weissbuch, I., Lahav, M., Leiserowitz, L., *Molecular Recognition at Crystal Interfaces*. Science 253, 637 (1991).
92. Mann, S., Ozin, G. A., *Synthesis of inorganic materials with complex form*. Nature 382, 313 (1996).
93. Aizenberg, J., Black, A. J., Whitesides, G. M., *Control of crystal nucleation by patterned self-assembled monolayers*. Nature 398, 495 (1999).
94. Mann, S., Sparks, N. H. C., Frankel, R. B., Bazylinski, D. A., Janasch, H. W., *Biomineralization of Ferrimagnetic Greigite(Fe_3S_4) and Iron Pyrite (FeS_2) in a Magnetotactic Bacterium*. Nature 334, 258 (1990).
95. Schaffer, T. E. *et al.*, *Does Abalone Nacre Form by Heteroepitaxial Nucleation of by Growth through Mineral Bridges?* Chem. Mater. 9, 1731 (1997).
96. Teng, H. H., Dove, P. M., Orme, C. A., De Yoreo, J. J., *Thermodynamics of Calcite Growth: Baseline for Understanding Biomineral Formation*. Science 282, 724 (1998).

97. Mann, S., *Mineralization in Biological Systems*. Structure and Bonding 54, 125 (1983).
98. Mann, S. *et al.*, *Crystallization at Inorganic-Organic Interfaces: Biominerals and Biomimetic Synthesis*. Science 261, 1286 (1993).
99. Calvert, P., Mann, S., *Synthetic and biological composites formed by in situ precipitation*. J. of Mat. Sci. 23, 3801 (1988).
100. Moradian-Oldak, J., Jimenez, I., Maltby, D., Fincham, A. G., *Controlled Proteolysis of Amelogenins Reveals Exposure of Both Carboxy- and Amino-Terminal Regions*. Biopolymers 58, 606 (2001).
101. Almqvist, N. *et al.*, *Methods for fabricating and characterizing a new generation of biomimetic materials*. Mat Sci & Engr C C7, 37 (1999).
102. Campbell, A. A., *Interfacial regulation of crystallization in aqueous environments*. Curr Opin Colloid & Interface Sci 4, 40 (1999).
103. Dove, P. M., Hochella Jr., M. F., *Calcite Precipitation Mechanisms and Inhibition by Orthophosphate: In Situ Observations by Scanning Force Microscopy*. Geochimica et Cosmochimica Acta 57, 705 (1993).
104. Wan Andrew, C. A., Khor, E., Hastings, G. W., *The influence of anionic chitin derivatives on calcium phosphate crystallization*. Biomaterials 19, 1309 (1998).
105. Bernard, J. P. *et al.*, *Inhibition of Nucleation and Crystal Growth of Calcium Carbonate by Human Lithostathine*. Gastroenterology 103, 1277 (1992).
106. Giannimaras, E. K., Koustsoukos, P. G., *The Crystallization of Calcite in the Presence of Orthophosphate*. J. Colloid & Interf. Sci. 116, 423 (1987).
107. Bigi, A., Boanini, E., Panzavolta, S., Roveri, N., *Biomimetic Growth of Hydroxyapatite on Gelatin Films Doped with Sodium Polyacrylate*. Biomacromolecules, A (2000).
108. Rodriquez-Lorenzo, L. M., Vallet-Regi, M., *Controlled Crystallization of Calcium Phosphate Apatites*. Chemisry of Materials 12, 2460 (2000).
109. Liu, Y., Wu, W., Sethuraman, G., Nancollas, G. H., *Intergrowth of calcium phosphates: an interfacial energy approach*. J. Crystal Growth 174, 386 (1997).
110. Mann, S., Williams, R. J. P., *Precipitation within Unilamellar Vesicles. Part I. Studies of Silver(1) Oxide Formation*. J. Chem. Soc. Dalton Trans. 21, 311 (1983).
111. Mann, S., Skarnulis, A. J., Williams, R. J. P., *Inorganic and Bio-inorganic Chemistry in Vesicles*. Israel J. Chem. 21, 3 (1981).
112. Mann, S., Hannington, J. P., Williams, R. J. P., *Phospholipid vesicles as a model system for biomineralization*. Nature 324, 565 (1986).
113. Li, C., Kaplan, D. L., *Biomimetic Composites via Molecular Scale Self-assembly and Biomineralization*. Curr. Opin. Solid St. & Mat. Sci. 7, 265 (2003).
114. Weiner, S., Addadi, L., Wagner, H. D., *Materials design in biology*. Materials Science & Engr. C 11, 1 (2000).
115. Nancollas, G. H., Wu, W., *Biomineralization mechanisms: a kinetics and interfacial energy approach*. J. Crystal Growth 211, 137 (2000).
116. Henisch, H. K., *Crystal Growth in Gels* (Dover Publications Inc., 1970), pp. 109.

117. Henisch, H. K., Garcia-Ruiz, J. M., *Crystal Growth in Gels and Liesegang Ring Formation I. Diffusion relationships*. J. Crystal Growth 75, 195 (1986).
118. Henisch, H. K., *Crystals in Gels and Liesegang Rings* (Cambridge University Press, Cambridge, 1988), pp.
119. Hickson, T. G. L., Polson, A., *Some Physical Characteristics of the Agarose Molecule*. Biochimica Et Biophysica Acta 165, 43 (1968).
120. Xiong, J.-Y. *et al.*, *Topology Evolution and Gelation Mechanism of Agarose Gel*. J. Phys. Chem. B 109, 5638 (2005).
121. Letherby, M. R., Young, D. A., *The Gelation of Agarose*. J. Chem. Soc. Faraday Trans. I 77, 1953 (1981).
122. Bica, C. I. D., Borsali, R., Geissler, E., Rochas, C., *Dynamics of Cellulose Whiskers in Agarose Gels. 1. Polarized Dynamic Light Scattering*. Macromolecules 34, 5275 (2001).
123. Owens, P. K., Karlsson, L., Lutz, E. S. M., Andersson, L. I., *Molecular imprinting for bio- and pharmaceutical analysis*. Trends in Analytical Chemistry 18, 146 (1999).
124. Kempe, M., Mosbach, K., *Separation of Amino Acids, Peptides and Proteins on Molecularly Imprinted Stationary Phases*. Journal of Chromatography A 691, 317 (1995).
125. Muldoon, M. T., Stanker, L. H., *Plastic antibodies: molecularly imprinted polymers*. Chem. & Indust., 204 (1996).
126. Ye, L., Mosbach, K., *Polymers Recognizing Biomolecules Based on a Combination of Molecular Imprinting and Proximity Scintillation: A New Sensor Concept*. J. Am. Chem. Soc. 123, 2901 (2001).
127. Vulfson, E. N. *et al.*, in *Drug Development Assay Approaches, Including Molecular Imprinting and Biomarkers* E. Reid, H. M. Hill, I. D. Wilson, Eds. (The Royal Society of Chemistry, Cambridge, UK, 1998), vol. 25, pp. 44-48.
128. Kobayashi, T., Wang, H. Y., Fujii, N., *Molecular Imprinting of Theophylline in Acrylonitrile-acrylic Acid Copolymer Membrane*. Chemistry Letters, 927 (1995).
129. Stevenson, D., *Molecular imprinted polymers for solid-phase extraction*. Trends in Analytical Chemistry 18, 154 (1999).
130. Hoyer, J. R., Shiraga, H. Min, W.,VanDusen, W.J., Clayman, M.D.,Miner, D., Terrell, C.H., Sherbotie, J.R., Foreman ,J.W., Przysiecki, C., Neilson, E.G., *Inhibition of Calcium Oxalate Crystal Growth in vitro by Uropontin: Another Member of the Aspartic Acid-rich Protein Superfamily*. Proceedings of the National Academay of Sciences, USA 89, 426 (1992).
131. Odian, G., *Principles of Polymerization* (Wiley Intersciences, New York, ed. 3rd, 1991), pp. 768.
132. Heinz-Helmut, Perkampus, *UV-VIS Atlas of Organic Compounds* (VCH, Weiheim, New York, ed. 2nd, 1992), pp.
133. Hargis, L., G.,, Howell, J. A., *Ultraviolet and Light Absorption Spectrometry*. Analytical Chem. 60, 131R (1988).

134. Howell, J. A., Hargis, L., G.,, *Ultraviolet and Light Absorption Spectrometry*. Analytical Chem. 62, 155R (1990).
135. Hargis, L., G.,, Howell, J. A., Sutton, R. E., *Ultraviolet and Light Absorption Spectrometry*. Analytical Chem. 68, 169R (June 15, 1996, 1996).
136. Wulff, G., in *Molecular Interactions in Bioseparations* T. T. Ngo, Ed. (Plenum Press, New York, 1993) pp. 363-381.
137. Vafai, S., Drake, B. D., Smith Jr., R. L., *Solid Molar Volumes of Interest to Supercritical Extraction at 298K: Atropine, Berberine Hydrochloride Hydrate, Brucine Dihydrate, Capsaicin, Ergotamine Tartrate Dihydrate, Naphthalene, Penicillin V, Piperine, Qunine, Strychnine, Theobromine, Theophylline, and Yohimbine Hydrochloride*. J. Chem. Eng. Data 38, 125 (1993).
138. Jahagirdar, D. V., Arbad, B. R., Walvekar, A. A., Shankarwar, A. G., Lande, M. K., *Studies in Partial Molar Volumes, Partial Molar Compressibilities and Viscosity B-Coefficients of Caffeine in Water at Four Temperatures*. Journal of Molecular Liquids 85, 361 (2000).
139. Li, S., Varadarajan, G. S., Hartland, S., *Solubilities of Theobromine and Caffeine in Supercritical Carbon Dioxide: Correlation with Density-based Models*. Fluid Phase Equlibria 68, 263 (1991).
140. Hayden, O., Dickert, F. L., *Selective Microorganism Detection with Cell Surface Imprinted Polymers*. Advanced Materials 13, 1480 (2001).
141. Crommelin, D. J. A., Modderkolk, J., de Blaey, C. J., *The pH Dependence of Rectal Absorption of Theophylline from Solutions of Aminophylline in situ in Rats*. International Journal of Pharmaceutics 3, 299 (1979).
142. Rogstad, K. N., Jang, Y. H., Sowers, L. C., Goddard III, W. A., *First Principles Calculations of the pKa Values and Tautomers of Isoguanine and Xanthine*. Chem. Res. Toxicol. 16, 1455 (2003).
143. Belcher, A. M. *et al.*, *Control of crystal phase switching and orientation by soluble mollusc-shell proteins*. Nature 381, 56 (1996).
144. Calvert, P., Rieke, P., *Biomimetic Mineralization in and on Polymers*. Chem. Mater. 8, 1715 (1996).
145. Hillner, P. E., Manne, S., Hansma, P. K., Gratz, A. J., *Atomic-Force Microscope - A New Tool For Imaging Crystal-Growth Processes*. Faraday Discuss. 95, 191 (1993).
146. Calvert P, O'Kelly J, C, S., *Solid freeform fabrication of organic-inorganic hybrid materials*. Materials Science and Engr. C 6, 165 (1998).
147. Liu, S. T., Nancollas, G. H., J. Colloid & Interf. Sci. 44 (1973).
148. Amjad, Z., *Calcium-Sulfate Dihydrate (Gypsum) Scale Formation On Heat-Exchanger Surfaces - The Influence Of Scale Inhibitors*. Journal Of Colloid And Interface Science 123, 523 (1988).
149. Oner, M., Calvert, P., *The effect of architecture of acrylic polyelectrolytes on inhibition of oxalate crystallization*. Mat. Sci. & Engr. C 2, 93 (1994).

150. Sikes, C. S., Yeung, M. L., Wheeler, A. P., in *Surface Reactive Peptides and Polymers* C. S. Sikes, A. P. Wheeler, Eds. (American Chemical Society, Washington, DC, 1990).
151. Manoli, F., Dalas, E., *Spontaneous precipitation of calcium carbonate in the presence of chondroitin sulfate*. J. Crystal Growth 217, 416 (2000).
152. Davis, S. A., Dujardin, E., Mann, S., *Biomolecular Inorganic Materials Chemistry*. Curr. Opin. Solid St. & Mat. Sci. 7, 273 (2003).
153. Nancollas, G. H., in *Biological Mineralization and Demineralization* G. H. Nancollas, Ed. (Springer-Verlag, Berlin, 1982), vol. 23, pp. 1-4.
154. Nielsen, A. E., Christoffersen, J., in *Biological Mineralization and Demineralization* G. H. Nancollas, Ed. (Springer-Verlag, Berlin, 1982), vol. 23, pp. 37-77.
155. Wada, N., Kanamura, K., Umegaki, T., *Effects of Carboxylic Acids on the Crystallization of Calcium Carbonate*. J. Colloid & Interf. Sci. 233, 65 (2001).
156. de Leeuw, N. H., Cooper, T. G., *A Computer Modeling Study of the Inhibiting Effect of Organic Adsorbates on Calcite Crystal Growth*. Crystal Growth & Design 4, 123 (2004).
157. Guo, J., Severtson, S. J., *Application of Classical Nucleation Theory to Characterize the Influence of Carboxylate-Containing Additives on $CaCO_3$ Nucleation at High Temperature, pH, and Ionic Strength*. Industrial Engineering and Chem. Res. 42, 3480 (2003).
158. Kim, I. W., Roberstons, R. E., Zand, R., *Effects of Some Nonionic Polymeric Additives on the Crystallization of Calcium Carbonate*. Crystal Growth & Design 5, 513 (2005).
159. Tako, M., Nakamura, S., *Gelation Mechanism of Agarose*. Carbohydrate Research 180, 277 (1988).
160. Piculell, L., Nilsson, S., *Effects of Salts on Association and Conformational Equilibria of Macromolecules in Solution*. Progress in Colloid & Polymer Science 82, 198 (1990).
161. Martell, A. E., Motekaitis, R. J., *Determination and Use of Stability Constants* (VCH Publishers, 1988), pp. 216.
162. Addadi, L., Moradian, J., Shay, E., Maroudas, N. G., Weiner, S., *A chemical model for the cooperation of sulfates and carboxylates in calcite crystal nucleation: Relevance to biomineralization*. Proc. Natl. Acad. Sci. USA 84, 2732 (1987).
163. Lee, I., Han, S. W., Choi, H. J., Kim, K., *Nanoparticle-Directed Crystallization of Calcium Carbonate*. Advanced Materials 12, 1617 (2001).
164. Dorozhkin, S. V., Epple, M., *Biological and Medical Significance of Calcium Phosphates*. Angew. Chem. Int. Ed. 41, 3130 (2002).